Report No. FAA-RD-80-50

(12)

20000727245

ADA085179

ENGINE INLET ANTI-ICING SYSTEM EVALUATION PROCEDURE

ALLYN HEINRICH
RICHARD ROSS
NICK GANESAN

JUN 6 1980

A

JANUARY 1980
FINAL REPORT

Document is available to the U.S. public through the National Technical Information Service, Springfield, Virginia 22161.

Prepared for

U.S. DEPARTMENT OF TRANSPORTATION
FEDERAL AVIATION ADMINISTRATION
Systems Research & Development Service
Washington, D.C. 20590

80 6 6 101

NOTICE

Technical Report Documentation Page

1. Report No. FAA/RD 80-50	2. Government Accession No. AD-A085 179	3. Recipient's Catalog No.
4. Title and Subtitle ENGINE INLET ANTI-ICING SYSTEM EVALUATION PROCEDURE.		5. Report Date January 1980
		6. Performing Organization Code
		8. Performing Organization Report No.
7. Author(s) Allyn Heinrich, Richard Ross and Nick Ganesan		
9. Performing Organization Name and Address GATES LEARJET CORPORATION P.O. Box 7707 Wichita, Kansas 67277		10. Work Unit No. (TRAIS)
		11. Contract or Grant No. DOT-FA76WA-3852
12. Sponsoring Agency Name and Address U.S. Department of Transportation Federal Aviation Administration Systems Research & Development Service Washington, D.C. 20590		13. Type of Report and Period Covered FINAL REPORT.
		14. Sponsoring Agency Code
15. Supplementary Notes		

16. Abstract The objectives of this work were to develop a procedure for predicting and evaluating the performance of engine inlet anti-icing systems for compliance with FAR 25 ice protection requirements without conducting flight tests in natural icing conditions. This must include consideration of water droplet impingment, collection efficiency, internal and external heat transfer and mass transfer of the impinging water.

The method of approach for developing these procedures was to survey current analysis methods involving physical theory and empirical methods and then to develop a computerized model for use in anti-icing system performance analysis. Icing wind tunnel tests were conducted using a three-dimensional nacelle test model to aid in the procedure development.

A typical engine-inlet anti-icing system was evaluated with the computer model in a variety of icing environments and operational conditions and compared with icing wind tunnel test results. Correlation between performance predictions and wind tunnel test results was found to have good agreement within the spectrum of conditions that were practicable in the wind tunnel.

17. Key Words ANTI-ICING, AIRCRAFT ENGINE INLETS, EVALUATION PROCEDURES, ANALYTICAL METHODS, ICING WIND TUNNEL TESTS	18. Distribution Statement DOCUMENT IS AVAILABLE TO THE PUBLIC THROUGH THE NATIONAL TECHNICAL INFORMATION SERVICE, SPRINGFIELD, VA 22151

19. Security Classif. (of this report)	20. Security Classif. (of this page)	21. No. of Pages	22. Price
UNCLASSIFIED	UNCLASSIFIED	142	

Form DOT F 1700.7 (8-72) Reproduction of completed page authorized

411784

PREFACE

This document, No. FAA-RD-80-50, is the final report of a study conducted by the Gates Learjet Corporation to develop an improved and simplified Procedure for predicting and evaluating engine inlet anti-icing systems. All work was performed in the Advanced Design, Aerodynamics, and Propulsion Analysis departments, under the coordination of Mr. A. M. Heinrich, Program Manager. The technical analysis was performed by Messrs. R. Ross, N. Ganesan, D.W. Newton and R. Sundquist. Development of the anti-icing analysis computer programs was originally formulated by Mr. T. M. Kutty prior to his departure from the company

Appreciation is gratefully extended for the cooperation and assistance provided by personnel of the NASA-Lewis Research Center in the conduct of icing wind tunnel tests.

TABLE OF CONTENTS

LIST OF ILLUSTRATIONS

List of Illustrations (Cont.)

LIST OF TABLES

SYMBOLS AND ABBREVIATIONS

		UNITS
A/A_E	Ratio of nacelle exit flow area with plug to unrestricted flow area	-
ALT	Altitude	ft
C	Nacelle chord length	ft
C_D	Drag coefficient	-
C_{D_o}	Profile drag coefficient	-
C_L	Lift coefficient	-
C_p	Specific heat at constant pressure	Btu/(lb-°R)
d	Distance along surface. Measured from inside nacelle inlet lip at aft limit of heated area. (See Figure 2-1 or 3-2).	ft
D	Drag	lb
DCD	Induced drag coefficient	-
D_D	Median droplet diameter	ft
D_{DM}	Median droplet diameter	μm
DIA	Nacelle highlight diameter	ft
DMWIH	Quantity of water impinging on the elemental area under analysis per foot circumference of the Nacelle lip.	lb/(hr-ft)
DQ	Heat transfered through elemental area under analysis	Btu/sec
DRB	Elemental runback	lb/(sec-ft^2)
DRBH	Water runback per foot circumference	lb/hr-ft
DS	Streamwise length of elemental area under analysis	ft
DT_B	Drop in bleed air temperature	°R
e	Partial pressure of water vapor for saturated air	lb/ft^2
EFF	Local channel efficiency	-
E_M	Water collection efficiency	-
EVAPH	Water evaporation rate per foot circumference	lb/hr-ft
exp	Base of Napierian logrithmic system	-
FN	Thrust/engine	lb
G	Acceleration due to gravity	ft/sec^2
H	Dry convective heat transfer coefficient	Btu(sec-ft^2-°R)
HORIZ	Horizontal extent of icing cloud	Statute miles

HPH	Heat transfer coefficient	Btu/(hr-ft^2)
IMPPH	Water impingement rate per foot of circumference	lb/hr-ft
J	Mechanical equivalent of heat	ft-lb/Btu
K	Evaporation fraction	-
K_1	Coefficient of thermal conductivity	Btu/(sec-ft -°R)
K_2	Inertia parameter	-
K_o	Impingement parameter	-
K_w	Water fraction	-
L	Latent heat of vaporization	Btu/lb
LOLS	Droplet range ratio	-
LWC	Liquid water content	grams/meter^3
M_w	Water collection rate	lb/(sec-ft^2)
MU	Coefficient of viscosity	lb/(ft-sec)
n	Exponent on Prandtl number	-
N1P	Engine speed	RPM
P	Pressure	lb/ft^2
P_C	Local surface pressure coefficient	-
PERC	Percent of water evaporated from section under analysis	-
P_r	Prandtl number	-
PSDAT	Matrix of surface position-pressure coefficient data (d, P_c) (See Section A.2)	-
Q	Quantity of heat	Btu/sec
R	Gas constant	(ft-lb)/(lb-°R)
RB	Runback rate	lb/(hr-ft)
RBPH	Water runback to next element per foot circumference	lb/hr-ft
RBS	Equivalent cross-sectional area of runback ice at aft limit of heated area.	in^2/ft
RHO	Air density	lb/ft^3
R_e	Reynolds number	-

$R_{e_{ft}}$	Reynolds number per foot	1/ft
R_{e_D}	Reynolds number based on water droplet diameter	-
$R_{e_{LE}}$	Reynolds number based on nacelle lip leading edge diameter (2 x R_{LE})	-
Re_s	Reynolds number based on local surface velocity and distance from stagnation point to point of analysis	-
R_{LE}	Leading edge radius	ft
S	Distance along surface from stagnation point to the point under consideration	ft
S'	Fraction of the distance from the stagnation point to the limit of impingement	-
S_H	Heated surface per foot circumference	ft^2/ft
SIN	Distance along surface from stagnation point to point of analysis	in
S_L	Distance along surface from stagnation point to limit of impingement	ft
S_w	Aircraft wing reference area	ft^2
t	Temperature	°F
t	Nacelle thickness	ft
t_T	Wind tunnel total temperature	°F
T	Temperature	°R
TAF	Ambient temperature	°F
TBF	Bleed air temperature	°F
TBFIN	Input bleed air temperature	°F
TEST	Test or run number	-
TOC	Nacelle thickness to chord ratio	-
TSDAT	Matrix of surface position - surface temperature data (d, T_S) (See Section A.2)	-
TSF	Surface temperature	°F
$T_{1,2,--5}$	Heat transfer temperature terms as defined in equations (2-33) through (2-37)	°R
V	Velocity	ft/sec
VKTAS	True airspeed	knots
V_1	True airspeed	miles/hr
V_2	True airspeed	knots

W	Aircraft weight	lb
W_w	Water flow rate	lb/hr
W_B	Bleed air mass flow rate per foot circumference	lb/sec-ft
WBM	Bleed air mass flow rate	lb/min
W_M	Water catch per foot circumference	lb/sec-ft
Z	Ratio - 1000/T	-
α	Nacelle angle of attack	deg
θ	Angle between lip radius line to the stagnation point and the lip radius line to the point of interest.	deg

SUBSCRIPTS

A	Ambient
B	Bleed air
o	Free stream
u	Upper
l	Lower
OUT	Output
CONV	Convection
EVAP	Evaporation
SENS	Sensible
W	Water
S	Surface
L	Local
IN	Input
TRAN	Transition
LAM	Laminar
TURB	Turbulent
H_2O	Water
air	Air
D	Reference value
AV	Average
LE	Leading edge
IMP	Impingement

1.0 INTRODUCTION

Gates Learjet introduced two new aircraft, Models 35 and 36, into their product line during 1974. These aircraft are powered by Garrett-AiResearch TFE 731-2 turbofan engines and use bleed-air for thermally anti-icing engine nacelle inlet lips, wings, and horizontal tail. During development of these aircraft it was found that existing techniques for predicting anti-icing system performance were either very complex or, when simplifying assumptions were made, were highly questionable in accuracy. In addition, current procedures for anti-icing system certification include a significant amount of flight testing in simulated and difficult to find natural icing conditions which is an expensive and time consuming process providing a very limited sample of the actual icing environment. Also, the validity of extrapolating data obtained from such flight tests to other FAR 25 Appendix C conditions has always remained questionable.

What has appeared to be needed is a simpler, less costly, and less time consuming technique where flight test requirements can be reduced to a minimum. To achieve this a procedure is needed which would utilize analytical prediction methods to evaluate the full scope of the icing environment and icing wind tunnel tests to confirm the method. The procedure must be sufficiently accurate and comprehensive to be acceptable to the FAA, but at the same time be simple and economical enough to be widely acceptable within the industry.

Against this background but focusing on only one area of a transport type airplane, a contract, No. DOT FA76WA-3852, was granted by the FAA, Washington, D.C., to develop a procedure for predicting and evaluating the performance of engine inlet anti-icing systems for compliance with FAR 25 ice protection requirements. The desire was to minimize the need for conducting flight tests in natural icing conditions. The procedure was to include consideration of water droplet impingment and collection efficiency, internal and external heat transfer, and mass transfer of the impinging water. A large spectrum of environmental and operational factors were to be analyzed in development of the procedure to identify those environmental/operational conditions which should be recommended for evaluation by the procedure. Icing wind tunnel tests were required to assist in the procedure development.

The following report describes the method of approach taken, icing wind tunnel tests conducted, and a correlation between predicted results, using the methodology, and the tunnel test results. Conclusions and recommendations are presented plus details of the computer programs developed.

2.0 ANALYSIS METHODOLOGY

Prediction of anti-icing system performance is based on a combination of aero-thermodynamic theory and empirical relationships. A summary of these methods, based on the works of many investigators, was prepared and published by the Federal Aviation Administration in 1964.[1] Solution of the general problem of internal heat transfer and of heat and mass transfer from a wetted surface in forced convection is quite involved and tedious. The method of solution customarily involves several trial-and-error calculations that are intermediate between the final answer and the basic factors that define a particular anti-icing situation. In order to lessen the burden of this effort a digital computer program was developed to perform these calculations.

The solution desired in anti-icing calculations is for the internal heat transfer rate of thermal heat systems, the external heat transfer by convection, evaporation of surface water, and the sensible heat change of the impinging water. After determining the heat transfer characteristics, the anti-icing performance (i.e., the rate of water impinging on the surface and the rate of evaporation) can be calculated for any known set of flight and atmospheric conditions. The difference between the rate of water impinging on the surface and the rate it is evaporated is the run-back rate. Knowing the run-back rate, the amount of run-back ice corres-pounding to the time taken to travel through the horizontal extent of the cloud is calculated.

The analysis is made using a point-by-point approach by dividing the heated area into several small segments. This method represents a more realistic evaluation because skin temperature and impingement rate gradients are generally too steep for use of average values.

---

1. Bowden, D.T., et. al.: "Engineering Summary of Airframe Icing Technical Data". Technical Report ADS-4, Federal Aviation Administration, March 1964.

2.1 Aero-Thermodynamic Relationships

The theoretical and empirical relationships used in calculating anti-icing performance of a system are arranged into several categories for convenience. The grouping is in a sequential order of calculation; i.e., the equations presented in a particular group use the known parameters mentioned in that group plus those that are mentioned (known or calculated) in preceding groups. Various parameters are identified by symbols which are identical or similar to the variables used in the computer program. This helps to easily understand the logical development of the computer programs from a listing of their statements.

Basic-Relationships

Known parameters:

Altitude (ALT), ft
Ambient Temperature (T_A), °R
True Airspeed (V_o), ft/sec
Gas Constant, R = 53.35 (ft-lb)/(lb-°R)

Based on the above, the following equations can be developed

Specific heat[2], $C_p = .2365 + 7.6 \times 10^{-6}\ T_A$ Btu/(lb-°R) (2-1)

Coefficient of viscosity[2]

$$MU = \frac{7.475 \times 10^{-7} T_A^{1.5}}{T_A + 216} \quad \text{lb/(ft-sec)} \qquad (2\text{-}2)$$

Coefficient of Thermal Conductivity[3]

$$K_1 = (.06944\ T_A + 4.722) \times 10^{-7} \quad \text{Btu/(ft-sec-°R)} \qquad (2\text{-}3)$$

2. Eshbach, O.W. and Souders, M.: "Handbook of Engineering Fundamentals". Third Edition, Wiley and Sons, New York, 1974, (P.843, Table 3).
2. ibid, (P.576, Figure 4)
3. Baumeister, T.: "Standard Handbook for Mechanical Engineers". 7th Edition, McGraw-Hill, New York, 1966, (P.4-93, Table 2).

Prandtl number, $P_r = (C_p)(MU)/K_1$ (2-4)

Ambient pressure

$$P_A = 2116.21/\ e^{[ALT/(27710\ -\ .098774\ ALT)]} \quad lb/ft^2 \qquad (2\text{-}5)$$

Density, $RHO = P_A/(R\ T_A)$ lb/ft^3 (2-6)

Reynolds Number per foot, $R_{e_{ft}} = (RHO)\ (V_o)/(MU)$ 1/ft (2-7)

The equations for specific heat, coefficient of viscosity and coefficient of thermal conductivity were developed by a curve fit to the data presented in the cited references.

The ICEOFF computer routine was written to calculate some basic aircraft performance parameters and, by calling an engine performance subroutine, determined extracted bleed air data for the given conditions. Since engine performance subroutines may not always be available and the desired data is otherwise known, the engine subroutine may be bypassed and bleed air data read in directly.

Thrust/Bleed-Air Calculations

Known parameters:

Airplane weight (W), lb

Airplane wing reference area (S_W), ft^2

Profile drag coefficient (C_{D_O})

Induced drag coefficient factor (DCD)

Nacelle highlight diameter (DIA), ft

Based on the above, the following equations can be written:

$$\text{Lift coefficient, } C_L = W/[\frac{RHO}{2G}\ V_o^2\ S_W] \qquad (2\text{-}8)$$

$$\text{Drag coefficient, } C_D = C_{D_o} + (DCD)\ C_L{}^2 \qquad (2\text{-}9)$$

$$\text{Drag, } D = C_D\ \frac{RHO}{2G}\ V_o^2\ S_W \quad \text{lbs} \qquad (2\text{-}10)$$

Thrust per engine, $F_N = D/2$ lbs (for 2 engines) (2-11)

Knowing F_N, ALT, V_o and T_A, the bleed-air temperature (T_B) and mass flow rate (W_B) can be determined from engine performance data.

Impingement Calculations

The inertia parameter, K_2, the Droplet Reynolds Number, R_{e_D}, and the water collection efficiency, E_M, are required to completely determine the rate of water catch and the region of impingement on a given airfoil shape.

Known parameters:

- Chord (nacelle length) (C), ft
- Thickness (t), ft
- Heated surface area per foot of circumference (S_H), ft^2/ft
- Droplet diameter (D_D), ft
- Liquid water content (LWC), g/m^3
- Acceleration due to gravity, $G = 32.174$ ft/sec^2
- Surface Pressure coefficient (P_c)

Figure 2-1 illustrates this geometry definition. Based on the above, the following relationships can be written:

Droplet Reynolds number, $R_{e_D} = (R_{e_{ft}})D_D$ (2-12)

Droplet range ratio (LOLS): droplet range is the distance the drop of water would travel before impingement if projected into still air with a given velocity

$$LOLS = \frac{\text{Droplet range projected into still air}}{\text{Droplet range projected into still air per Stoke's Law}}$$

Physically this is an average value of drag force times R_{e_D} for a drop projected into still air.

$LOLS = .98 - .134 \ln (R_{e_D})$ $\quad R_{e_D} \leq 200$ (2-13)

$LOLS = .74 - .0887 \ln (R_{e_D})$ $\quad R_{e_D} > 200$ (2-14)

These relations for LOLS were obtained by a curve fit of information presented by Bowden[1].

Inertia Parameter, $K_2 = .108 \dfrac{G\,V_0}{C(MU)} \; D_D^2$ (2-15)

1. op. cit.

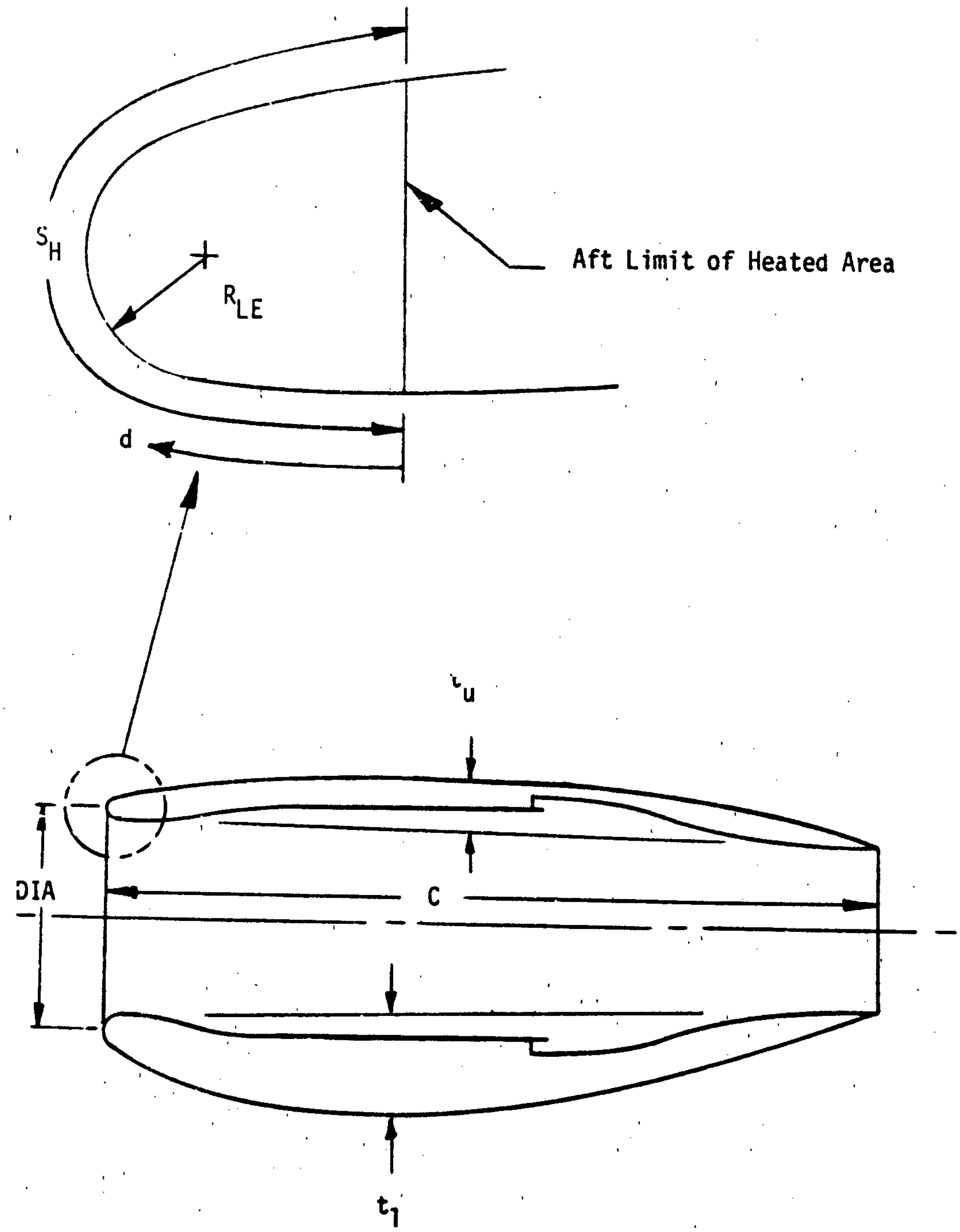

FIGURE 2-1 Nacelle Configuration Definition

K_2 is obtained by a curve fit of information presented by Bowden[1].

Impingement parameter, $K_0 = K_2$ (LOLS) (2-16)

K_0 is a parameter introduced by Langmuir and Blodgett[4] so that the collection efficiency, E_M, versus the inertia parameter curves for various droplet Reynold's numbers may be collapsed into a single curve for bodies of the same geometrical shape. Collection efficiency is given by:

$$E_M = 0 \qquad K_0 < .004 \qquad (2\text{-}17)$$

$$E_M = .0873\ [5.522 + \ln K_0] \qquad .004 \le K_0 < .01 \qquad (2\text{-}18)$$

$$E_M = .08 + .31\ [2 + .4342 \ln K_0] \qquad .01 \le K_0 < .4 \qquad (2\text{-}19)$$

E_M is the ratio of the amount of water intercepted by the airfoil to the amount of water contained in the volume of cloud swept out by the airfoil. The expressions shown for E_M are obtained by a curve fit of information presented by Bowden[1].

Water catch,

$$W_M = .623\ V_0\ (LWC)\ \frac{t}{C}\ C\ E_M\ 10^{-4} \qquad \text{lb/sec-ft} \qquad (2\text{-}20)$$

Water collection rate (average),

$$M_{W_{AV}} = W_M/S_H \qquad \text{lb/(sec-ft}^2) \qquad (2\text{-}21)$$

Water collection rate at leading edge,

$$M_{W_{LE}} = 2\ M_{W_{AV}} \qquad \text{lb/(sec-ft}^2) \qquad (2\text{-}22)$$

---

1. op. cit.

4. Lagmuir, I. and Blodgett, K.: "A Mathematical Investigation of Water Droplet Trajectories". AAFTR 5418, Feb. 19, 1946

1. op. cit. (Figure 2-9)

Water collection rate at any point due to impingement,

$$M_{W_{IMP}} = M_{W_{LE}} \; [1-.385(3S')^{1.75}] \qquad 0 < S' \le 1/3 \quad lb/(sec\text{-}ft^2) \quad (2\text{-}23)$$

$$M_{W_{IMP}} = 1.177 \; M_{W_{LE}} [(1-S')^{1.6}] \qquad 1/3 < S' < 1 \quad lb/(sec\text{-}ft^2) \quad (2\text{-}24)$$

Where S = distance (ft) along surface from stagnation point to the point under consideration, $S' = S/S_L$ and $S_L = S_H/2$ (S_L = Distance along surface from stagnation point to limit of impingement, ft). These expressions for $M_{W_{IMP}}$ were obtained by a curve fit of data presented by Neel[5].

Heat Transfer Calculations

Heat transfer calculations are based on the fact that at any point on the surface, the skin temperature attains a steady value which allows equilibrium between internal and external heat flows. The formulation of the problem is based essentially on the development presented by Gray[6] and Gelder[7]. The equations are quite lengthy and a number of simplifying assumptions and considerable manipulation reduce them to a manageable level as described in the following material.

Heat transfer in forced convection from a surface subjected to water impingement is represented by the total heat transferred by convection, evaporation, and the sensible heat change of the impinging water. An accounting is made for heat generated by friction and the kinetic energy of the water droplets. The expression for heat output can be written in several ways depending on how the various terms are grouped. Following the development of Gelder[7]:

---

5. Neel. C.G.: "A Procedure for the Design of Air-Heated Ice Prevention". NACA TN 3130, 1954. (Figure 16a)
6. Gray, V.H.: "Simple Graphical Solution on Heat-Transfer and Evaporation from Surface Heated to prevent Icing". NACA TN 2799, 1952.
7. Gelder, F.P., et. al.: "Icing Protection for a Turbojet Transport Airplane: Heating Requirements, Methods of Protection, and Performance Penalties". NACA TN 2866, 1953.

$$Q_{OUT} = Q_{CONV} + Q_{EVAP} + Q_{SENS} \tag{2-25}$$

Where:

$$Q_{CONV} = H\, S_H \left\{ T_S - T_A - \frac{V_o^2}{2GJ\, C_p}\left[1 - \left(\frac{V_L}{V_o}\right)^2 (1 - P_r^n)\right]\right.$$

$$\left. + .622\, \frac{LK_w}{C_p} \left(\frac{e_D - e_L}{P_L}\right)\right\} \quad \text{Btu/sec-ft} \tag{2-26}$$

$$Q_{EVAP} = 0.622\, H\, \frac{S_H L K_w}{C_p} \left(\frac{e_S - e_D}{P_L}\right) \quad \text{Btu/sec-ft} \tag{2-27}$$

$$Q_{SENS} = S_H\, M_w\, C_{P_W} \left(T_S - T_A - \frac{V_o^{\,2}}{2\, GJC_{P_W}}\right) \quad \text{Btu/sec-ft} \tag{2-28}$$

Substituting equations (2-26), (2-27) and (2-28) into (2-25) and rearranging gives:

$$Q_{OUT} = S_H\, H \left\{ \left(T_S - T_A\right) \left(1 + M_w\, C_{P_W}/H\right)\right.$$

$$- \frac{V_o^{\,2}}{2GJ\, C_p} \left[1 - \left(\frac{V_L}{V_o}\right)^2 \left(1 - P_r^n\right) + \frac{M_w\, C_p}{H}\right]$$

$$\left. + \frac{0.622\, L\, K_w}{C_p}\left[\frac{e_S}{P_L} - \frac{e_L}{P_L}\right]\right\} \quad \text{Btu/sec-ft} \tag{2-29}$$

In order to eliminate the lengthy calculation involved in the solution of the equation (2-29), the following set of assumptions were made:

a. The flow over the body being almost adiabatic, the local stream vapor pressure can be represented by[6]:

$$e_L = e_A \, P_L/P_A \qquad \text{lb/ft}^2 \qquad (2\text{-}30)$$

b. The local velocity and pressure may be related by the incompressible dry air relation[5]:

$$V_L = \left[V_o^2 - \frac{2G}{RHO_A}\left(P_L - P_A\right)\right]^{.5} \qquad \text{ft/sec} \qquad (2\text{-}31)$$

c. The exponent on the Prandt number is chosen as .5 corresponding to the conservative case of laminar flow rather than 1/3 corresponding to the case of turbulent flow.

d. Radiation is small and is neglected.

e. Conduction along the skin is neglected because the thickness is small and the conduction is small compared to convection.

f. The specific heat of water at constant pressure, C_{P_W} is 1 Btu/(lb -°R)

With the use of the above assumptions, the equations can be combined and reduced to the final form[7]:

$$\begin{aligned} Q_{OUT} = H\,S_H \Big\{ & (T_s - T_A) \quad (1 + M_W/H) \\ & - V_o^{\,2}\left(P_r^{.5} + M_W\,Cp/H\right)/2GJC_p \\ & + 0.622\,\frac{LK_W}{Cp}\left(\frac{e_S}{P_L} - \frac{e_A}{P_A}\right) \\ & + R\,T_A\left(1 - P_r^{.5}\right)\left(1 - P_L/P_A\right)/JC_p \Big\} \quad \text{Btu/sec-ft} \qquad (2\text{-}32) \end{aligned}$$

---

6. op. cit.
7. op. cit.

From (2-32) the following temperature terms can be obtained[6]:

$$T_1 = (T_s - T_A)\ (1 + M_W/H) \qquad {}^oR \qquad (2\text{-}23)$$

$$T_2 = V_o^{\,2}\ (P_r^{.5} + M_W Cp/H)/2GJ\ C_p \qquad {}^oR \qquad (2\text{-}34)$$

$$T_3 = 0.622\ L(e_S/P_L)/C_p \qquad {}^oR \qquad (2\text{-}35)$$

$$T_4 = 0.622\ L(e_A/P_A)/C_p \qquad {}^oR \qquad (2\text{-}36)$$

$$T_5 = RT_A\ (1-P_r^{.5})(1-P_L/P_A)/JC_p \qquad {}^oR \qquad (2\text{-}37)$$

Equation (2-32) can then be written as:

$$Q_{OUT} = H\ S_H \left[T_1 - T_2 + K_W\ (T_3-T_4) + T_5\right] \quad \text{Btu/sec-ft} \qquad (2\text{-}38)$$

The analytical procedure developed by Gray[6] defines the terms T_3 and T_4 as follows:

$$T_3 = 2760\ e_S/P_L \qquad {}^oR \qquad (2\text{-}39)$$

$$T_4 = 2760\ e_A/P_A \qquad {}^oR \qquad (2\text{-}40)$$

Where L and C_p were assumed to be 1066 Btu/lb and 0.24 Btu/(lb-^{o}R) respectively and e_S, e_A are partial pressures of water vapor (corresponding to saturated air unless otherwise noted), at surface and ambient conditions, respectively. Curves of these values, good for a wide range of temperature, were presented by Gray[6]. However for computer use, a curve fit to a psychrometric chart vapor pressure line presented in Eshbach[2] is used for e_S and e_A.

$$e_S,\ e_A = 144\ \exp^{(A + BZ + CZ^2 + DZ^3 + EZ^4)} \quad \text{lb/ft}^2 \qquad (2\text{-}41)$$

Where:

exp is the base of the Napierian logarithm system

$Z = \frac{1000}{T}$, where T is static temperature, ^{o}R

and,

---

6. op. cit.
2. op. cit.

If: $T \le 491.688$ Ice	If; $491.688 < T \le 671.688$ Water	If: $T > 671.688$ Vapor
A = +19.598997	A = +13.435296	A = +16.825544
B = -10.431025	B = -5.0988424	B = -14.213106
C = -0.27550673	C = -1.6896174	C = +7.5567694
D = +0.03904393	D = +0.17829154	D = -4.0151569
E = 0	E = 0	E = +0.71697364

Additional parameters that are required for completing the calculations are latent heat of vaporization, L, evaporation fraction, K, elemental runback rate, DRB, water collection rate, M_w and the change in bleed air temperature along the heated surface.

The latent heat of vaporization for water is represented by:

$$L = 1348.21 - 0.5620\, T_s \qquad 460^\circ R \le T_s \le 660^\circ R \quad \text{Btu/lb} \tag{2-42}$$

This relation was developed by a curve fit to information prepared by the SAE[8].

The evaporation fraction is defined as:

$$K = (T_3 - T_4)\, H/L\, M_w \tag{2-43}$$

The value of K depends on equilibrium conditions and is solved by iteration during the calculation.

The elemental runback rate is:

$$DRB = (1-K)\, M_w \qquad \text{lb/(sec-ft}^2) \tag{2-44}$$

For the succeeding element the water collection rate is:

$$M_w = M_{w_{IMP}} \text{ (at that point)} + DRB \qquad \text{lb/(sec-ft}^2) \tag{2-45}$$

The drop in bleed air temperature is:

$$DT_B = Q_{out}/(W_B\, C_{P_B}) \qquad {}^\circ R \tag{2-46}$$

This leads to the necessity of calculating the heat transfer coefficients.

---

8. "SAE Aerospace Applied Thermodynamics Manual". Second Edition, Society of Automotive Engineers, Inc., New York, Oct. 1969. (P. 165, Fig. 2C-1).

Internal Heat Transfer

Known parameters:

Bleed-air flow rate (W_B), lb/sec-ft

Bleed-air temperature (T_B), °R

Skin temperature (T_S), °R

Local channel efficiency (EFF)

Based on the above the following equations can be written:

Specific heat of bleed-air[2],

$$C_{P_B} = .2365 + 7.6 \times 10^{-6} T_B \quad \text{Btu/(lb-°R)} \qquad (2\text{-}47)$$

Heat input, $Q_{IN} = W_B(C_{P_B})(T_B - T_S)$ Btu/sec-ft (2-48)

External Heat Transfer

Known parameters:

Leading-edge radius (R_{LE}), ft

Local pressure coefficient (P_c)

Mechanical equivalent of heat, J = 778 ft-lb/Btu

The following relationships can now be developed:

Reynolds number in the leading-edge region,

$$Re_{LE} = Re_{ft} R_{LE} \qquad (2\text{-}49)$$

Local velocity, $V_L = V_o\,(1-P_c)^{.5}$ (2-50)

Reynolds number at any point, $Re_S = Re_{ft}\, S\, V_L/V_o$ (2-51)

The dry air convective heat transfer coefficient is determined by the method of Gelder[7]. In the region of the stagnation point, an empirical equation for a cylinder is used:

$$H = \left[0.57 K_1 P_r^{.4}\ Re_{LE}^{.5}/R_{LE}\right]\left[1 - (\theta/90)^3\right] \quad \text{Btu/(sec-ft}^2\text{-°R)} \qquad (2\text{-}52)$$

2. op. cit.

7. op. cit.

where Θ is the angle in degrees from the stagnation point to the point of interest. This equation is used up to $\Theta = 25$ degrees. Beyond $\Theta = 25$ degrees, a flat plate laminar flow equation is used:

$$H = 0.332\ K_1\ P_r^{1/3}\ P_r^{1/3}\ R_{e_S}^{.5}/S \qquad \text{Btu/(sec-ft}^2\text{-°R)} \quad (2\text{-}53)$$

where S is the distance along the surface from the stagnation point to the point of interest. This equation is used up to a Reynolds number of 2×10^5. From $R_{e_S} = 2 \times 10^5$ up to the point where $R_{e_S} = 1.2 \times 10^6$ is treated as a transition region and for R_{e_S} greater than 1.2×10^6 is considered fully turbulent flow. For a flat plate in turbulent flow:

$$H = 0.0296\ K_1\ P_r^{1/3}\ R_{e_S}^{.8}/S \qquad \text{Btu/(sec-ft}^2\text{-°R)} \quad (2\text{-}54)$$

For the transition region a linear variation of the heat transfer coefficient with Reynolds number between laminar flow and turbulent flow is used. If the computed Reynolds number indicates a transition flow region, the following procedure is used.

1. Determine the position on the surface, S_{TRAN}, where $R_{e_S} = 2 \times 10^5$ and a compute a laminar flow heat transfer coefficient for conditions at that point using equation (2-53), H_{LAM}
2. Determine the position on the surface, S_{TURB} where $R_{e_S} = 1.2 \times 10^6$ and compute a turbulent flow heat transfer coefficient for conditions at that point using equation (2-54), H_{TURB}
3. Calculate the heat transfer coefficient for the point of interest from:

$$H = H_{LAM} + \frac{H_{TURB} - H_{LAM}}{1 \times 10^6}\left(R_{e_S} - 2 \times 10^5\right) \qquad \text{Btu/(sec-ft}^2\text{-°R)} \quad (2\text{-}55)$$

The local static pressure is determined from the incompressible relation.

$$P_L = P_A + \frac{RHO}{2G} V_o^2 P_c \qquad \text{lb/ft}^2 \qquad (2\text{-}56)$$

Channel Efficiency

Dry air test data is used in determining an effective anti-icing efficiency. This is a measure of the effectiveness of the hot bleed air in heating the external surface. For dry air, M_w and K_w are zero and (2-38) reduces to:

$$Q_{out} = H\ S_H\ (T_1 - T_2 + T_5) \qquad \text{Btu/sec-ft} \qquad (2\text{-}57)$$

and

$$T_1 = T_S - T_A \qquad {}^0R \qquad (2\text{-}58)$$

$$T_2 = V_o^2\ P_r^{.5}/2GJ\ C_p \qquad {}^0R \qquad (2\text{-}59)$$

T_5 is the same as given in (2-37).

The heat supplied, Q_{IN}, can be computed from (2-48) and the channel efficiency is then given by:

$$Eff = Q_{out}/Q_{in} \qquad (2\text{-}60)$$

2.2 COMPUTER PROGRAMS

The Channel Efficiency Computer program, CHANEFF, is described in Appendix A. A flow chart, a program listing, an example of the input format and an example of the output are presented. In a similar fashion the icing analysis computer program, ICEOFF, is described in Appendix B.

Included in Appendix A is a listing of a function subprogram, TRP, that is called by both CHANEFF and ICEOFF to interpolate the input data arrays for values of pressure coefficient, surface temperature and channel efficiency intermediate to those supplied. Included in Appendix B, is a listing of a function subprogram, PP, that is used to compute the partial pressure of water vapor at saturation temperature.

3.0 ICING WIND TUNNEL TESTS

Icing wind tunnel tests were conducted to provide experimental data that would assist in the development of evaluation procedures for engine inlet anti-icing systems. The scope of testing was selected to cover a wide spectrum of environmental conditions that were practicable in the wind tunnel described in the following section.

3.1 Wind Tunnel Facility

Through sponsorship by the Federal Aviation Administration, approval was obtained for use of the NASA Lewis Research Center Icing Research Tunnel (IRT) located at Cleveland, Ohio. This facility is a closed return tunnel having a 6 x 9 foot (1.83 M x 2.74 M) test section. Performance capabilities are outlined in the following table:

- Airspeed: 260 KTAS (483 KM/Hr) maximum without model installed
- Air Temperature: -22°F(-30°C) to 32°F (0°C)
- Liquid Water Content: Approximately 0.5 to 2.0 g/m^3
- Median Droplet Size: 11 to 20 μm

Airspeed capability with the TFE731 nacelle installed was approximately 240 KTAS.

Air temperature in the tunnel was measured by three (3) total temperature thermocouples calibrated by NASA-Lewis personnel and located at the upstream corner from the test section. These were located on cross-bars attached to the turning vanes and sensed air temperature at the top, center, and bottom in the tunnel cross section. Tunnel temperatures were monitored by both the tunnel and the refrigeration plant operators and adjusted to match as closely as possible.

Test section static (ambient) temperature was obtained by subtracting from the measured total temperature the stagnation temperature increment as follows:

$$t_A = t_T - \frac{V^2}{2G\, C_p\, J} \qquad (3\text{-}1)$$

Where: V = true airspeed, ft/sec

G = acceleration of gravity, 32.174 ft/sec^2

C_p = mean specific heat of air, 0.24 Btu/(lb - ^oR)

J = meachanical equivalent of heat in engineering units, 778.2 ft-lbs/Btu

Liquid water content (LWC) capabilities of the tunnel are limited to some extent by an interdependence on airspeed and median droplet size because higher LWC is achievable only at the lower airspeeds. Median droplet size, in an approximately Langmuir "D" size distribution, is somewhat dependent on LWC and airspeed in that larger median droplet sizes cannot be obtained at a combination of high LWC and high airspeed.

A desired combination of LWC and median droplet size is obtained by setting tunnel controls for the spray system air and water pressures. To determine these pressures the following method was provided by NASA:

Given: LWC, D_{DM}, V (e.g., V_1 or V_2)

Obtain:

$$W_w = 11.667\ LWC(V_1) \tag{3-2}$$

$$P_{H_2O}-P_{air} = \frac{1}{38.7}\left(\frac{W_w}{77}\right)^2 \tag{3-3}$$

$$P_{air} = \frac{1.13[43.9-(4V_2)^{.5}]\ [38.7(P_{H_2O}-P_{air})^{.5}]\left(\frac{T_{air}}{536}\right)^{.5}}{D_{DM} - 0.006(V_2) - 4} - 11.3 \tag{3-4}$$

$$P_{H_2O} = (P_{H_2O} - P_{air}) + P_{air} \tag{3-5}$$

Where: LWC = liquid water content, g/m^3

D_{DM} = median droplet size, μm

V_1 = mph true airspeed

V_2 = knots true airspeed

W_w = water flow rate, lb/hr

P_{H_2O} = water pressure, lb/in^2 gage

P_{air} = air pressure, lb/in^2 gage

T_{air} = $180 + 460 = 640°R$

The tunnel spray system water and air pressures were calibrated by NASA-Lewis personnel.

3.2 Model and Instrumentation

The wind tunnel model employed for icing tests was adapted from a full-scale nacelle for the Garret-AiResearch Corporation TFE731-2 turbofan engine. Modification to the nacelle included incorporation of a roll-formed and welded steel duct with flanges for mounting of fore and aft nacelle bodies and the wrap cowls. A strut assembly was fabricated from square steel tubes which was then welded to the duct and to mounting plates for installation on the wind tunnel turntable. The nacelle was mounted on its side in the tunnel, as shown in Figure 3-1, to facilitate angle-of-attack changes by rotation of the turntable.

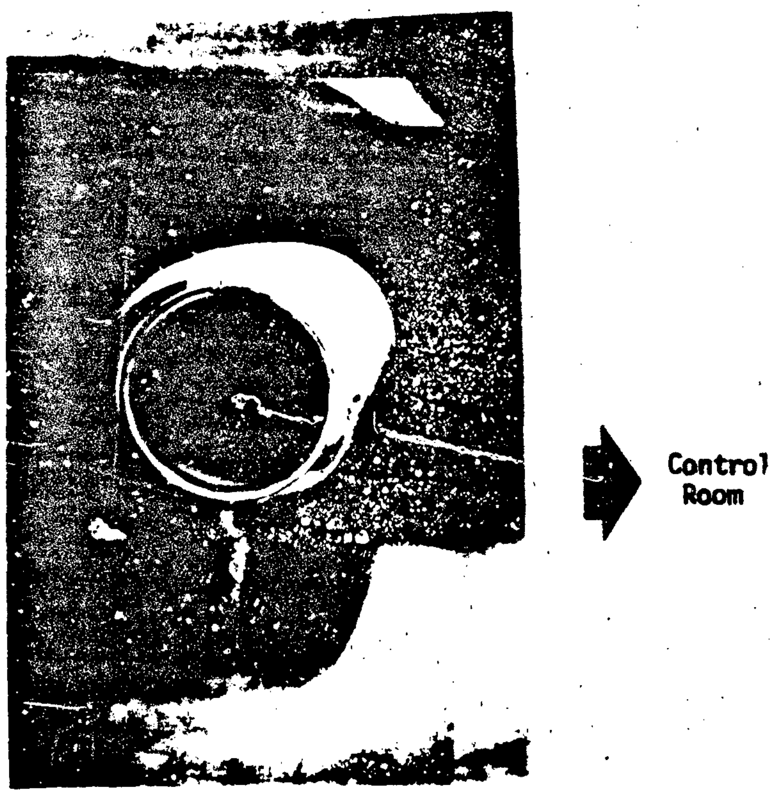

Figure 3-1 Test Nacelle Installation

An aluminum plug was attached to the nacelle exit for certain tests to provide a variation of air mass flow through the nacelle and consequently a shift of the stagnation point on the inlet lip. The plug was adjustable in fore and aft position through use of threaded attachment rods. The forward cone of the plug was electrically heated to prevent icing.

Instrumentation was provided on the nacelle inlet lip to measure outside surface temperatures and static pressures along three chordwise positions* located at radials of 6, 9, and 12 o'clock. Figure 3-2 illustrates typical instrument positions on the lip. These positions are relative to nacelle orientation as installed on the aircraft. In the wind tunnel, with the nacelle mounted on its side, the 12 o'clock position faced towards the control room and the 9 o'clock position was on the top. At each radial position thermocouples and pressure taps were separated circumferentially by approximately two (2) inches. Pressure tubing and thermocouple wires were routed inside the lip chamber in order to present a smooth exterior lip surface.

Hot air mass flow provided to the inlet lip heat distribution system was supplied by a gas-heated tunnel supply system. Air mass flow was measured with a calibrated orifice located outside and beneath the tunnel test section. From there the hot air was ducted up through the test section turntable, into the forebody of the nacelle, and then into the inlet lip anti-icing system. Temperature and pressure of the hot air entering the anti-icing system were measured with total temperature and pressure probes.

Air temperature was controlled by a NASA provided Brown Recorder/Controller which regulated a natural gas fired air heater. Air pressure was controlled by a NASA provided pneumatic servo valve which adjusted a remote pressure regulator.

---

* The turbofan engine used with this nacelle produced neglible inlet swirl.

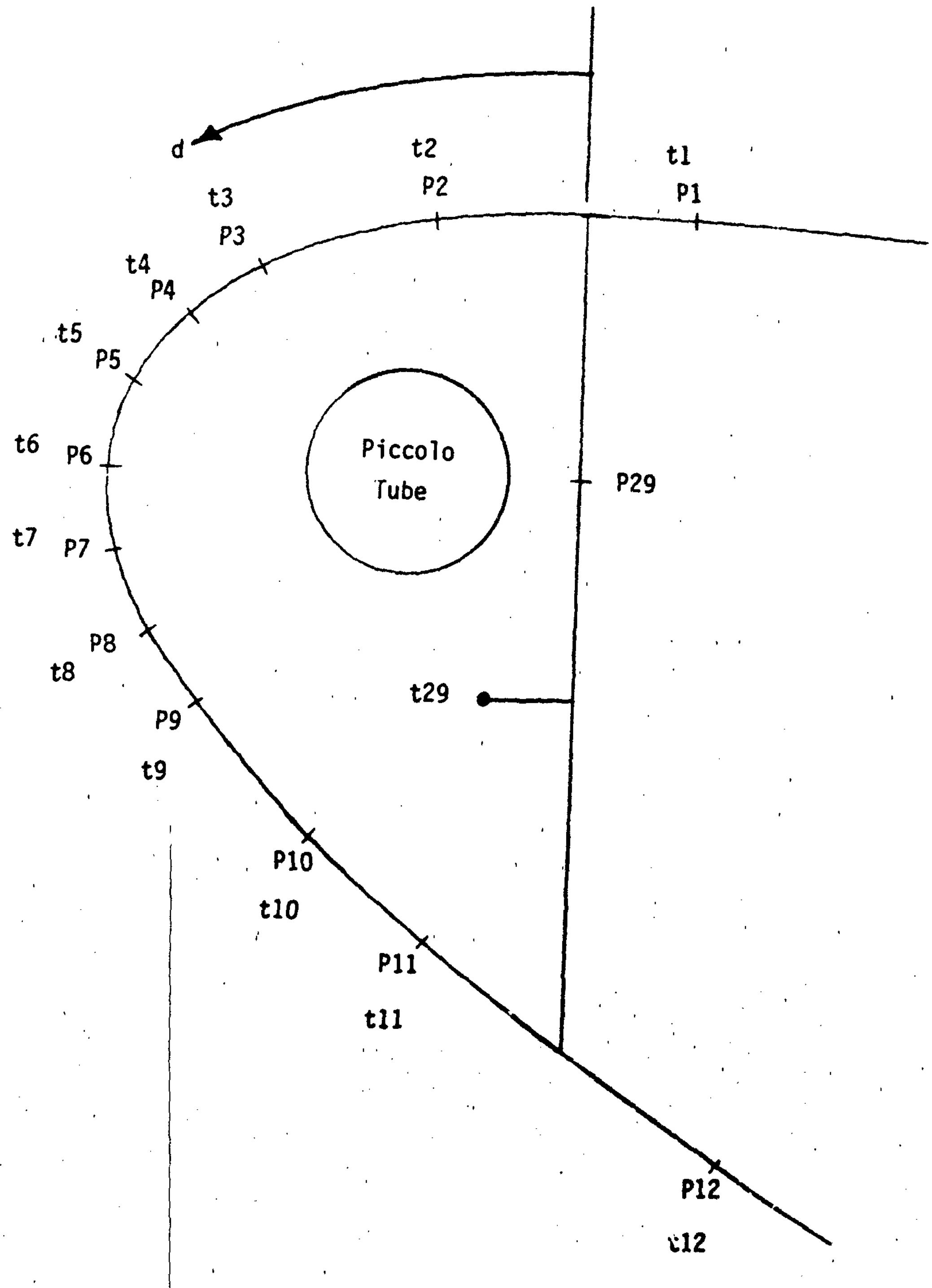

Figure 3-2 Typical Instrumentation Points on Nacelle Inlet Lip - 6 O'clock Position

All pressures and temperatures on the model, tunnel airspeed, and the heated air flow provided to the model were measured and recorded with the following contractor supplied equipment:

a. Pressures were measured using a scanning valve and pressure transducers.

b. Temperatures were measured using iron-constantan thermocouples, a 150°F temperature controlled reference, and amplifier.

c. Electrical outputs from pressure transducers and thermocouples were measured by a Hewlett Packard 3455A digital micro-voltmeter with an accuracy of ±(0.007% of reading +4 digits) in the 0.1 volt range.

d. Test data from the voltmeter were further processed with a Hewlett-Packard 9825A desk-top digital computer to apply instrument calibrations, convert voltmeter outputs to engineering units, calculate tunnel airspeed and hot air mass flow, annotate output, record data on magnetic cassette tape, and print outputs on paper tape.

Calibration of contractor supplied equipment was accomplished prior to the icing tunnel tests. This equipment included all instrumentation employed to measure model temperatures, pressures, tunnel air speed, pressure altitude, and hot air bleed mass flow rate. Tunnel air speed was obtained with an existing pitot-static-probe installed in the test section. Total and static pressures were picked off the tunnel plumbing system for measurement by contractor instrumentation.

3.3 Scope of Tests

The scope of tests conducted, listed in Table 3-1, were performed over a period of six weeks. The conditions shown in Table 3-1 were set as test objectives and were not always what was achieved during this test. Actual test conditions are presented in Appendix C. Installation and check-out of the test model and instrumentation required four days.

TABLE 3-1. ICING WIND TUNNEL TEST SCHEDULE

Dry Air Runs - Configuration A*

NOTE: Conditions shown are test objectives. Corrected test conditions are shown in Appendix C.

Run No.	t_R (°F)	W_B (lb/min)	D_{DM} µm	LWC (g/m^3)	t_T (°F)	V (KIAS)	Spray Time (min.)
1A	350	12	--	--	30	225	--
2A	350	15	--	--	30	225	--
3A	400	12	--	--	30	225	--
4A	400	15	--	--	30	225	--
5A	450	12	--	--	30	225	--
6A	450	15	--	--	30	225	--
7A	350	12	--	--	14	225	--
8A	350	15	--	--	14	225	--
9A	400	12	--	--	14	225	--
10A	400	15	--	--	14	225	--
11A	450	12	--	--	14	225	--
12A	450	15	--	--	14	225	--
13A	350	12	--	--	-4	150	--
14A	350	15	--	--	-4	150	--
15A	400	12	--	--	-4	150	--
16A	400	15	--	--	-4	150	--
17A	450	12	--	--	-4	150	--
18A	450	15	--	--	-4	150	--
19A	350	12	--	--	-15	200	--
20A	350	15	--	--	-15	200	--

* Single skin inlet lip configuration.

Dry Air Runs - Configuration A (Cont):

Run No.	t_B (°F)	W_B (lb/min)	D_{DM} μm	LWC (g/m^3)	t_T (°F)	V (KIAS)	Spray Time (min.)	
21A	400	12	--	--	-15	200	--	
22A	400	15	--	--	-15	200	--	
23A	450	12	--	--	-15	200	--	
24A	450	15	--	--	-15	200	--	
25A-28A (Not used)								
29A**	400	12	--	--	14	225	--	
30A**	400	12	--	--	14	225	--	
31A†	350	12	--	--	14	225	--	$\alpha = -2$
32A†	350	12	--	--	14	225	--	$\alpha = -4$

** Variable stagnation point using nacelle exit plug.

† Variable nacelle angle of attack conditions.

Wet Air Runs - Configuration A

NOTE: Conditions shown are test objectives. Corrected test conditions are shown in Appendix C.

Run No.	t_B (°F)	W_B (lb/min)	D_{DM} μm	LWC (g/m^3)	t_T (°F)	V (KIAS)	Spray Time (min.)
60A	350	12	15	0.78	30	225	4.63
61A	350	15	15	0.78	30	225	4.63
62A	400	12	15	0.78	30	225	4.63
63A	400	15	15	0.78	30	225	4.63
64A	450	12	15	0.78	30	225	4.63
65A	450	15	15	0.78	30	225	4.63
66A	350	12	15	0.6	14	225	4.63
67A	350	15	15	0.6	14	225	4.63
68A	400	12	15	0.6	14	225	4.63
69A	400	15	15	0.6	14	225	4.63
70A	450	12	15	0.6	14	225	4.63
71A	450	15	15	0.6	14	225	4.63
72A	350	12	20	1.72	-4	150	2.0
73A	350	15	20	1.72	-4	150	2.0
74A	400	12	20	1.72	-4	150	2.0
75A	400	15	20	1.72	-4	150	2.0
76A	450	12	20	1.72	-4	150	2.0
77A	450	15	20	1.72	-4	150	2.0
78A	350	12	20	1.28	-15	200	2.0
79A	350	15	20	1.28	-15	200	2.0
80A	400	12	20	1.28	-15	200	2.0
81A	400	15	20	1.28	-15	200	2.0

Wet Air Runs - Configuration A (Cont):

Run No.	t_B (°F)	W_B (lb/min)	D_{DM} μm	LWC (g/m^3)	t_T (°F)	V (KIAS)	Spray Time (min.)
82A	450	12	20	1.28	-15	200	2.0
83A	450	15	20	1.28	-15	200	2.0
84A-94A (not used)							
95A*	400	12	15	0.6	14	225	4.63
96A*	400	12	15	0.6	14	225	4.63
97A**	350	12	15	0.6	14	225	4.63 $\alpha = -2°$
98A**	350	12	15	0.6	14	225	4.63 $\alpha = -4°$

* Variable stagnation point.

** Variable nacelle angle of attack. Note: These two conditions were not run due to lack of time in tunnel schedule.

Dry Air Runs - Configuration B*

NOTE: Conditions shown are test objectives. Corrected test conditions are shown in Appendix C.

Run No.	t_B (°F)	W_B (lb/min)	D_{DM} μm	LWC (g/m³)	t_T (°F)	V (KIAS)
35B	350	12	--	--	30	225
36B	350	15	--	--	30	225
37B	400	12	--	--	30	225
38B	400	15	--	--	30	225
39B	450	12	--	--	30	225
40B	450	15	--	--	30	225
41B	350	12	--	--	14	225
42B	350	15	--	--	14	225
43B	400	12	--	--	14	225
44B	400	15	--	--	14	225
45B	450	12	--	--	14	225
46B	450	15	--	--	14	225
47B-52B (not used)						
53B	350	12	--	--	-15	200
54B	350	15	--	--	-15	200
55B	400	12	--	--	-15	200
56B	400	15	--	--	-15	200
57B	450	12	--	--	-15	200
58B	450	15	--	--	-15	200

* Double skin inlet lip configuration.

Wet Air Runs - Configuration B

NOTE: Conditions shown are test objectives. Corrected test conditions are shown in Appendix C.

Run No.	t_B (°F)	W_B (lb/min)	D_{DM} μm	LWC (g/m^3)	t_T (°F)	V (KIAS)	Spray Time (min.)
100B	350	12	15	0.78	30	225	4.63
101B	350	15	15	0.78	30	225	4.63
102B	400	12	15	0.78	30	225	4.63
103B	400	15	15	0.78	30	225	4.63
104B	450	12	15	0.78	30	225	4.63
105B	450	15	15	0.78	30	225	4.63
106B	350	12	15	0.6	14	225	4.63
107B	350	15	15	0.6	14	225	4.63
108B	400	12	15	0.6	14	225	4.63
109B	400	15	15	0.6	14	225	4.63
110B	450	12	15	0.6	14	225	4.63
111B	450	15	15	0.6	14	225	4.63
112B	350	12	20	1.28	-15	200	2.0
113B	350	15	20	1.28	-15	200	2.0
114B	400	12	20	1.28	-15	200	2.0
115B	400	15	20	1.28	-15	200	2.0
116B	450	12	20	1.28	-15	200	2.0
117B	450	15	20	1.28	-15	200	2.0

3.4 Icing Wind Tunnel Test Procedures

Dry air testing was conducted prior to icing tests to determine the inlet lip skin temperature and surface static pressure profiles. Various combinations of tunnel airspeed, tunnel temperature, hot air bleed mass-flow rate and temperature, and nacelle angle-of-attack, as indicated in Table 3-1, were run with dry air conditions. Following the dry runs, wet-air tests were conducted for the same conditions except that cloud characteristics were simulated using the tunnel water spray system.

The procedure employed during dry air runs is described as follows:

a. Start tunnel and set at idle speed.
b. Start tunnel cool-down.
c. When tunnel has reached the approximate temperature desired, increase airspeed to test condition and re-adjust tunnel temperature.
d. While (c) is in progress, fire air-bleed gas heater.
e. Adjust air heater temperature and bleed-air pressure to obtain desired mass flow rate and temperature at entrance to nacelle inlet lip anti-icing system.
f. When all conditions are stabilized, conduct instrumentation data scans, convert to engineering units, and record data.
g. Hold tunnel conditions constant and adjust bleed air temperature or mass flow rate to next test point and again stabilize and record data.
h. When all test conditions at a given tunnel airspeed or temperature are complete, adjust to next test point and repeat procedure above.

Following completion of dry runs for a particular test model configuration the procedure is repeated for wet runs, except that the tunnel water/air spray system is used to simulate icing cloud conditions. Dry air test procedures are repeated through item (g) with the following additional steps used during icing test runs:

h. When all conditions are stabilized, including pre-adjustment of spray system water and air pressure, switch spray system on, adjust water flow rate rotameters for uniform spray across tunnel cross section, record data after a predetermined interval, and at completion of spray time switch spray system and hot air bleed flow off.

i. As soon as spray system and bleed air are off, conduct a rapid shut-down of the tunnel fan motor. This procedure freezes the "iced" condition of the model because tunnel temperature has a tendancy to cool-down further by 10-15°F and to hold this condition due to the cold-soaked state of the all metal tunnel.

j. Conduct an inspection of the ice formation on the model, take measurements and samples if desired, and remove ice from the model using a steam hose.

k. Following the above, subsequent runs are conducted repeating the procedure outlined.

Spray duration during a test run was selected corresponding to the approximate time it would take to fly through the cloud size being simulated at the tunnel airspeed. During simulation of maximum continuous cloud characteristics, corresponding to low levels of LWC, tunnel airspeed was run at 225 KIAS (approximately 230-235 KTAS, depending on tunnel temperature).

For intermittent maximum cloud simulation conditions, however, airspeed was limited to either 200 KIAS (approximately 196 KTAS) or 150 KIAS (approximately 142 KTAS) because the tunnel spray system is limited in maximum water flow rate. Run time based on the time of transit through intermittent cloud size at these speeds, however, is insufficient to allow data acquisition so run time was increased to two (2) minutes as was seen in Table 3-1.

Although time in a cloud may have no significance in developing an analytical method there is other rationale for limiting the exposure time. For the nacelle and anti-icing system employed there are design limits to which icing can be prevented at any bleed air temperature and/or mass flow rate when testing in conditions of either maximum continuous or maximum intermittent icing. It was to avoid exceeding these limits that the approach was taken to use FAA defined cloud sizes and tunnel velocity to determine exposure time. In addition, longer exposure time to the icing cloud results in an undesirable amount of ice forming on the unheated nacelle support structure, especially under glaze icing conditions.

4.0 CORRELATION OF RESULTS

Dry air wind tunnel test data were used with the computer program CHANEFF to determine effective channel efficiencies for each set of data corresponding to a different nacelle lip pressure coefficient distribution and internal heat distribution system. These are related to changes in nacelle angle of attack, nacelle air flow, circumferential position around the lip and double versus single skin internal distribution systems. Although it would appear that a change of internal bleed air flow or bleed air temperature would result in different channel efficiencies, this is not the case. For a given type of internal distribution system, the surface temperature, which is used in determining the channel efficiency, is directly related to the quantity of heat provided whether by virtue of higher bleed mass flow or bleed air temperature. Thus the calculated efficiency, for the range of bleed flows and temperatures tested, is independent of these two parameters. Hence in order to use a larger data base for improved accuracy of the channel efficiency, the individual test efficiencies for a given physical arrangement are averaged. There will be efficiencies related to the 6, 9 and 12 o'clock measurement positions for each variation in nacelle angle of attack, mass flow and internal distribution system. In total 18 different efficiency distributions were computed, corresponding to three angles of attack, two mass flows and two distribution systems for each of three clockwise measuring stations. Table 4-1 presents a matrix of which dry test runs were used to calculate the efficiency and to which wet test runs they apply.

Table 4-1 Efficiency - Run matrix

Runs used for EFF	Runs EFF applies for T_s Calculations: Dry	Wet
10A-24A	1A-24A	60A-83A
29A	29A	95A
30A	30A	96A
31A	31A	-
32A	32A	-
35B-45B 53B-58B	35B-46B 53B-58B	100B-117B

A typical averaged surface pressure coefficient is presented in Figure 4-1. It is noted that the peak pressure coefficient from this test data is greater than 1.0. Since this is physically impossible the Pc curve was faired to 1.0 at the stagnation point as shown. This appeared to be a common occurance with the measured pressure data. This first came to attention during the running of the test and an effort was made to determine the cause of it. No reason for its occurance would be determined. Corresponding measured surface temperature distributions are shown in Figure 4-2 and the resulting averaged channel efficiencies from program CHANEFF are presented in Figure 4-3. Utilizing the pressure data from Figure 4-1 and efficiencies from Figure 4-3 surface temperatures were computed with program ICEOFF. A comparison of calculated and measured surface temperature for these dry air conditions is presented in Figure 4-4. It is seen that the agreement is excellant.

A comparison of surface pressure coefficient at the three nacelle inlet lip measuring stations is shown in Figure 4-5 for both wet and dry air. As would be expected the presence of water has little if any effect on the pressure coefficient. The corresponding channel efficiencies for dry air for the three inlet lip measuring stations is given in Figure 4-6 and the comparison of calculated and measured surface temperature for the three inlet lip measuring stations for both single and double skin bleed air distribution systems is presented in Figure 4-7. It is noted in Figure 4-6 that at the 6 o'clock position, the calculated channel efficiency exceeds 1.0. Although it is physically impossible to exceed 100% efficiency, the mechanics of the calculation process allow this to happen on rare occasions. Detailed checks revealed no mathematical or computational error and the use of this efficiency in program ICEOFF gave an exact reproduction of the measured surface temperature. It is concluded that there must be some of the basic assumptions underlying the method of channel efficiency that allows this to happen. Examination of the equation used to compute EFF reveals how this can occur. From equation (2-48), (2-57), (2-58) and (2-60):

$$EFF = \frac{HS_H \, (T_S - T_A - T_2 + T_5)}{C_{P_B} \, W_B \, (T_B - T_S)} \tag{4-1}$$

It can be shown that, compared to T_S and T_A, T_2 and T_5 are relatively unimportant for the test conditions of this report. Hence it is easily seen that for conditions such that T_B and T_S are quite close in magnitude and T_S and T_A are quite different in magnitude, the result for EFF could exceed 1.0. This is undoubtedly due to some of the simplifications that resulted from early assumptions concerning the flow and heat transfer characteristics. Understanding how it can occur makes it no more desirable but in the final analysis it will reproduce accurate surface temperatures and thus will be tolerated. Examination of Figures 4-4 and 4-7 reveals that the agreement for dry air is excellent but for wet air it is less good. It appears that the method tends to over predict the temperature near the stagnation point and to under predict it near the aft limit of the heated area. Although the amount of difference between calculated and measured T_S varies with various conditions the trend noted above is fairly consistant. This could be caused by a somewhat inaccurate modeling of either the evaporation process or the heat transfer process that resulted from simplifying assumptions.

The balance of the figures in this section present the effects of independent parameters on the pressure coefficient, the resulting efficiency and a comparison of calculated and measured surface temperature. Figures 4-8, 4-9 and 4-10 present this information as influenced by nacelle angle of attack. Only dry air temperatures are presented because time did not allow the testing of the wet air counterparts.

Figures 4-11, 4-12 and 4-13 present pressure coefficient, efficiency and temperature comparison for changes in inlet mass flow. Here again one of the efficiency curves (Run 29A) exhibits a value greater than 1.0. In this case 2.44. Although appearing to be unreasonable at first, the same arguments as set forth before apply and again the calculated dry air surface temperature agrees well with measured values.

Figures 4-14 and 4-15 present channel efficiency and comparison of temperatures for single and double skin anti-icing systems.

The last four figures (4-16, 4-17, 4-18 and 4-19) show only comparative temperatures because they were aerodynamically and geometrically similar to other configurations and used pressure coefficients and efficiencies defined for them. These similarities are distinguished in Table 4-1.

The effects of bleed air temperature are illustrated in Figure 4-16. Here the comparison includes wet and dry air as well as single and double skin systems.

Temperature comparison for changes in bleed air mass flow are shown in Figure 4-17. Included are data for wet and dry air as well as single and double skin systems.

Figure 4-18 gives comparative temperature for a variety of liquid water contents. It should be noted here that it was not possible to hold all other test parameters constant during the test while varying liquid water content alone. Hence a direct comparison for the effects of liquid water content alone cannot be made. Again both single and double skin systems are shown.

The comparison of temperature while changing water droplet diameter is given in Figure 4-19 for both single and double skin systems. As for liquid water content, it was not possible to change droplet diameter alone while holding all other test parameters constant. Thus a direct comparison to determine effects of droplet diameter alone is not possible.

For all of these comparisons, the results are nearly the same: very good agreement for dry air and moderately good agreement for wet air. It is noted that even minute as well as large fluctuations in surface temperature are reproduced for dry air calculations. Although not as accurate as for dry air, the wet air temperature distributions generally give the correct trend and do display the gross variations that exist in the measured data. This leads to the belief that the method is very useful and needs only some refinements as applied to wet air calculations.

A correlation of all calculated and measured data was performed. For the 966 calculated dry air temperatures the mean deviation from measured temperature is 6°F and for the 924 wet air temperatures the mean deviation is 19°F.

During the data analysis, it was noted that the calculated surface temperatures for wet air consistantly gave better correlation with the measured results for the double skin system than for the single skin system. There are at least two reasons why this is so. First the double skin will give a more uniform temperature distribution (i.e. nearly constant) and second, the deviations from this nearly constant value will be smaller. Both of these will work in favor of better accuracy from the calculation method. These are well illustrated by the tabulated data, (Tables C-4, C-5 and C-6) and Figures 4-17 and 4-18.

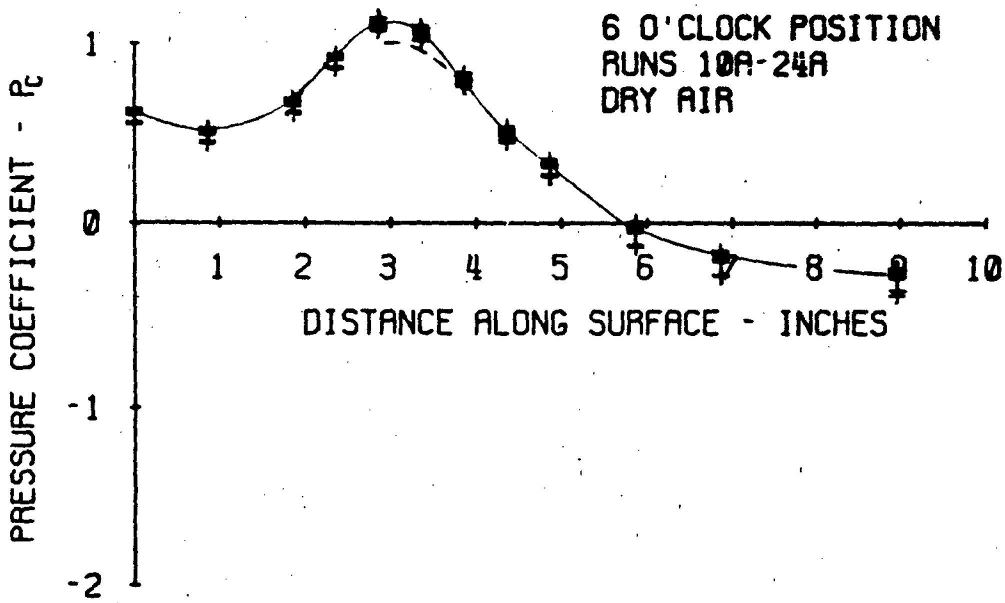

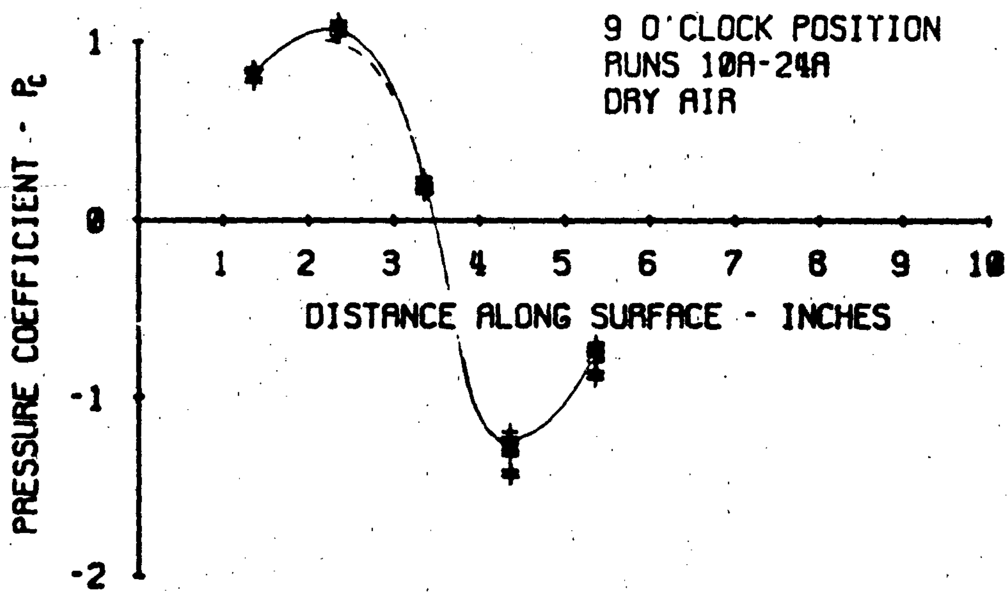

Figure 4-. Averaged Surface Pressure Coefficients

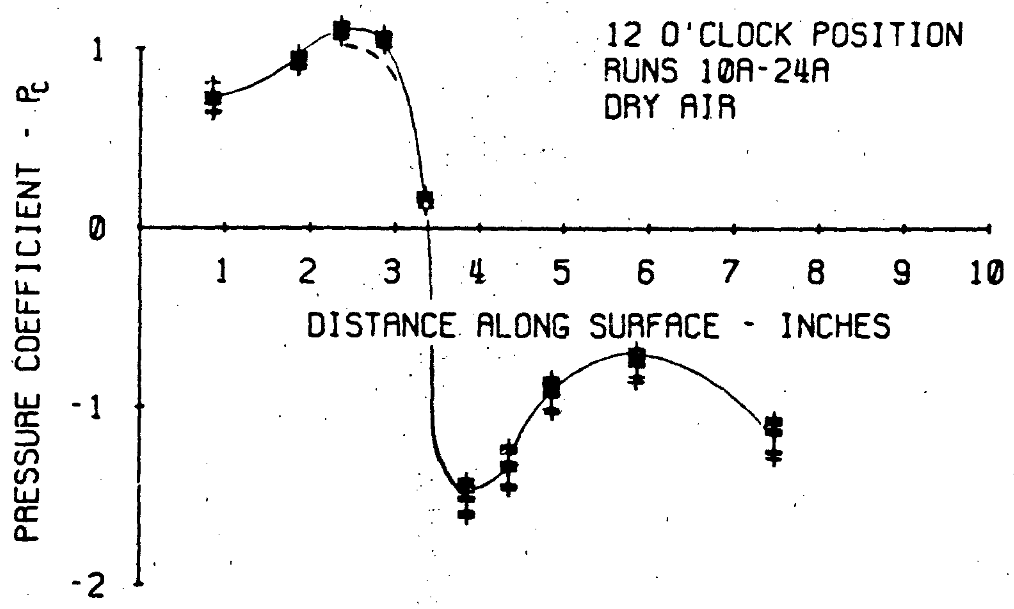

Figure 4-1 (Cont.)

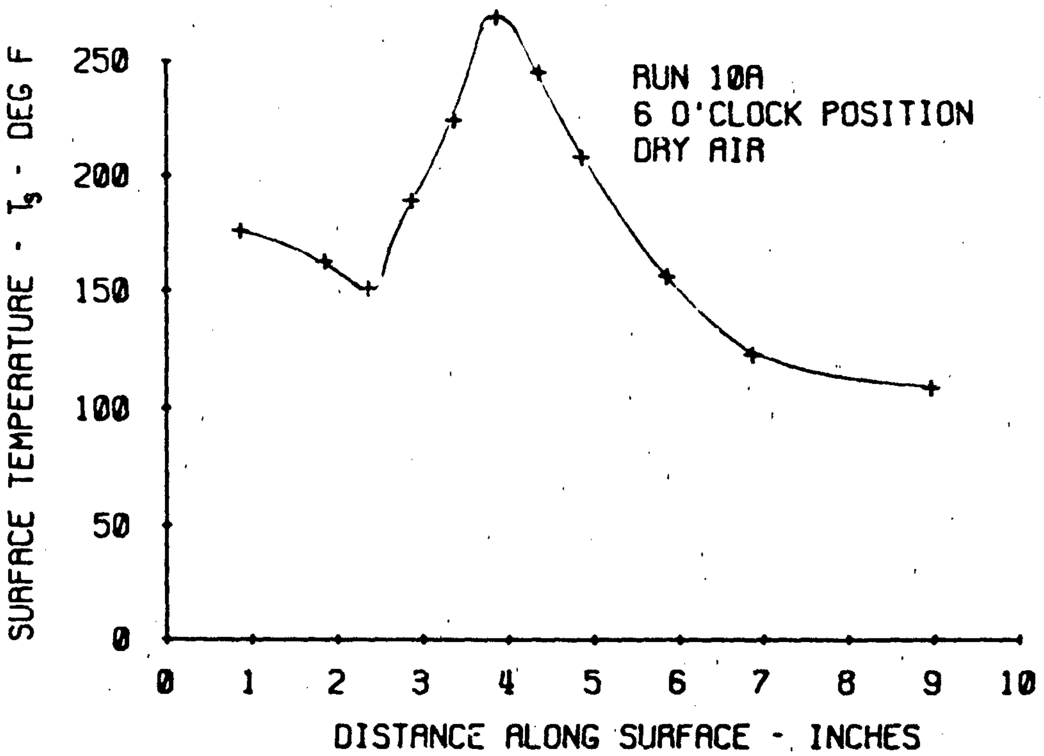

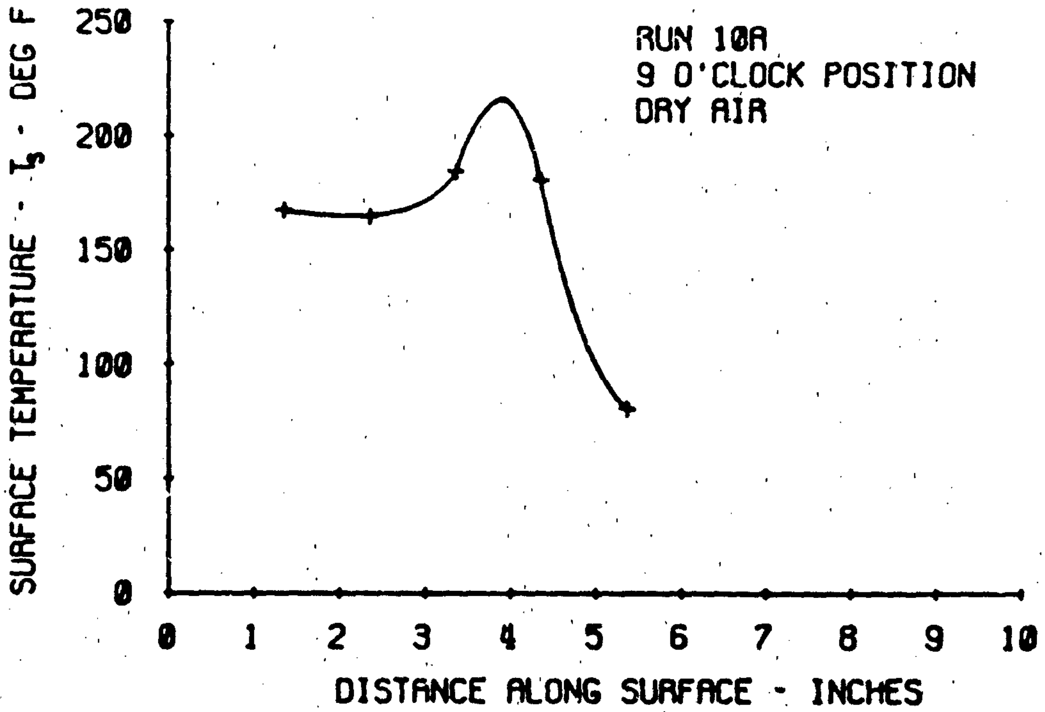

Figure 4-2 Typical Measured Surface Temperature Distribution

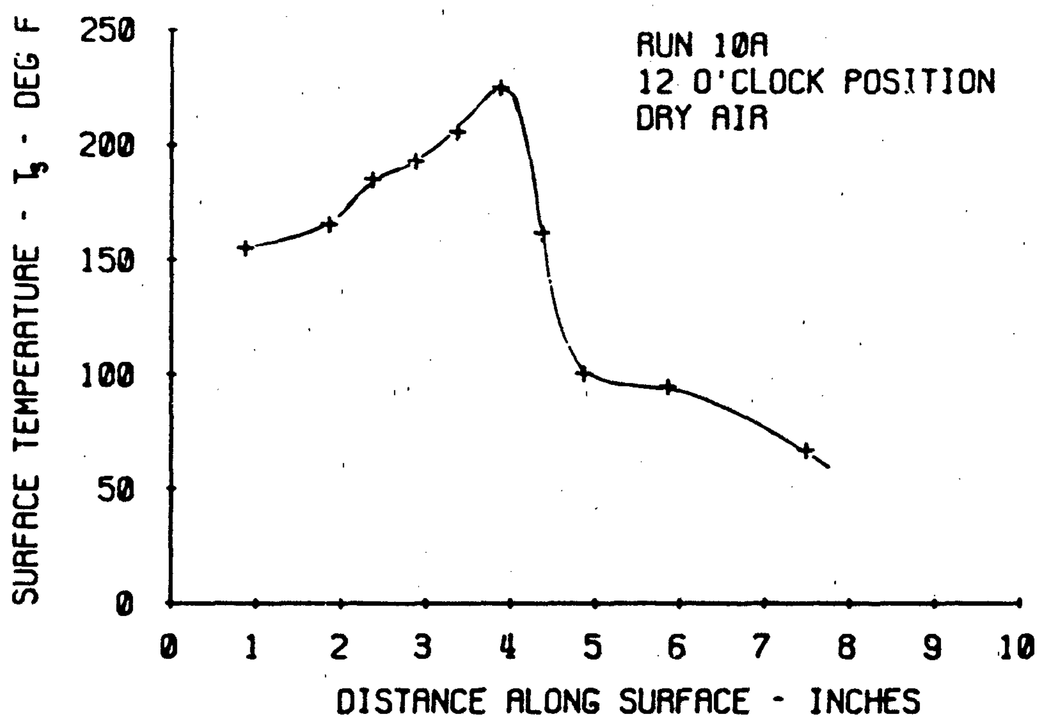

Figure 4-2 (Cont.)

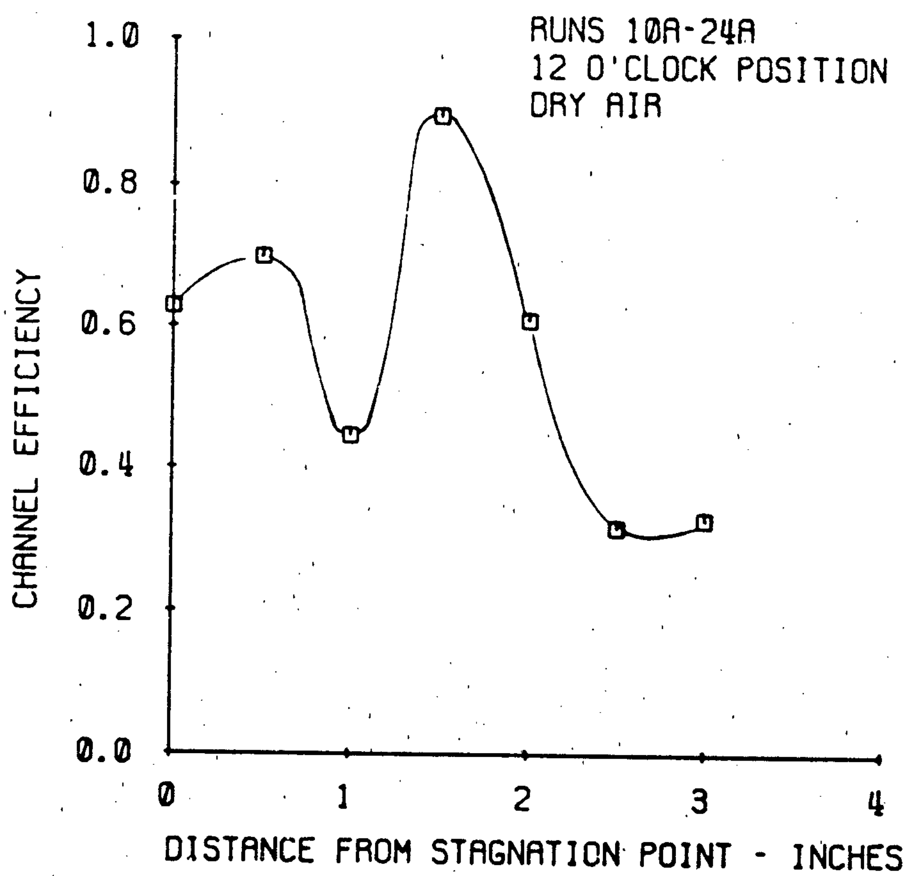

Figure 4-3 Average Channel Efficiency

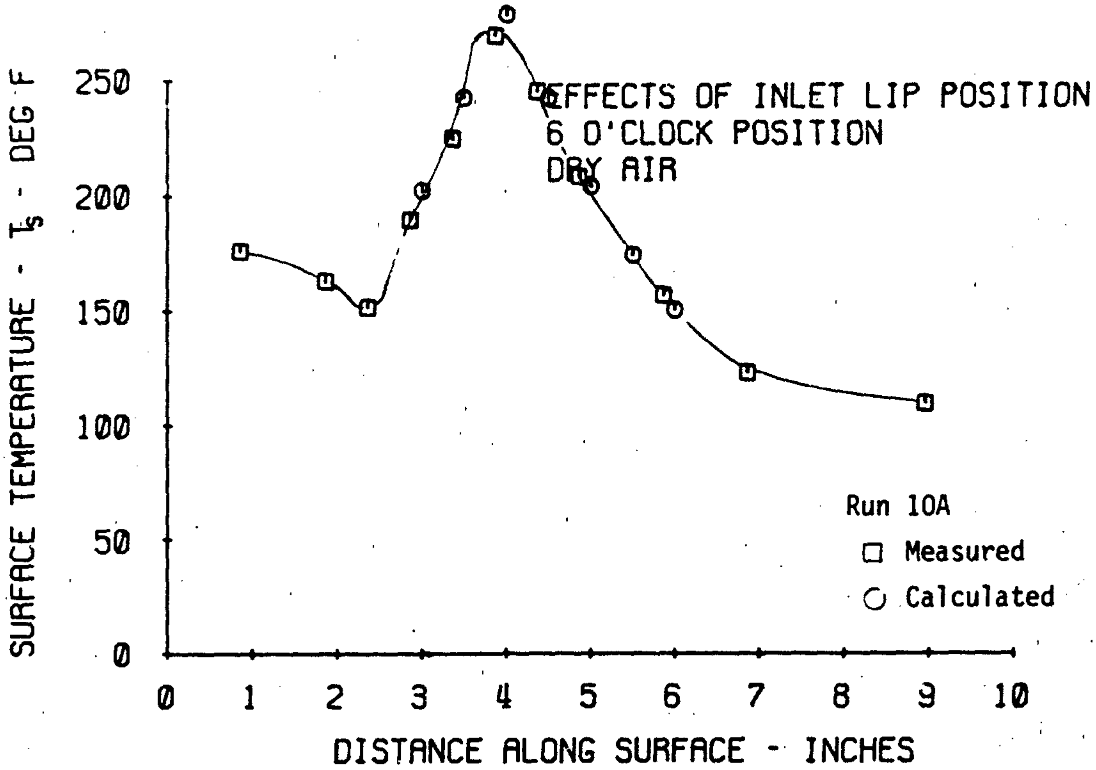

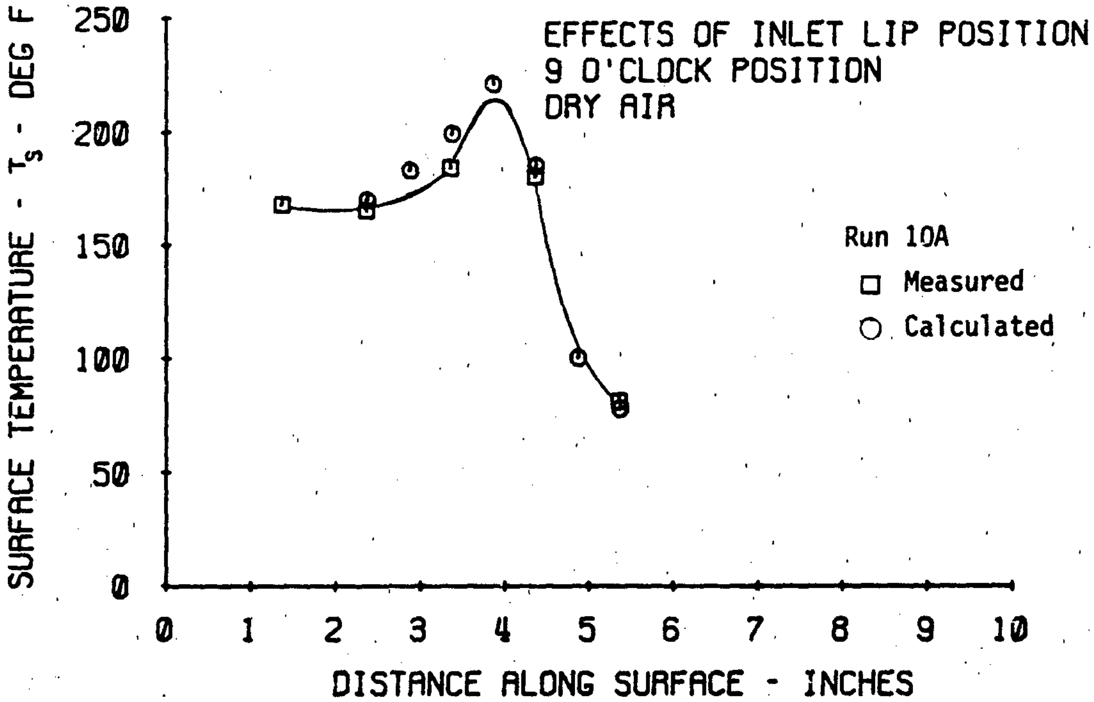

Figure 4-4 Comparison of Calculated and Measured Surface Temperature

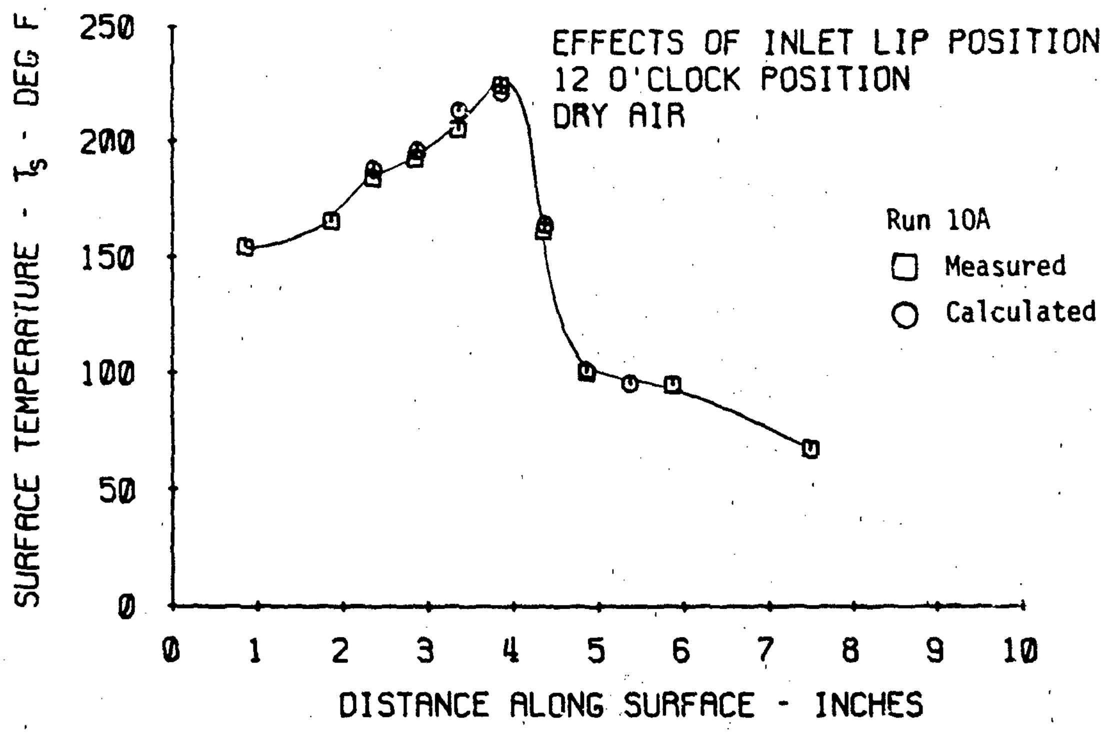

Figure 4-4 (Cont.)

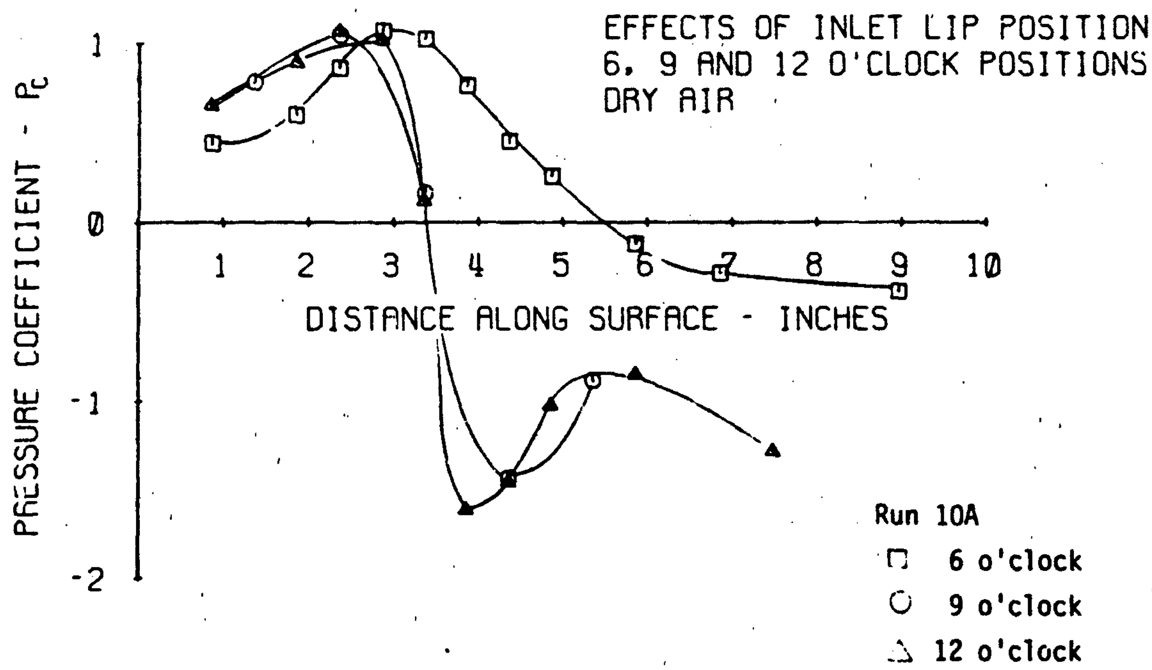

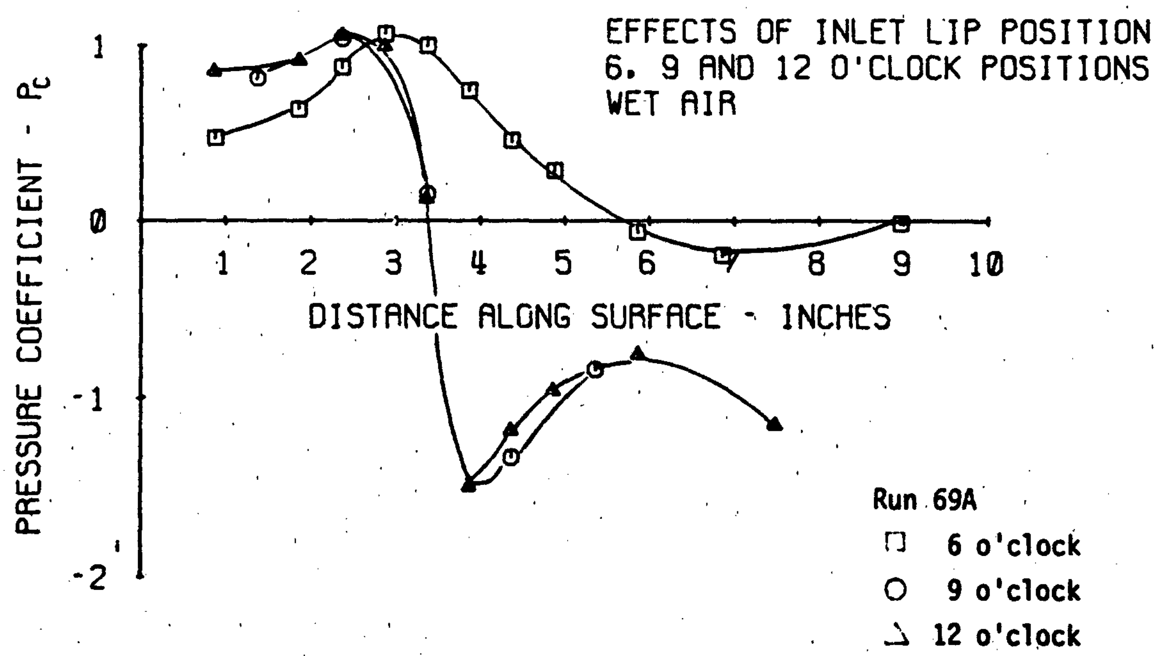

Figure 4-5 Effects of Nacelle Lip Position on Surface Pressure Coefficient

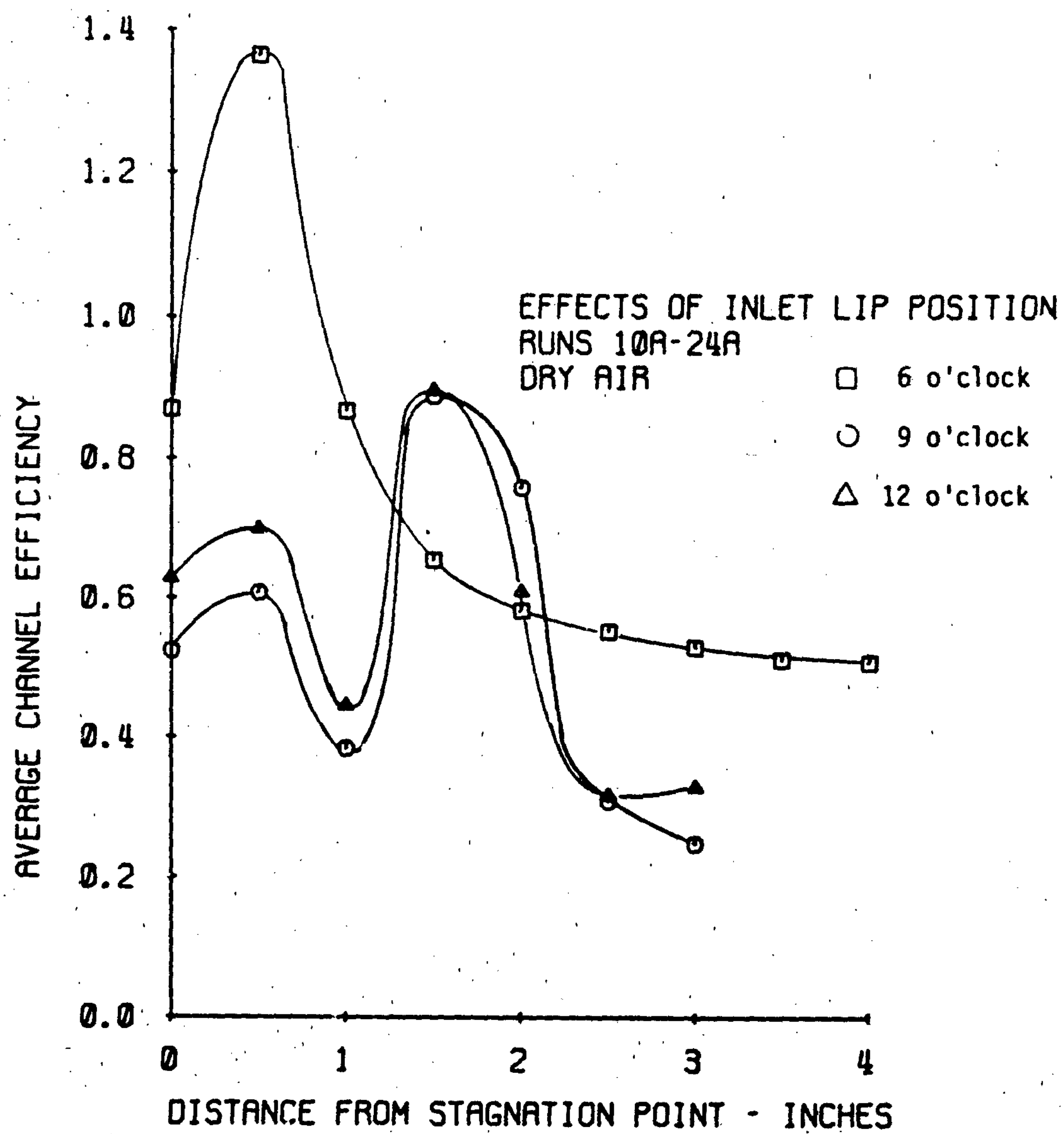

Figure 4-6 Effects of Nacelle Lip Position on Efficiency Distribution

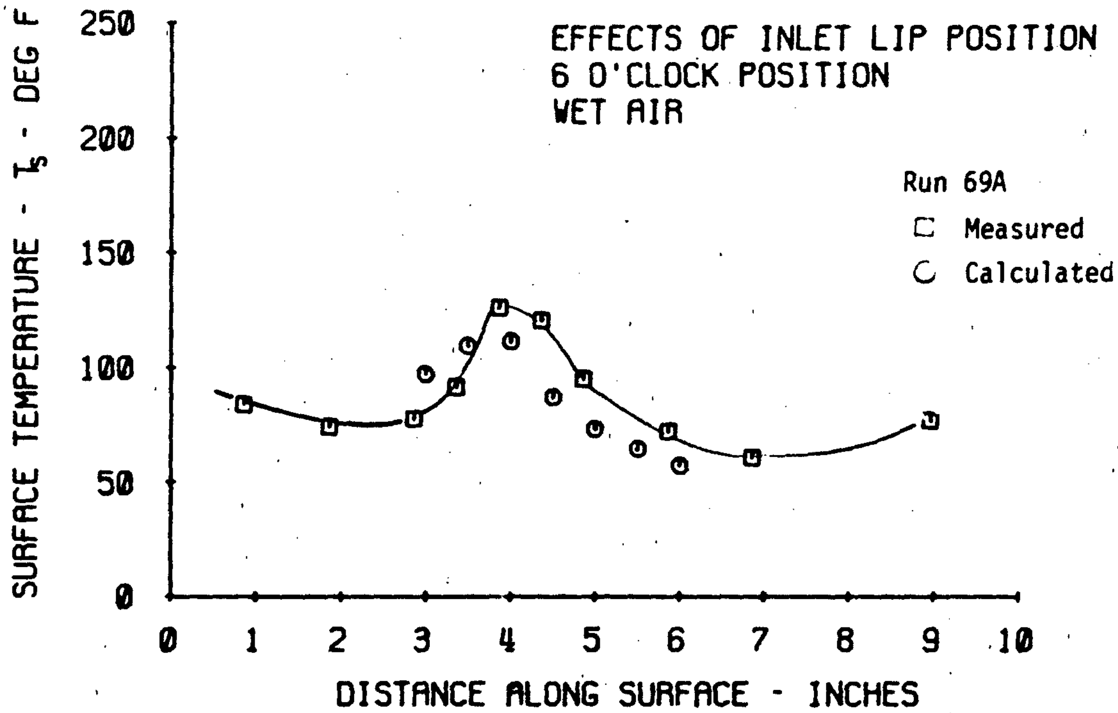

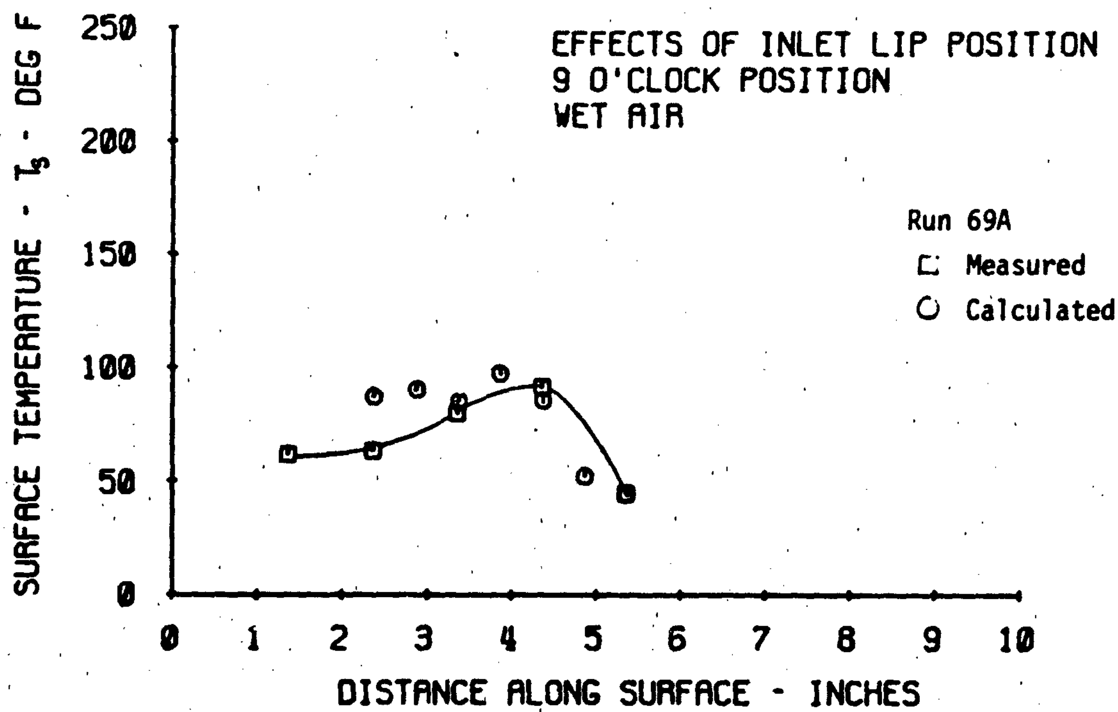

Figure 4-7 Comparison of Calculated and Measured Surface Temperature for Three Nacelle Lip Positions.

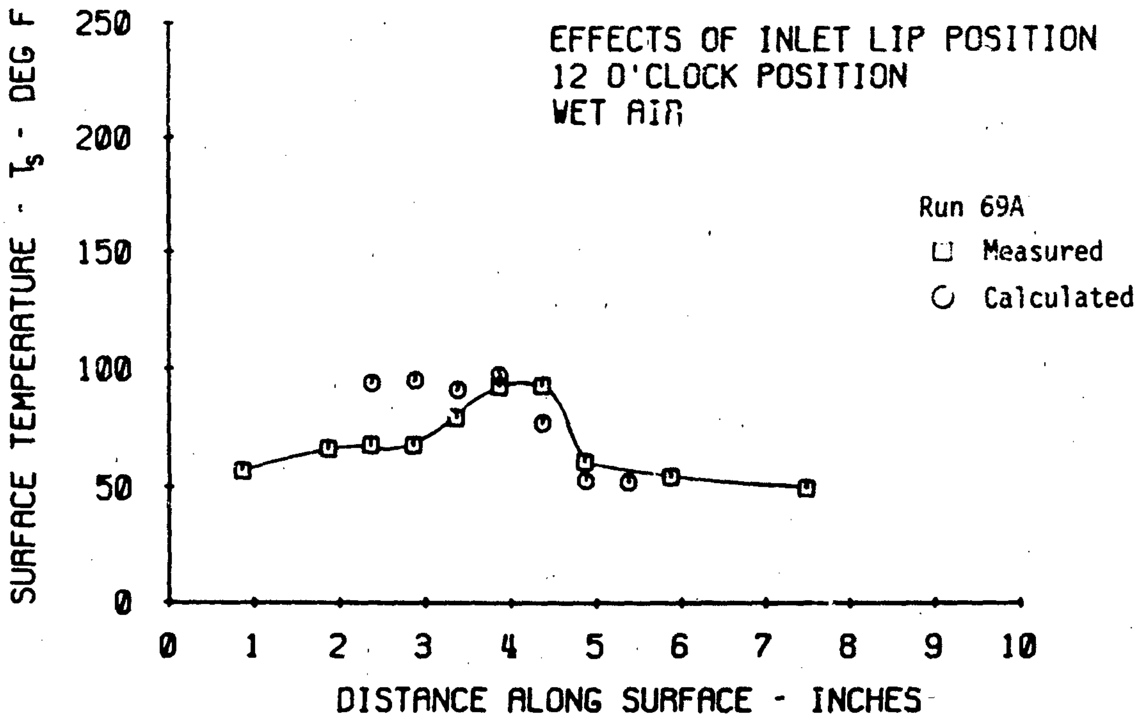

Figure 4-7 (Cont.)

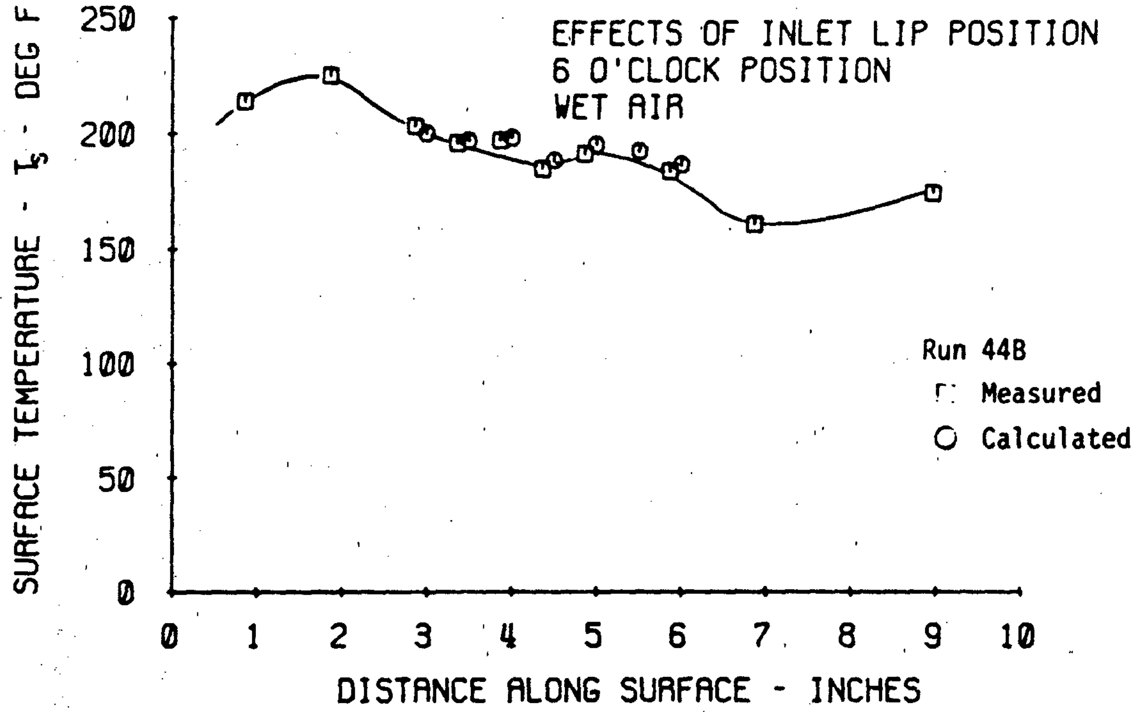

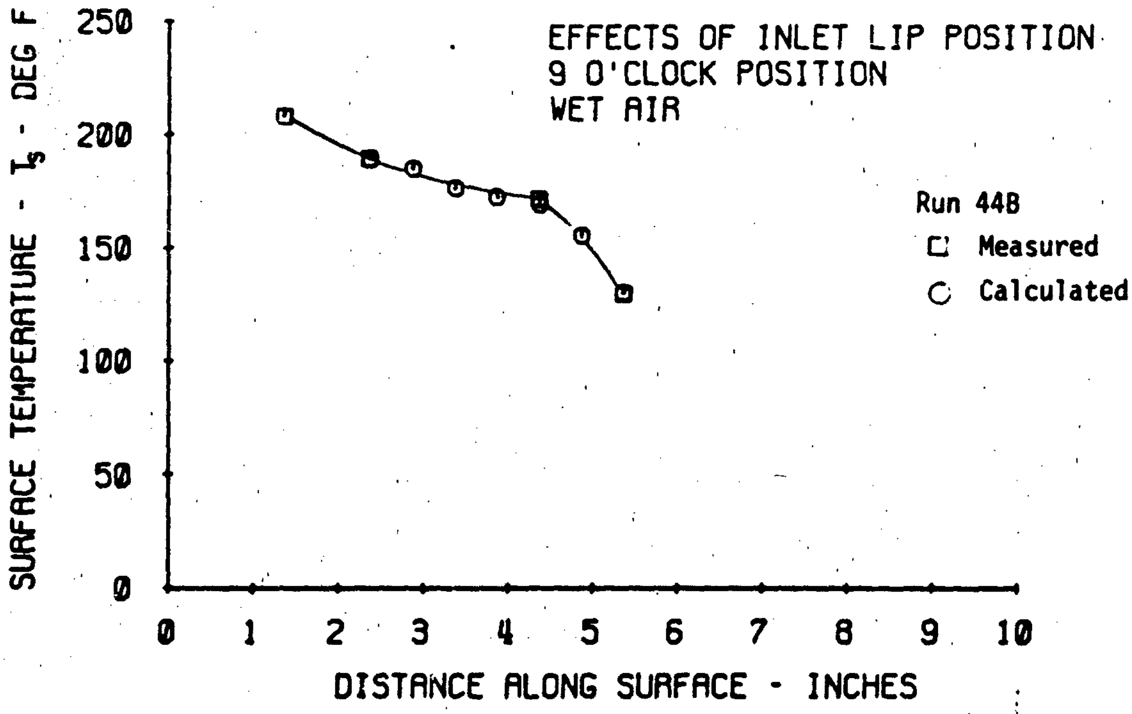

Figure 4-7 (Cont.)

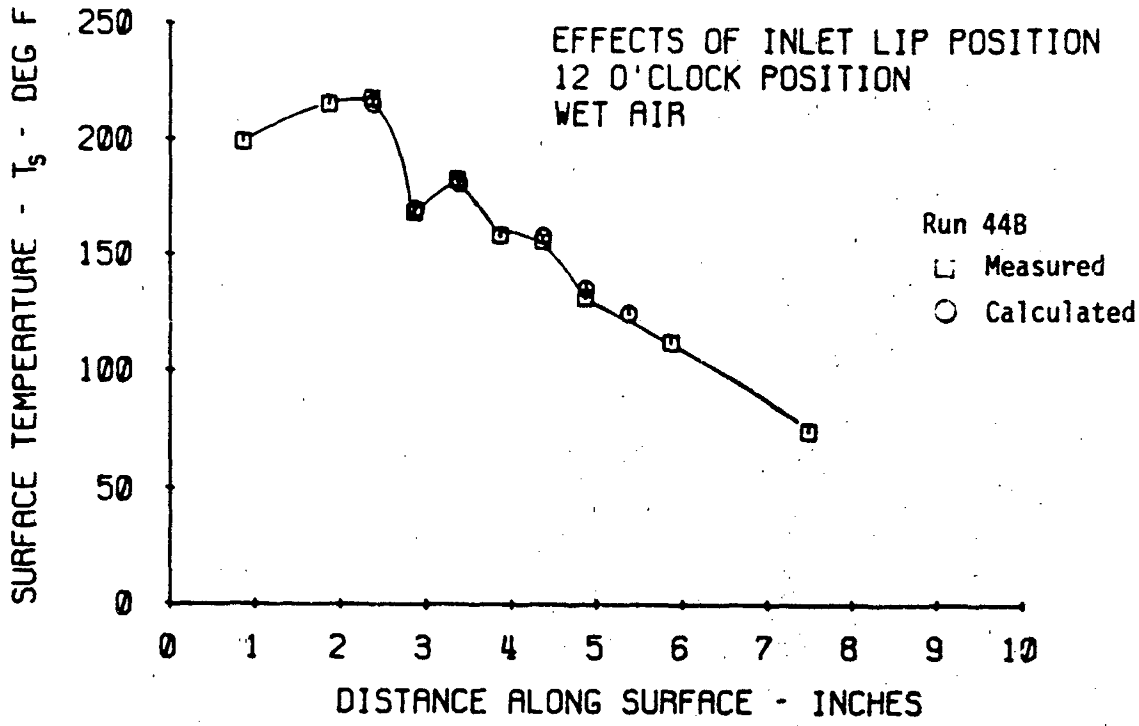

Figure 4-7 (Cont.)

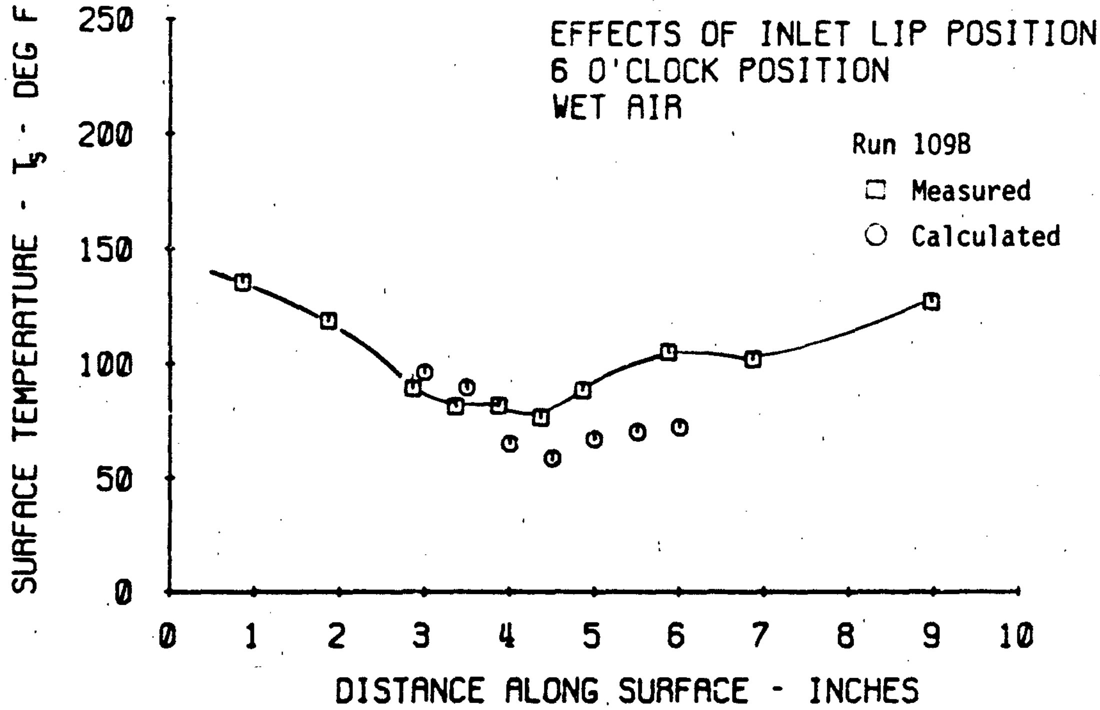

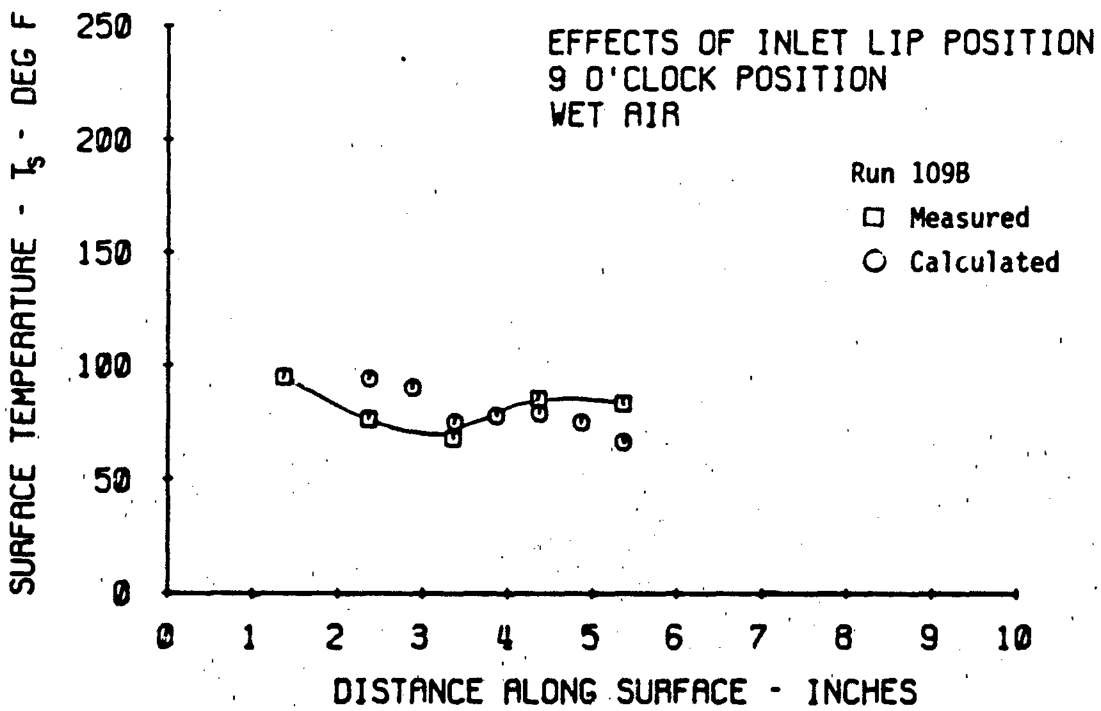

Figure 4-7 (Cont.)

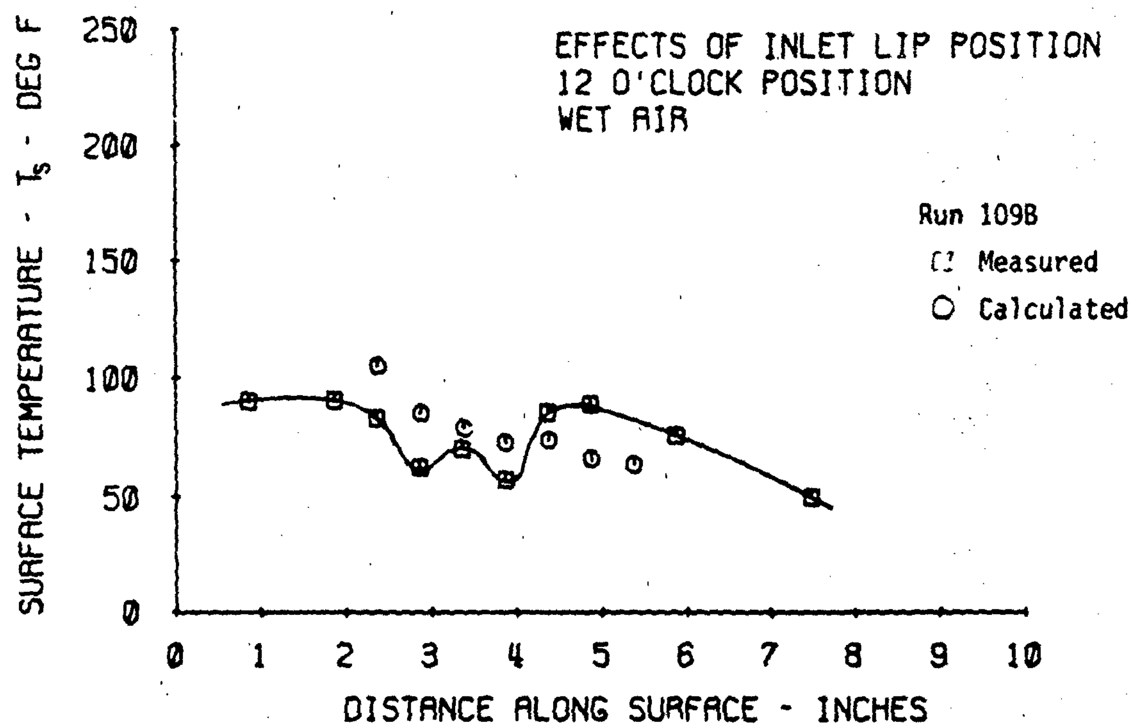

Figure 4-7 (Cont.)

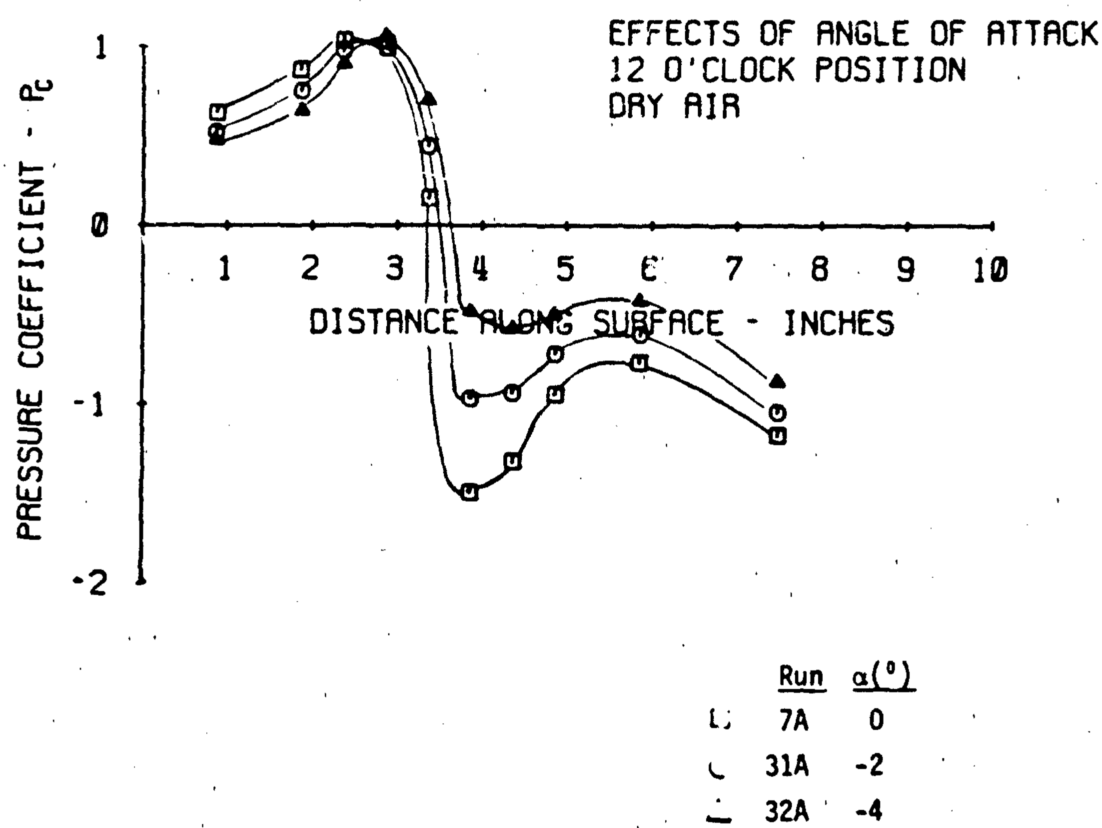

Figure 4-8 Effects of Nacelle Angle of Attack on Surface Pressure Coefficient

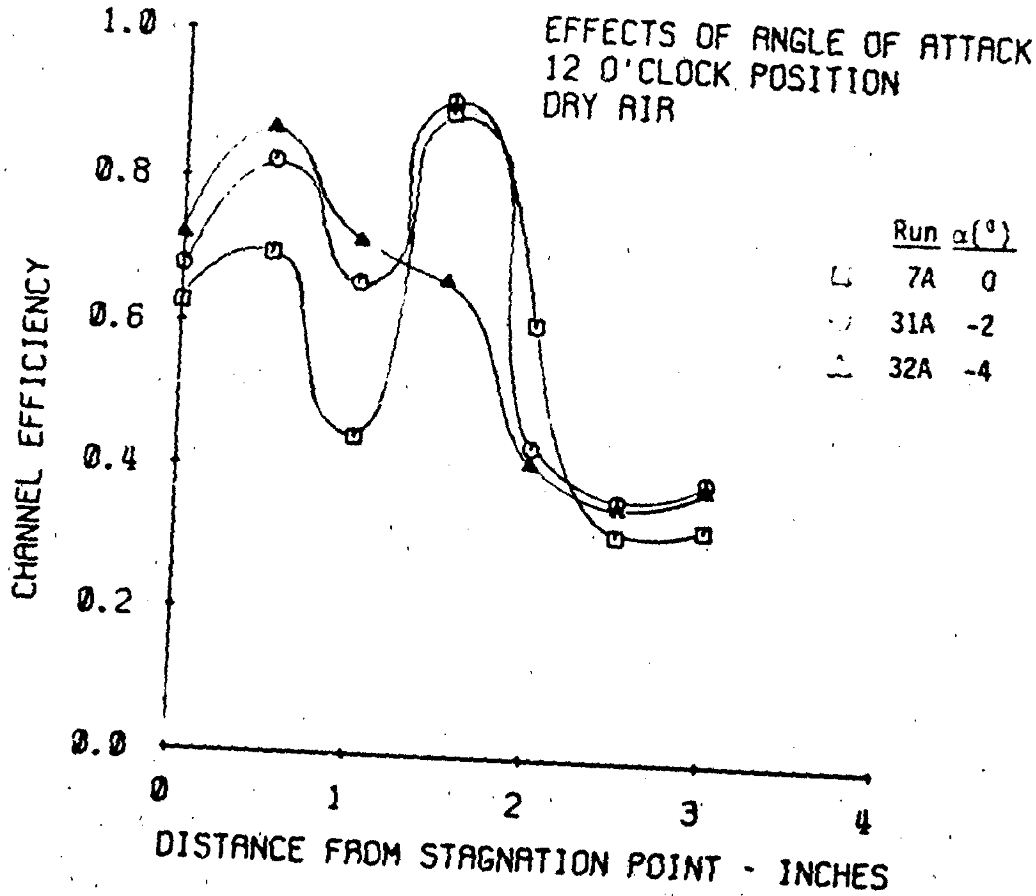

Figure 4-9 Effects of Nacelle Angle of Attack on Channel Efficiency

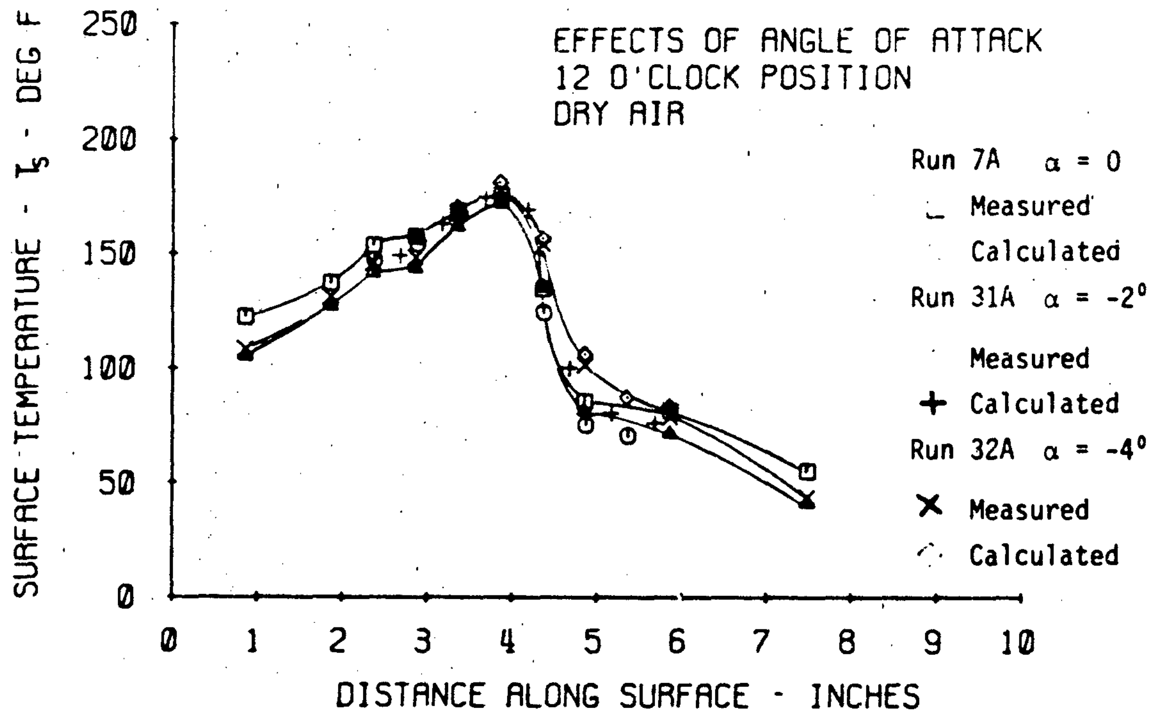

Figure 4-10 Comparison of Calculated and Measured Surface Temperature for 3 Nacelle Angles of attack

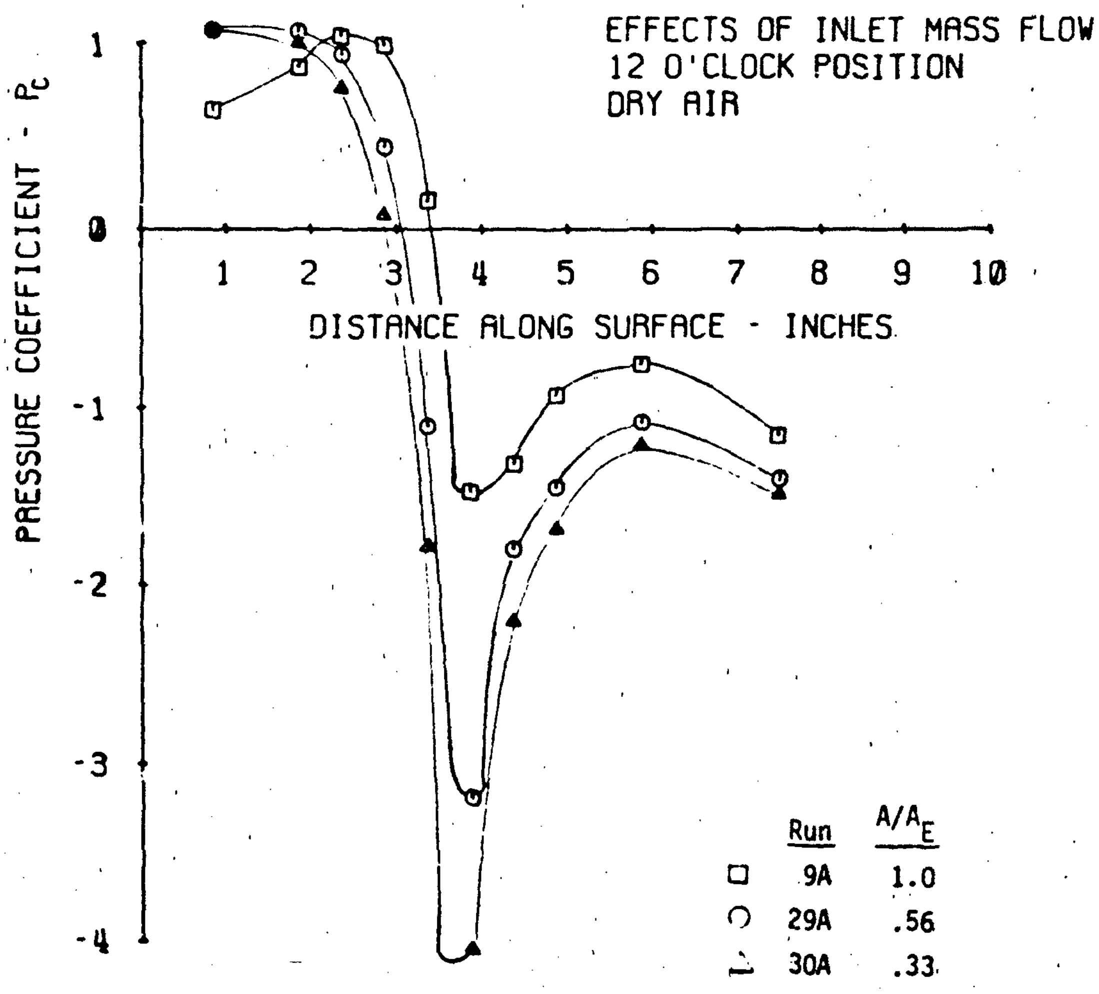

Figure 4-11 Effects of Nacelle Inlet Mass Flow on Surface Pressure Coefficient

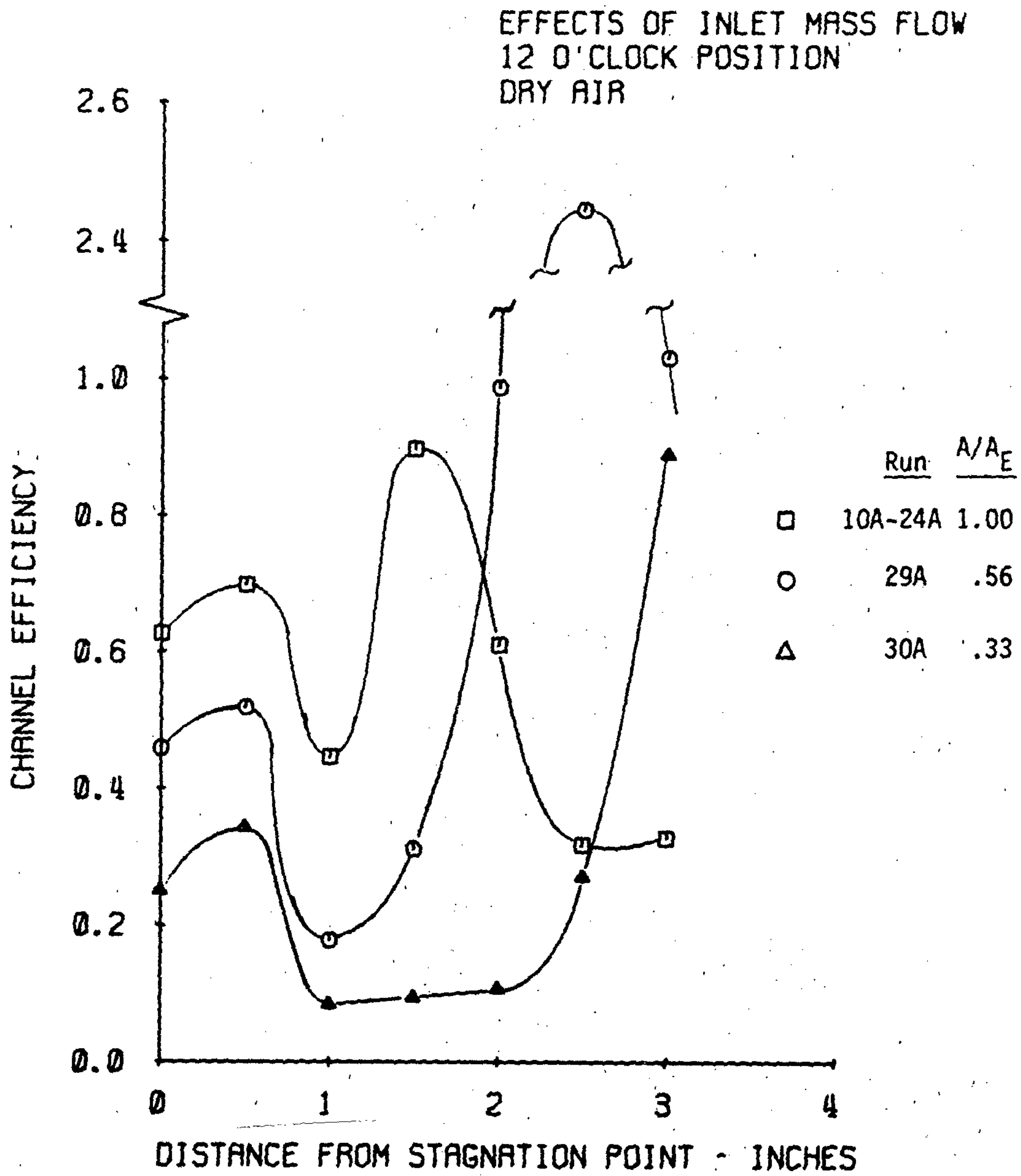

Figure 4-12 Effects of Nacelle Inlet Mass Flow on Channel Efficiency

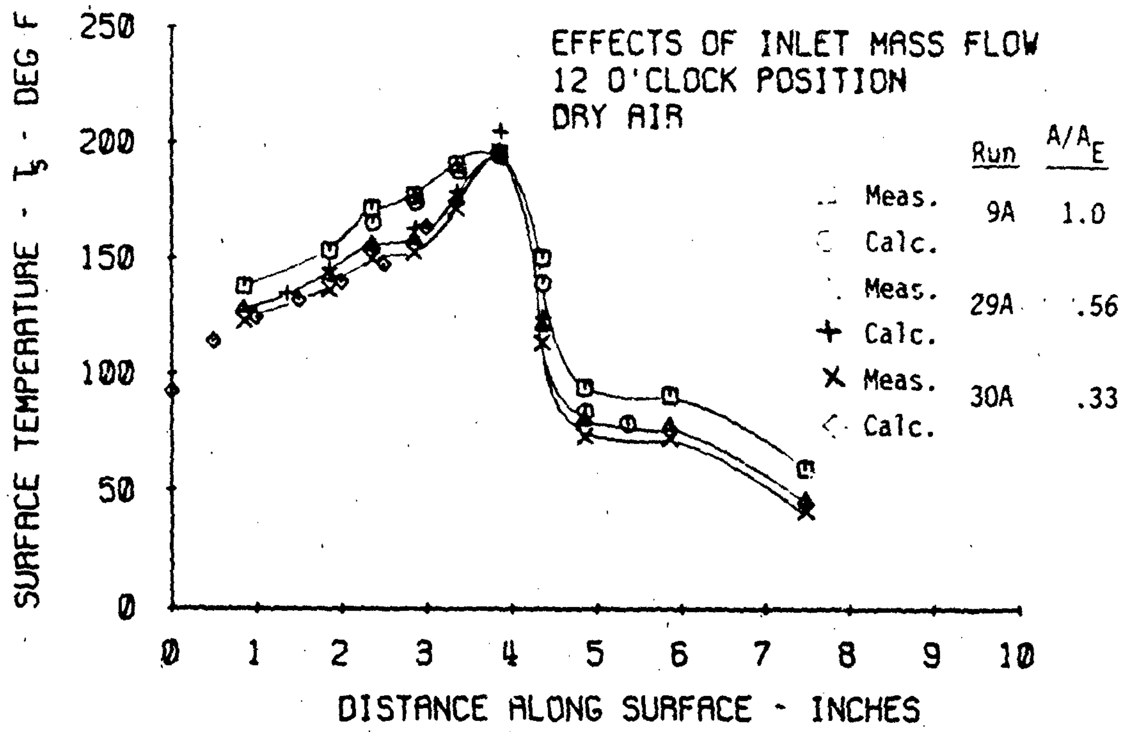

Figure 4-13 Comparison of Calculated and Measured Surface Temperature for three Nacelle Inlet Mass Flows.

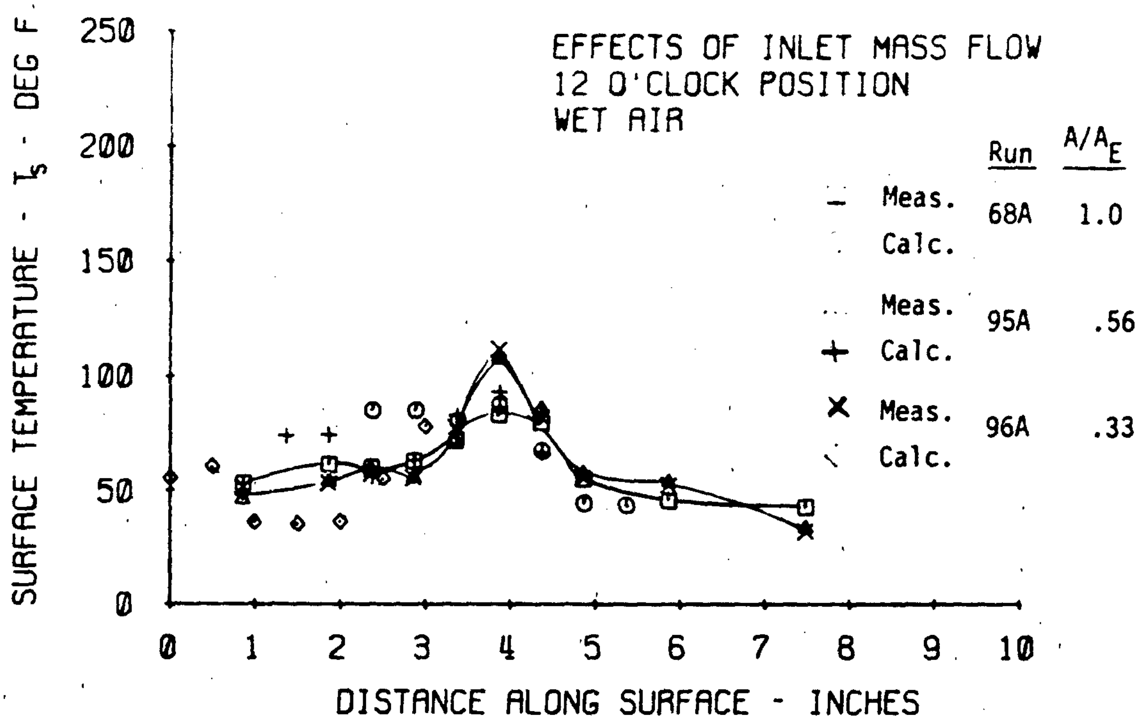

Figure 4-13 (Cont.)

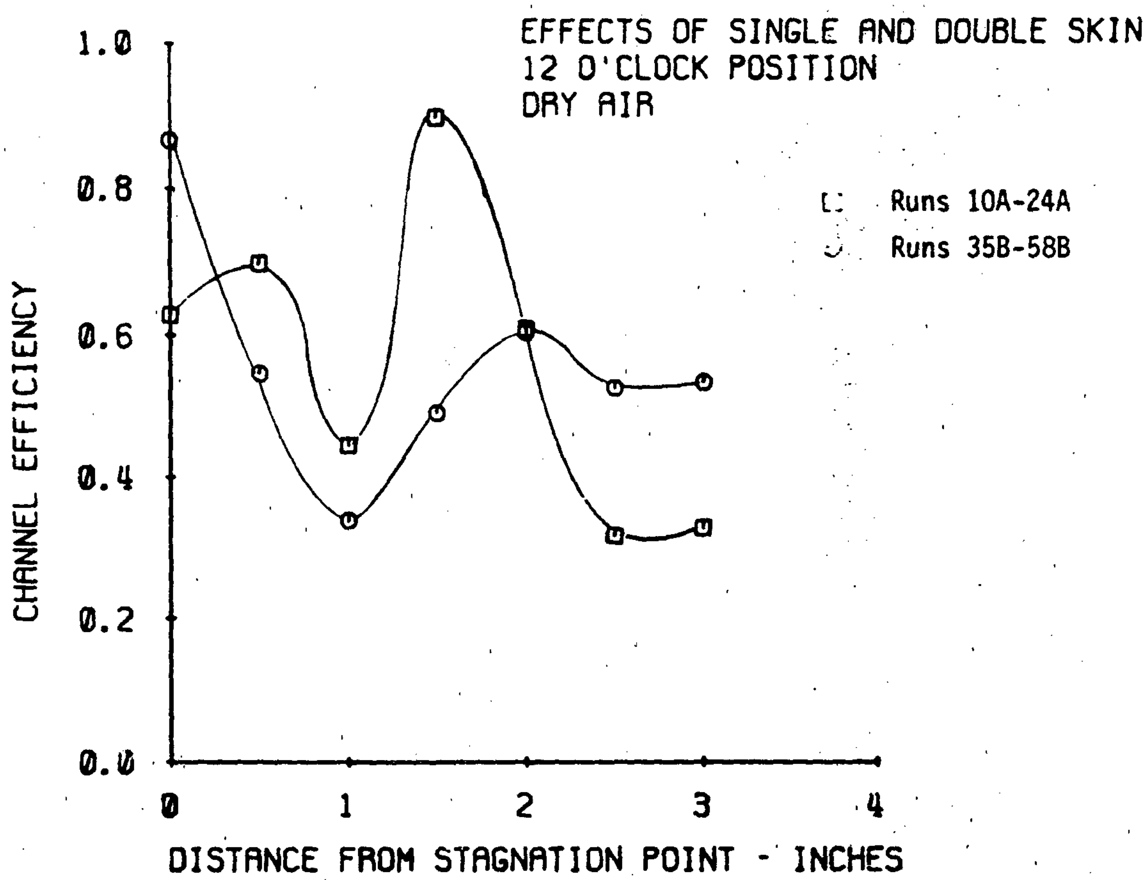

Figure 4-14 Effects of Internal Flow Distribution on Channel Efficiency.

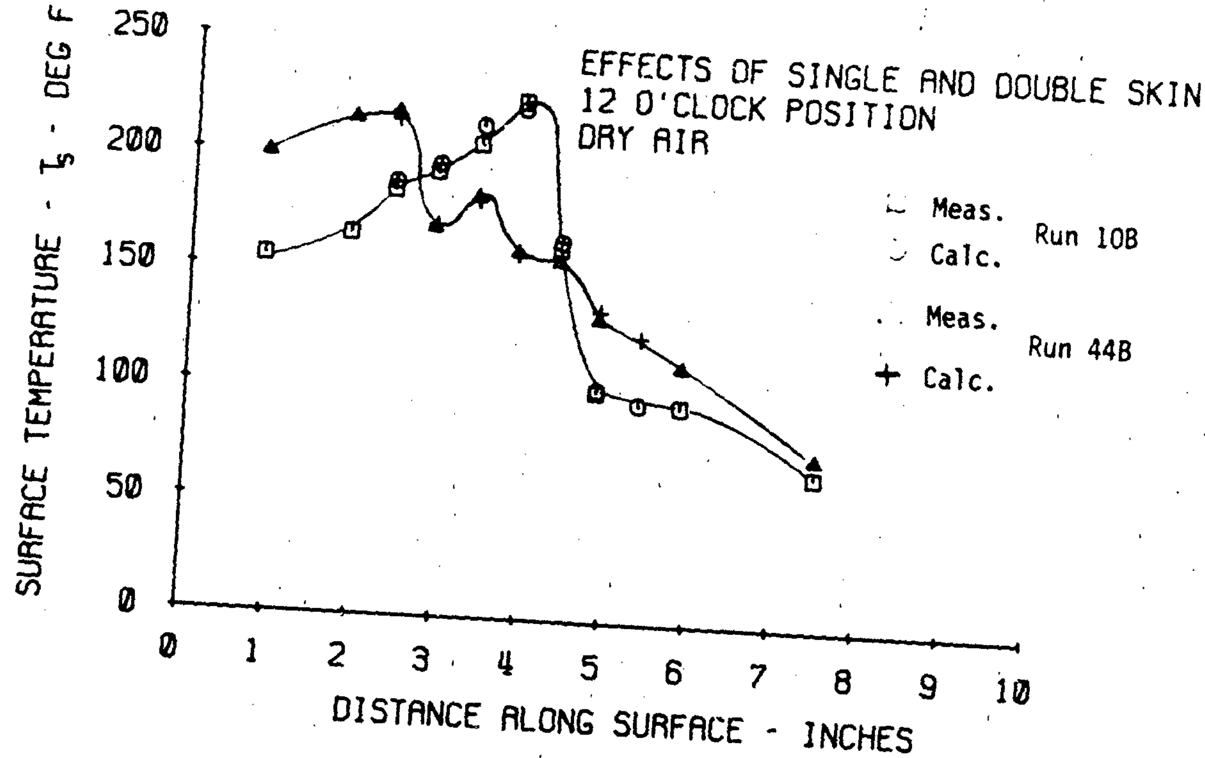

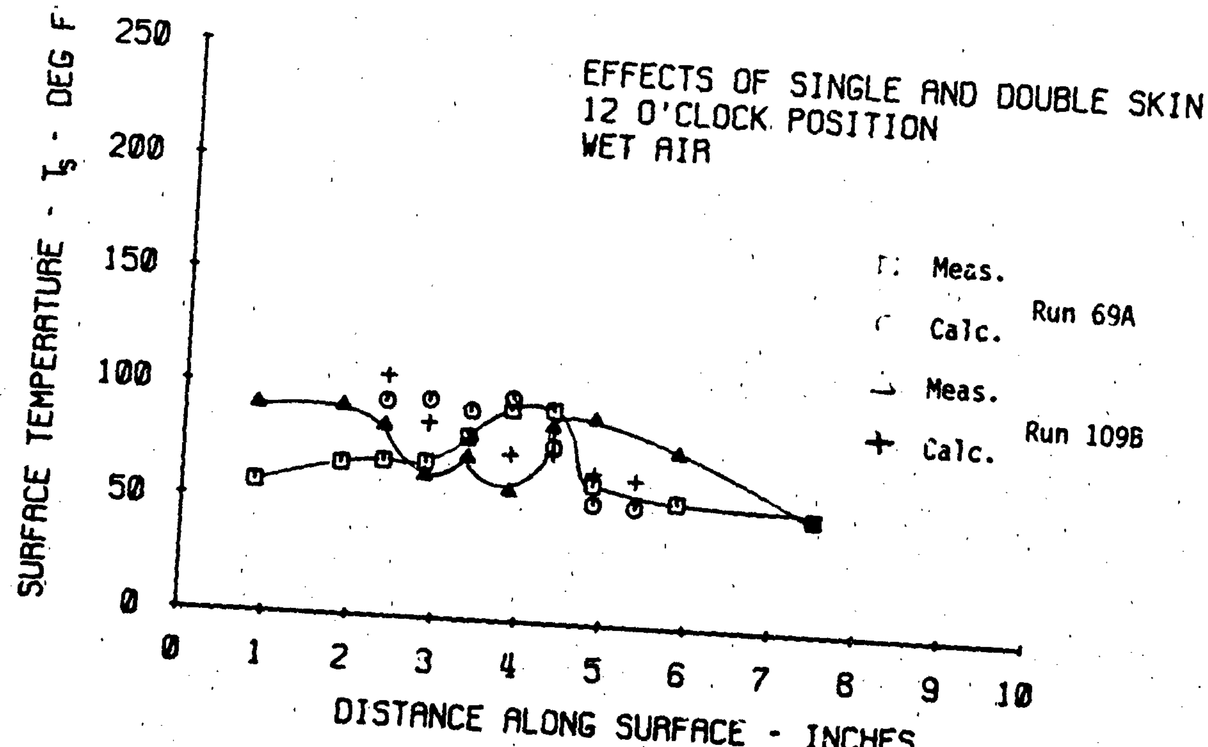

Figure 4-15 Comparison of Calculated and Measured Surface Temperature for Single and Double Skin Distribution Systems.

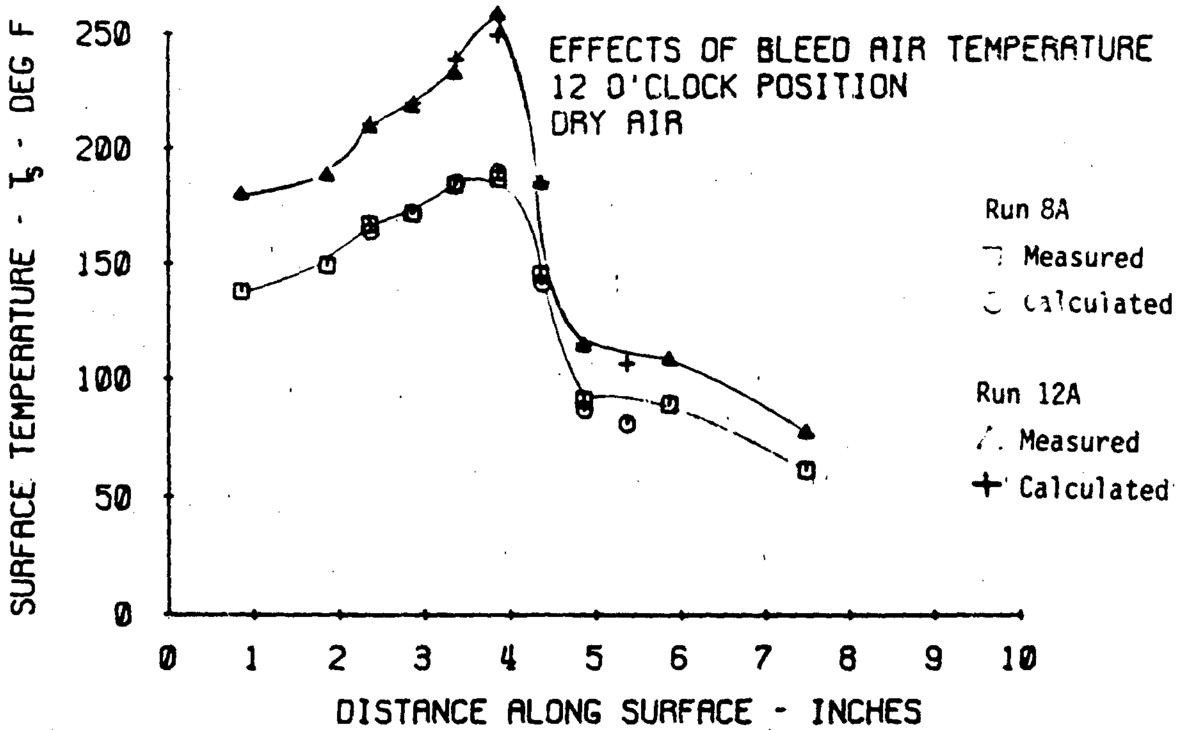

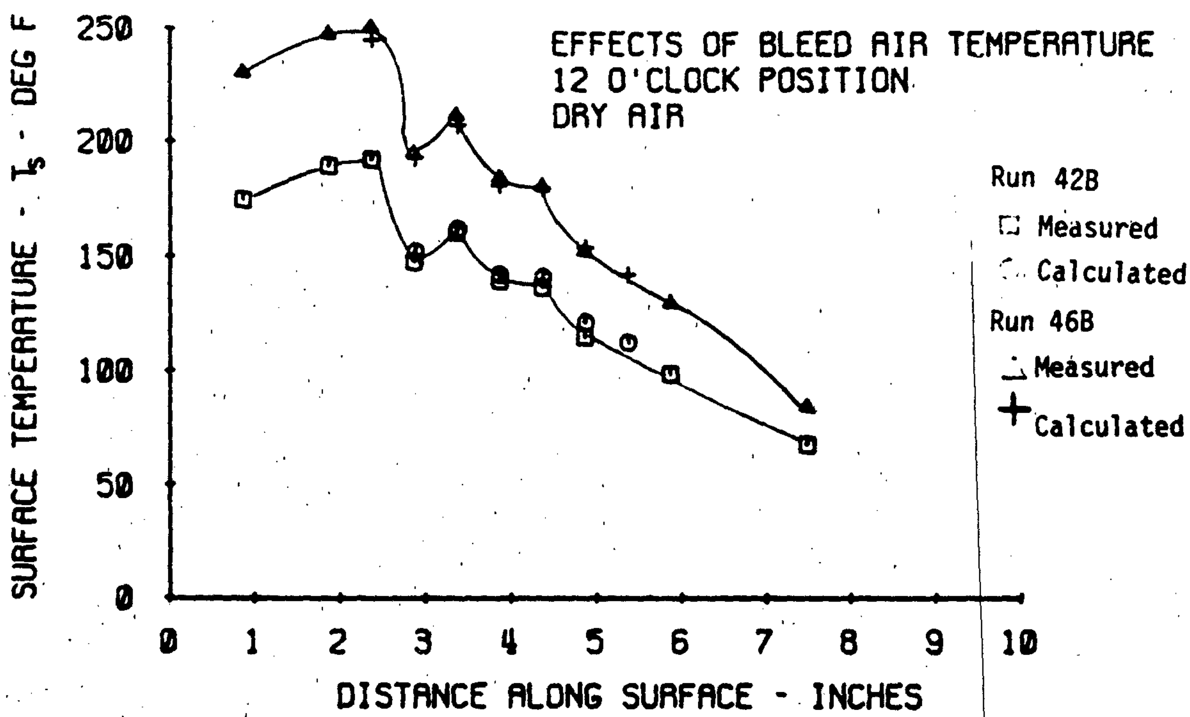

Figure 4-16 Comparison of Calculated and Measured Surface Temperature for Two Bleed Air Temperatures. - Dry Air

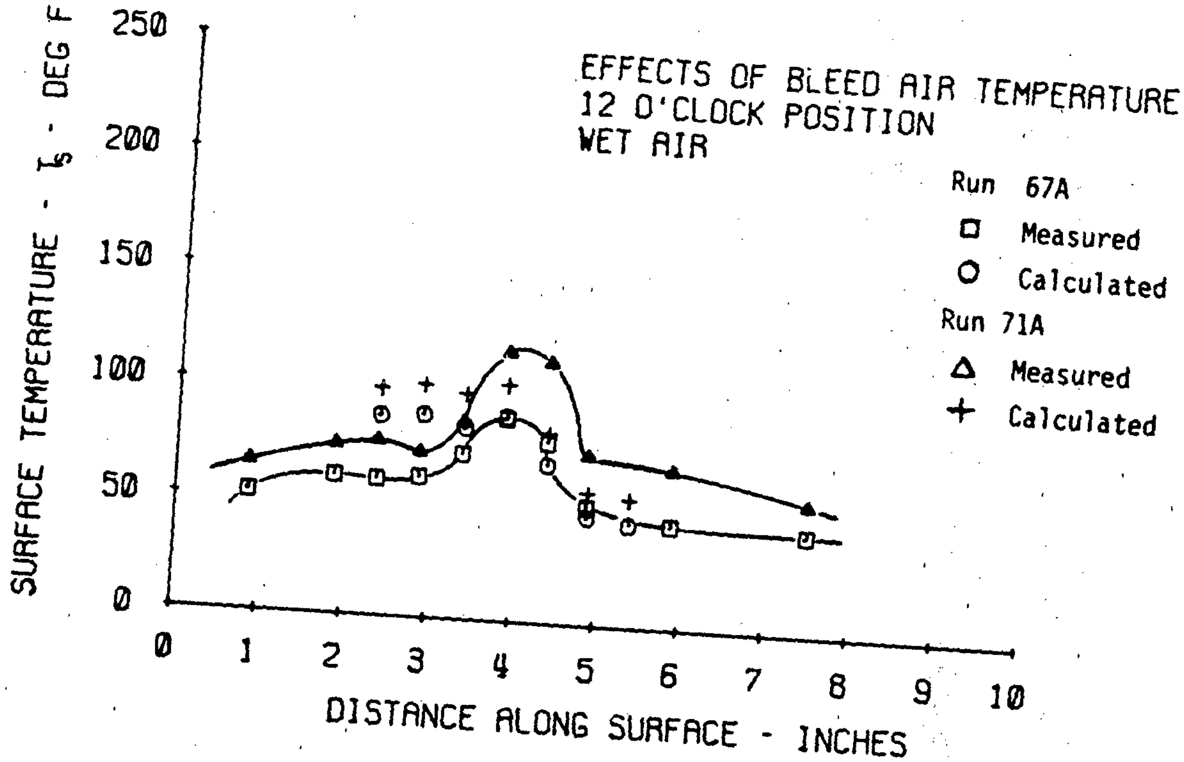

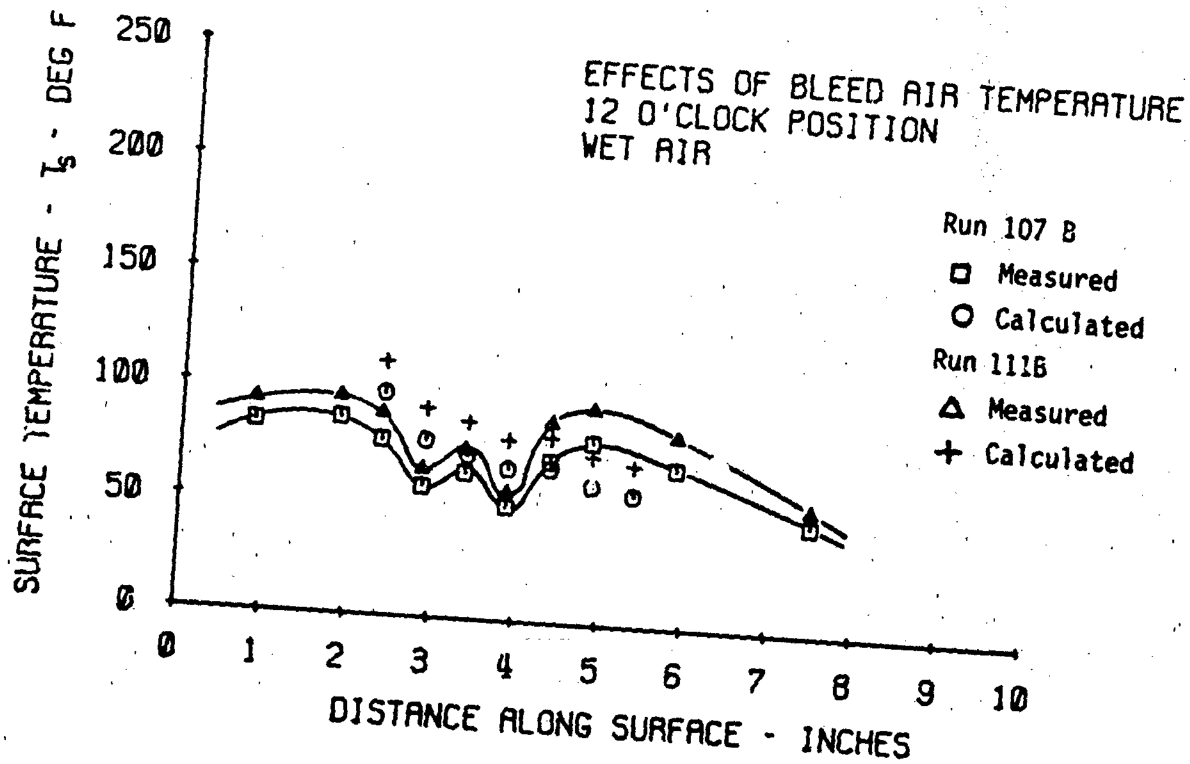

Figure 4-16 (Cont.) - Wet Air

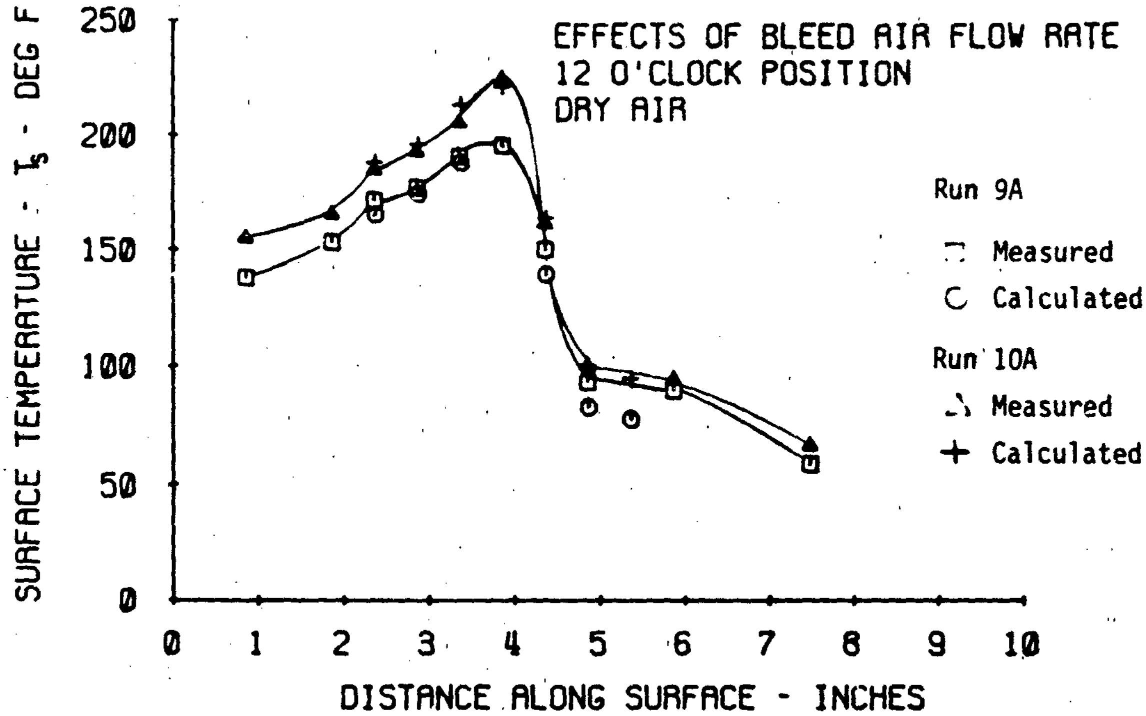

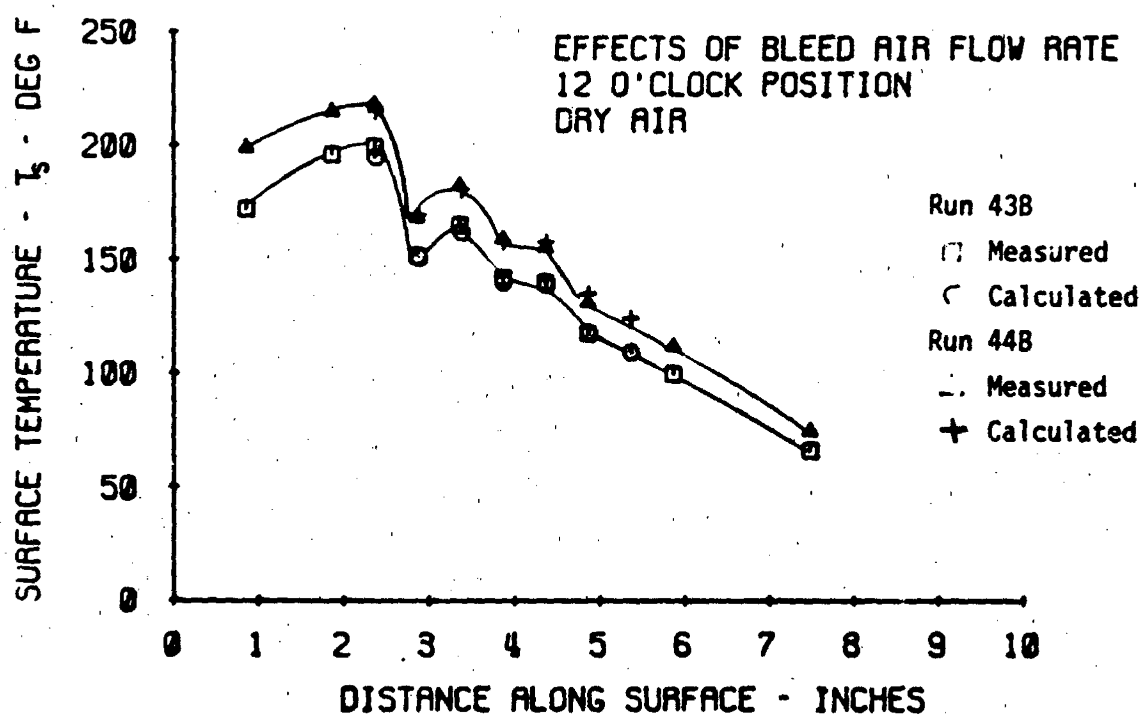

Figure 4-17 Comparison of Calculated and Measured Surface Temperature for Two Bleed Air Flow Rates.

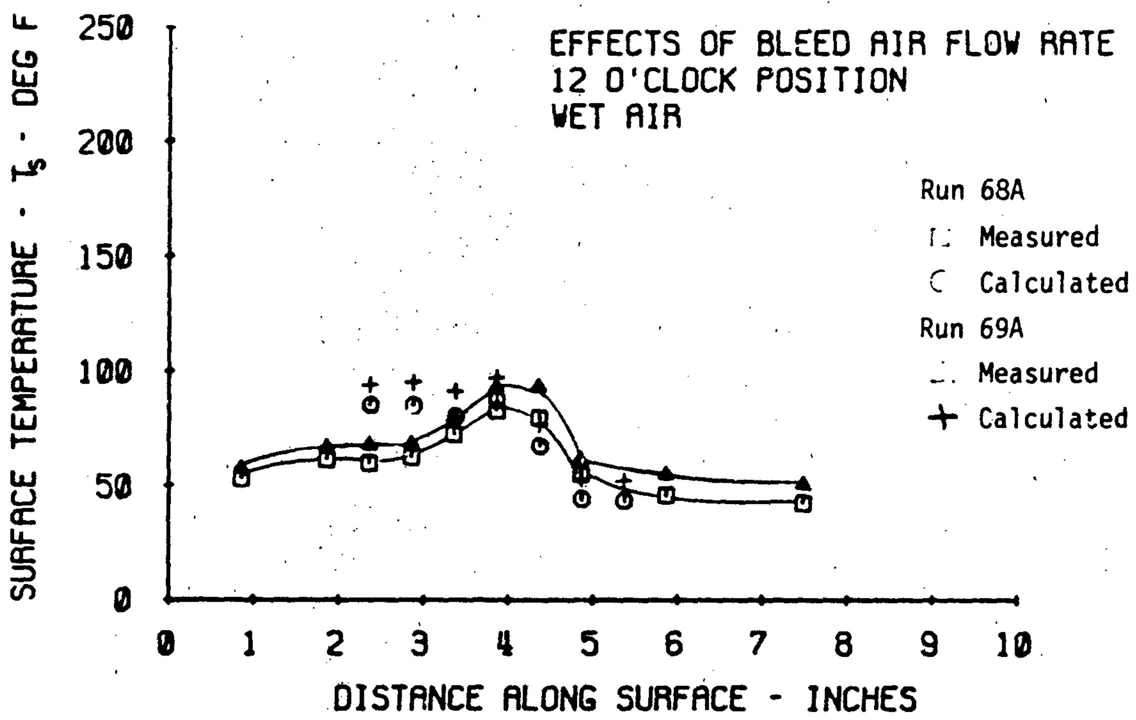

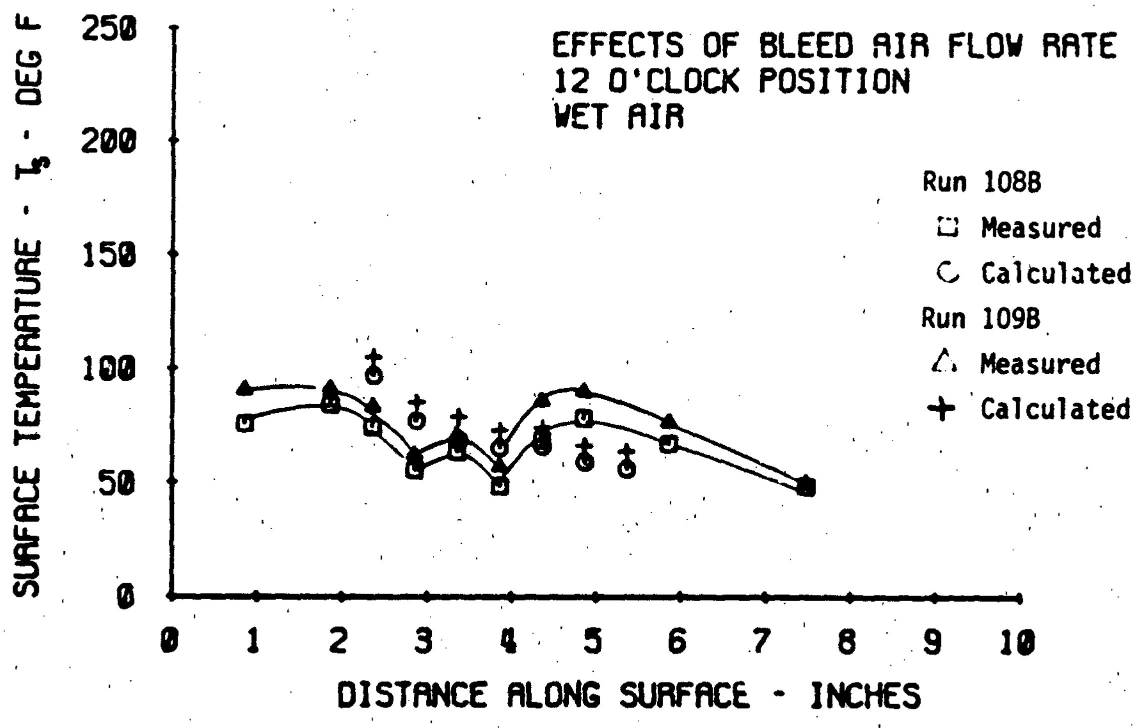

Figure 4-17 (Cont.)

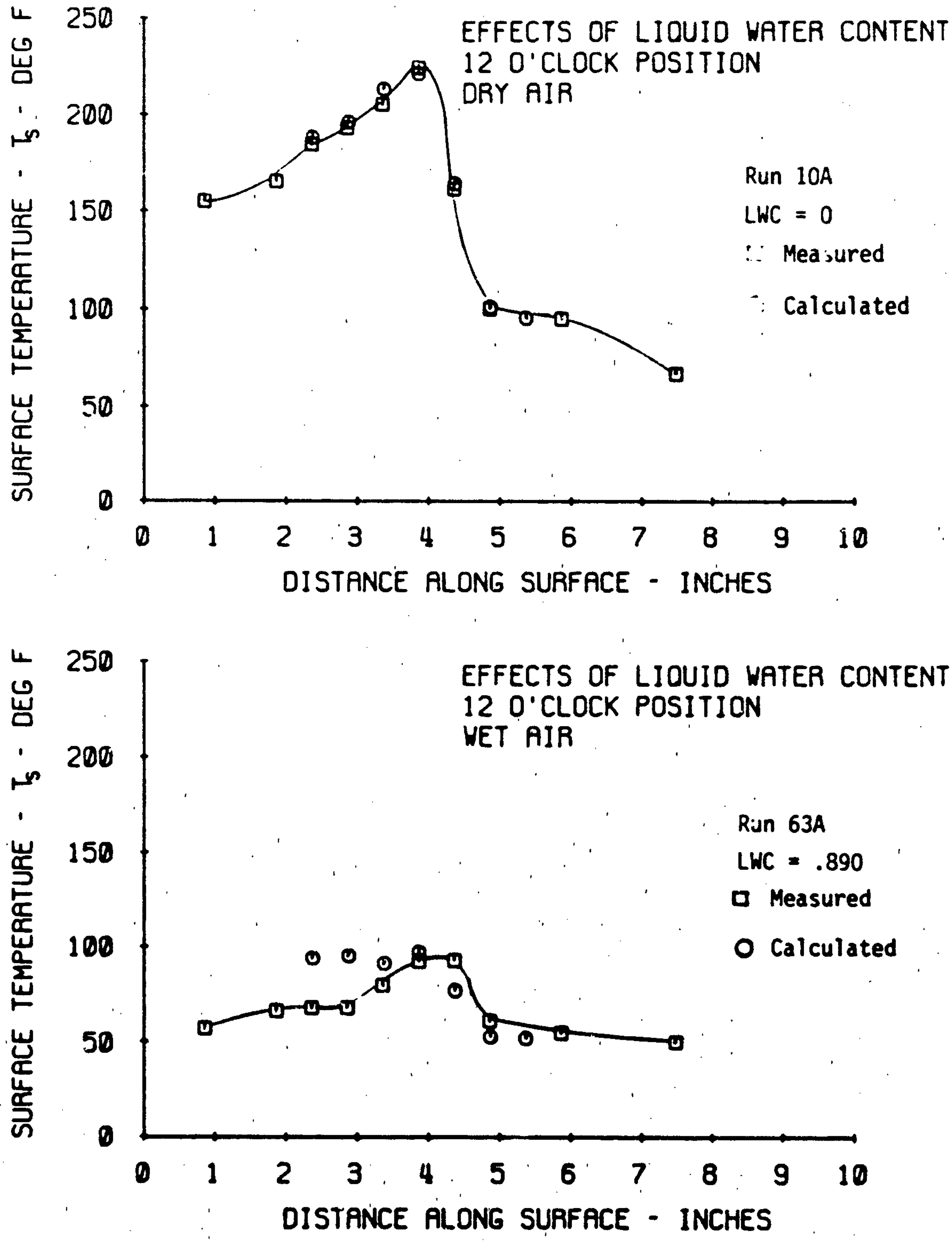

Figure 4-18 Comparison of Calculated and Measured Surface Temperature for Different Liquid Water Content.

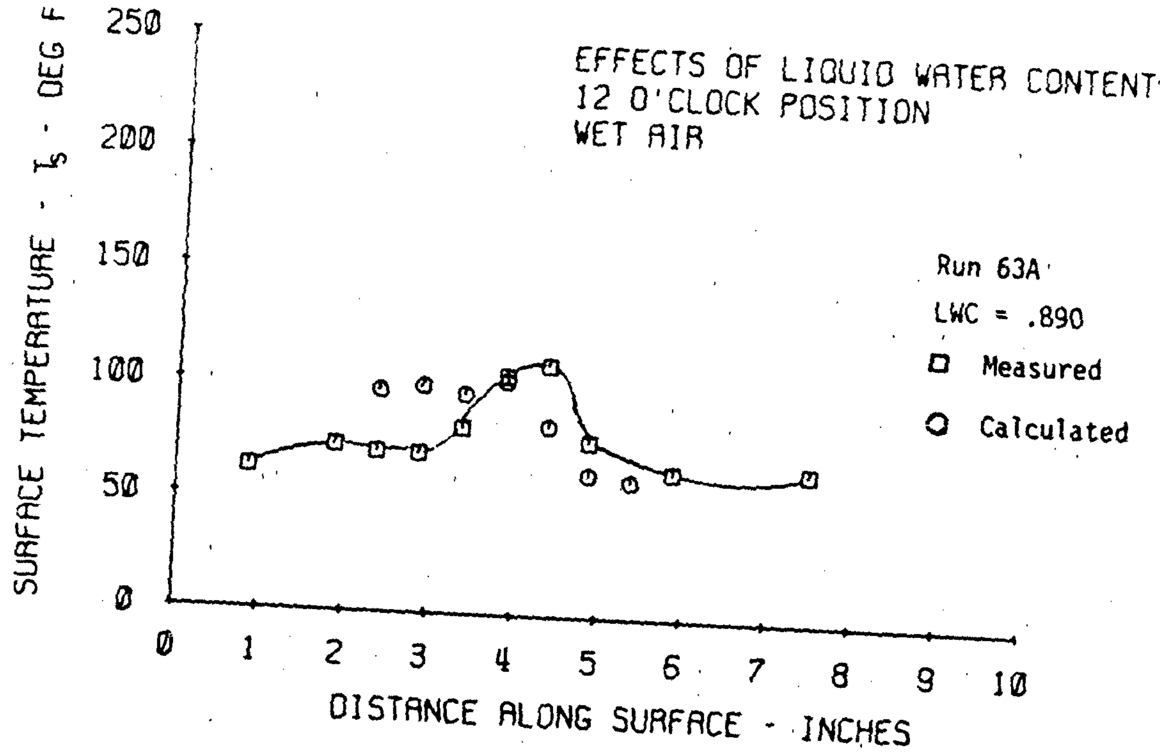

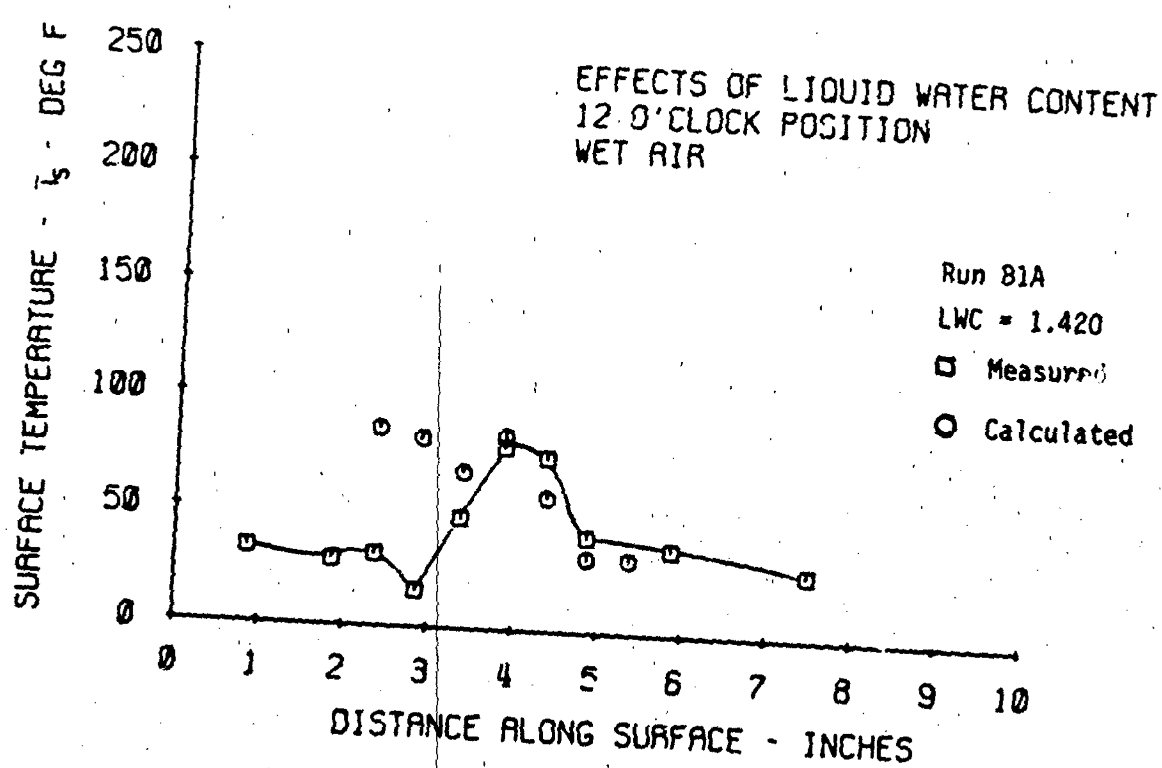

Figure 4-18 (Cont.)

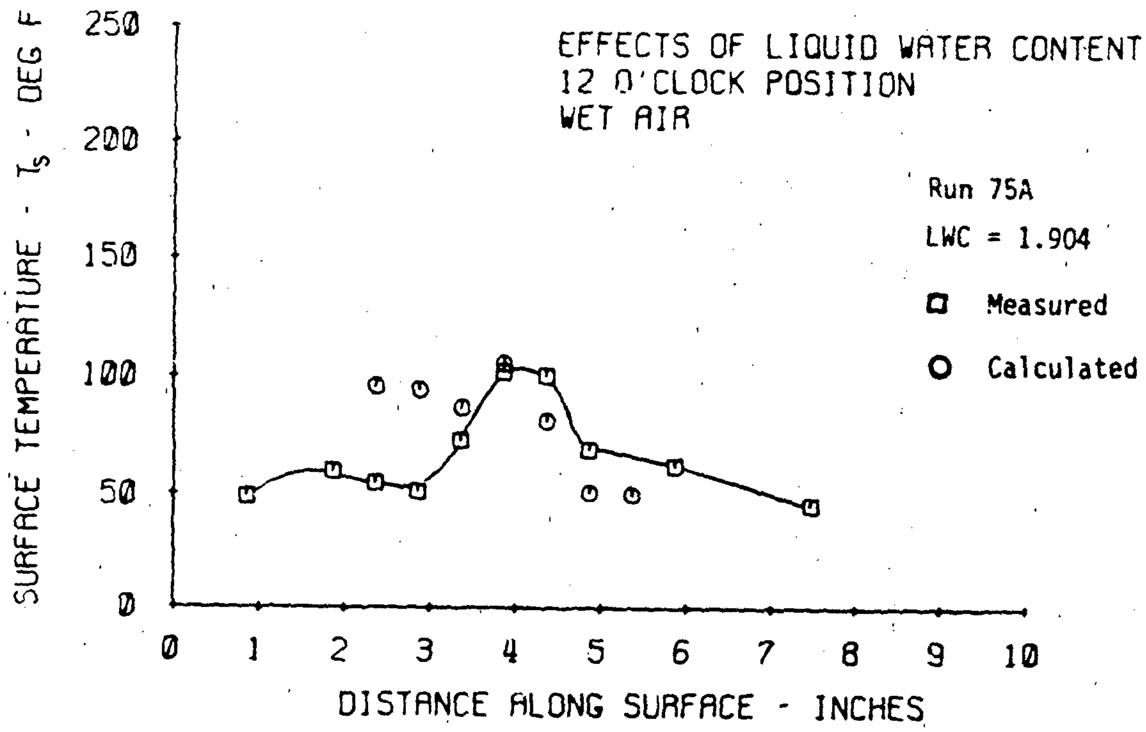

Figure 4-18 (Cont.)

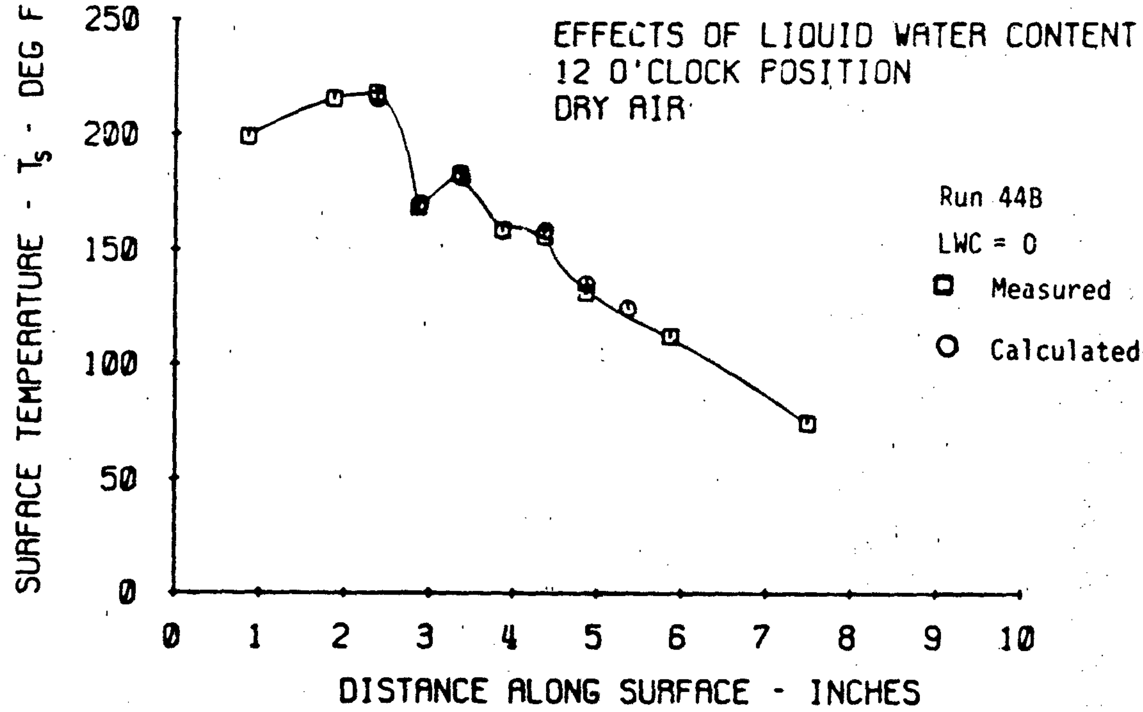

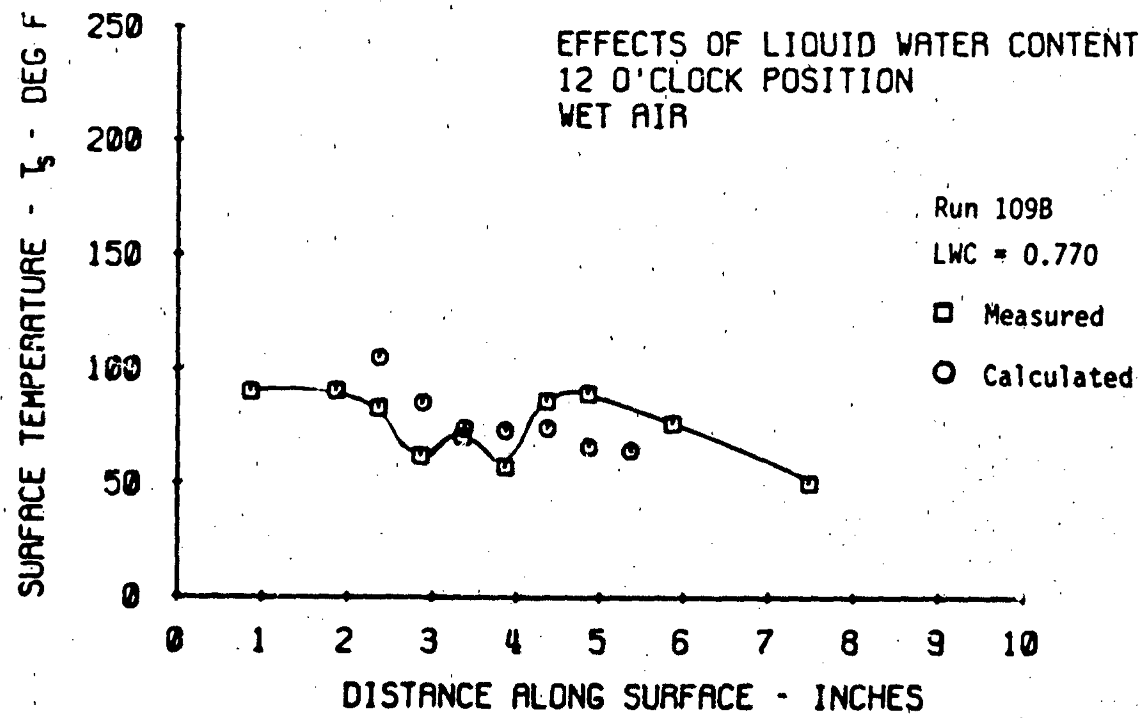

Figure 4-18 (Cont.)

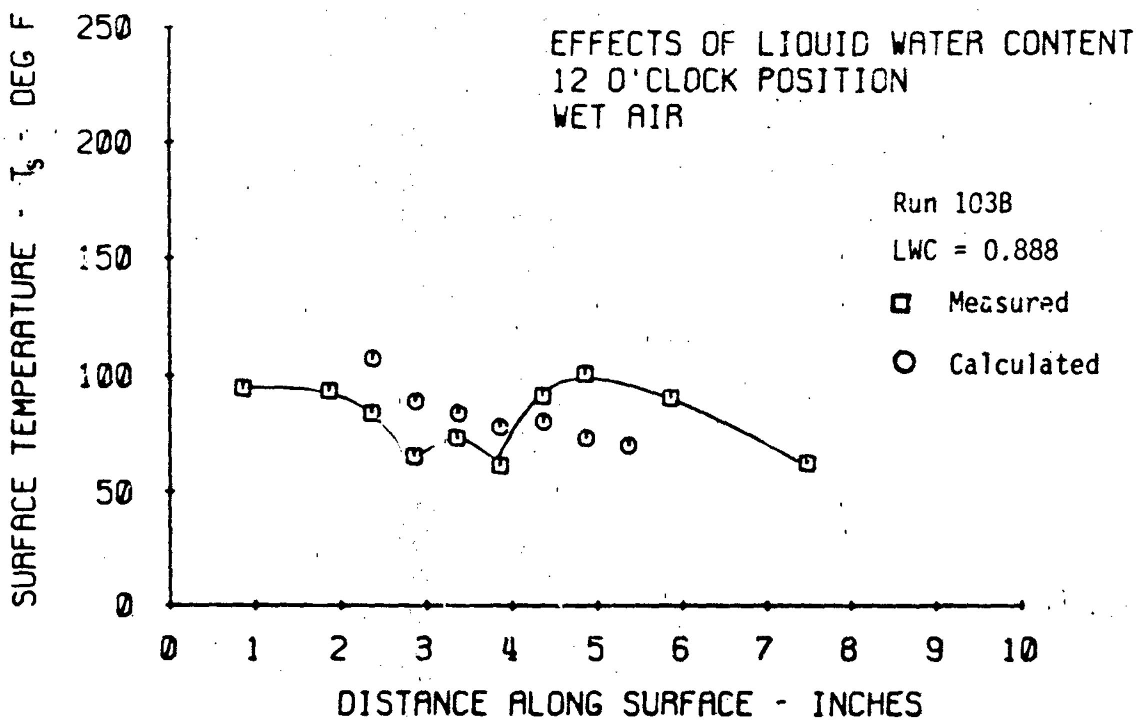

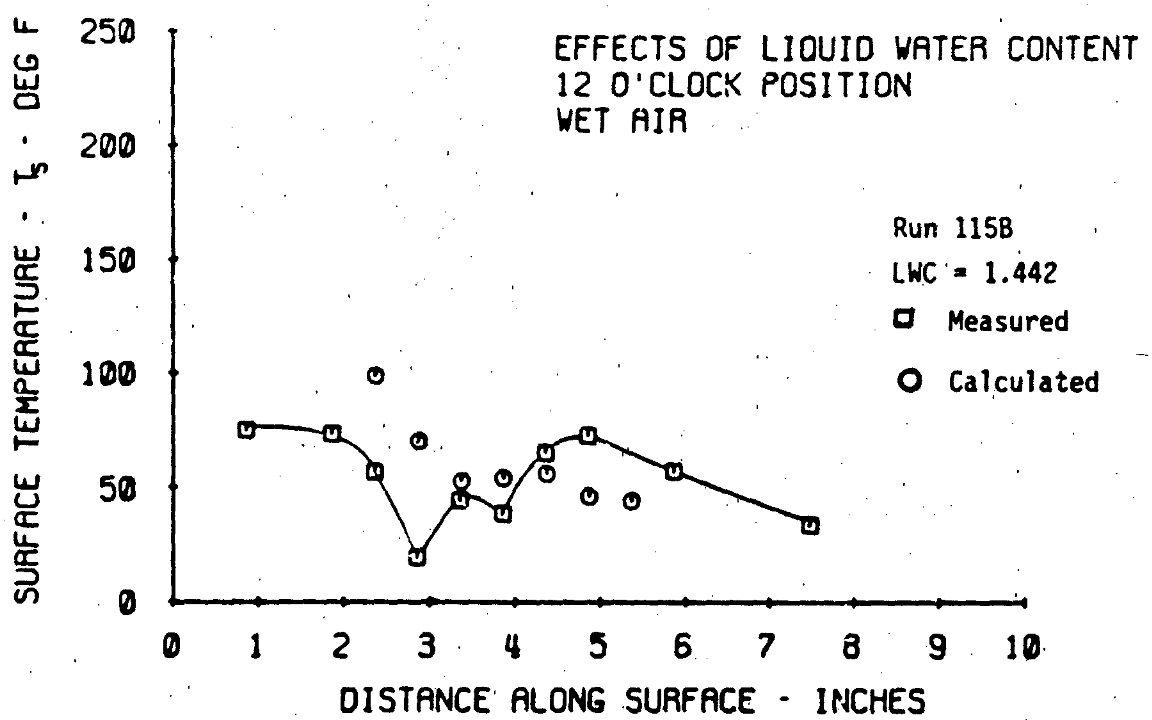

Figure 4-18 (Cont.)

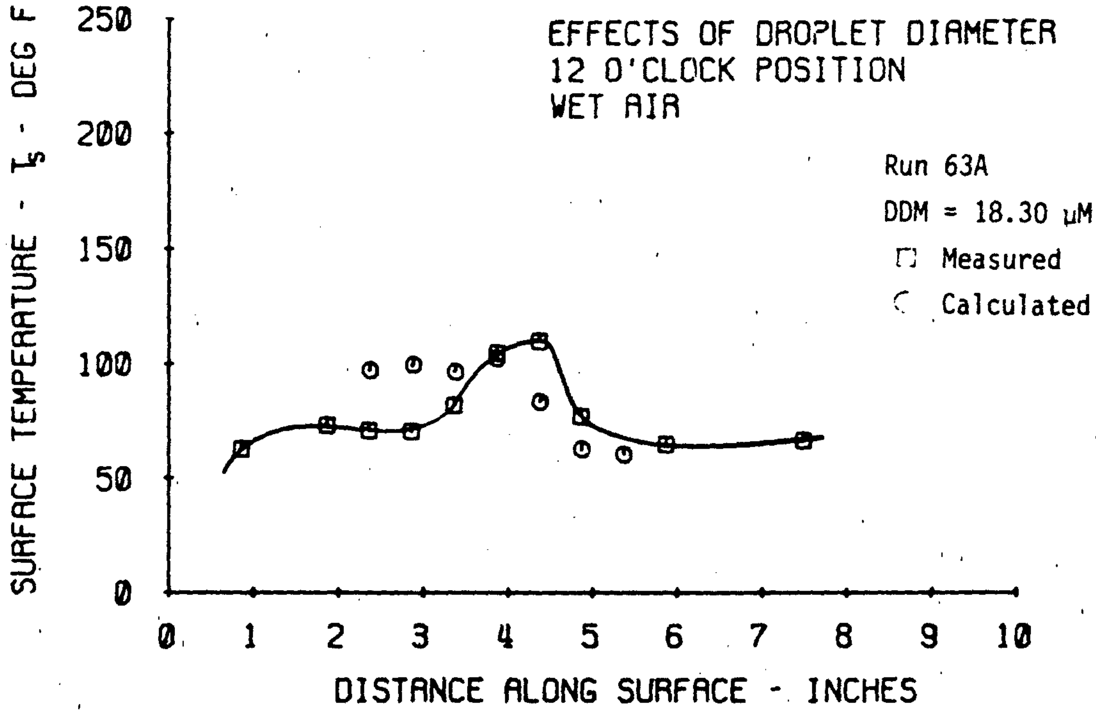

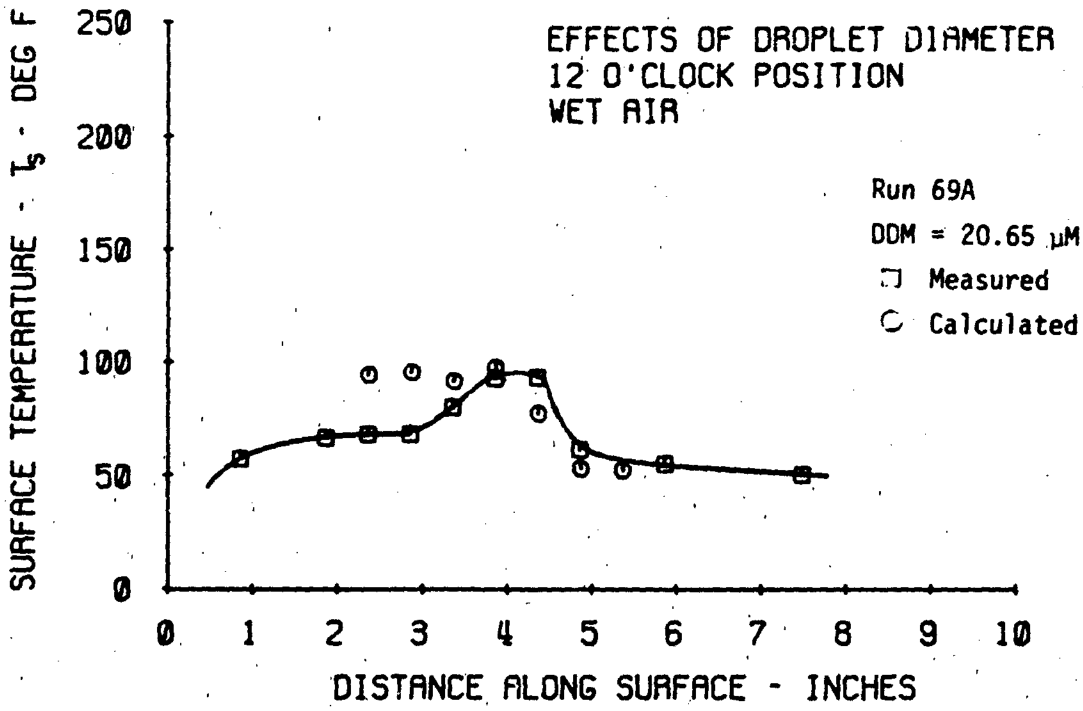

Figure 4-19 Comparison of Calculated and Measured Surface Temperature for Different Water Droplet Diameters. - Single skin.

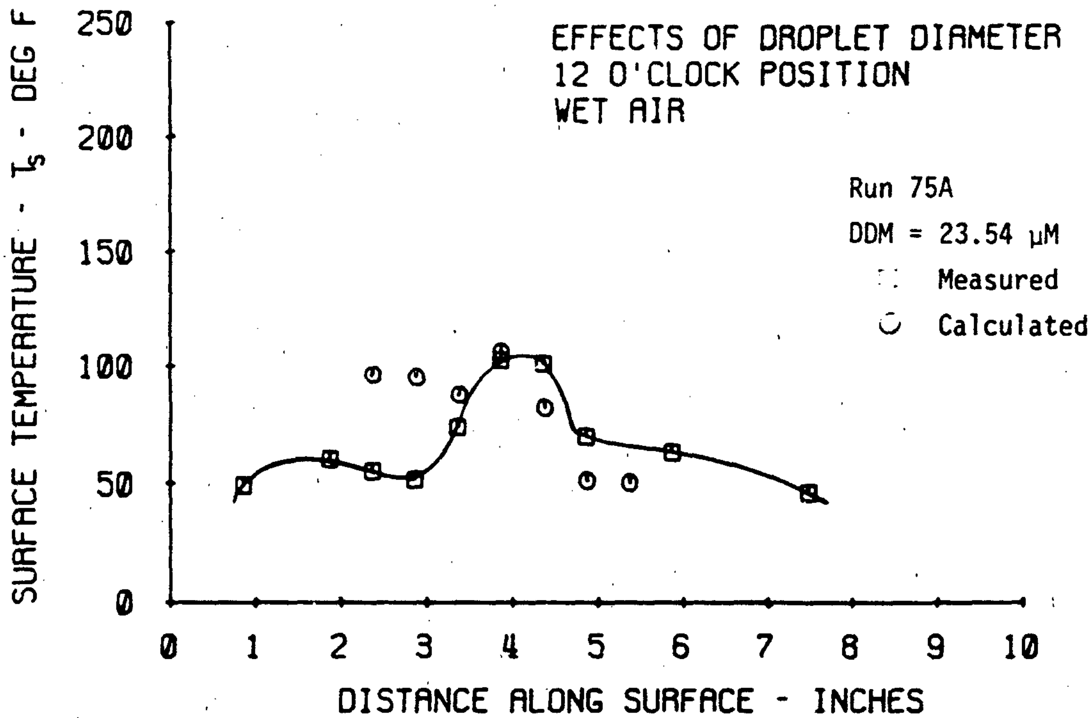

Figure 4-19 (Cont.)

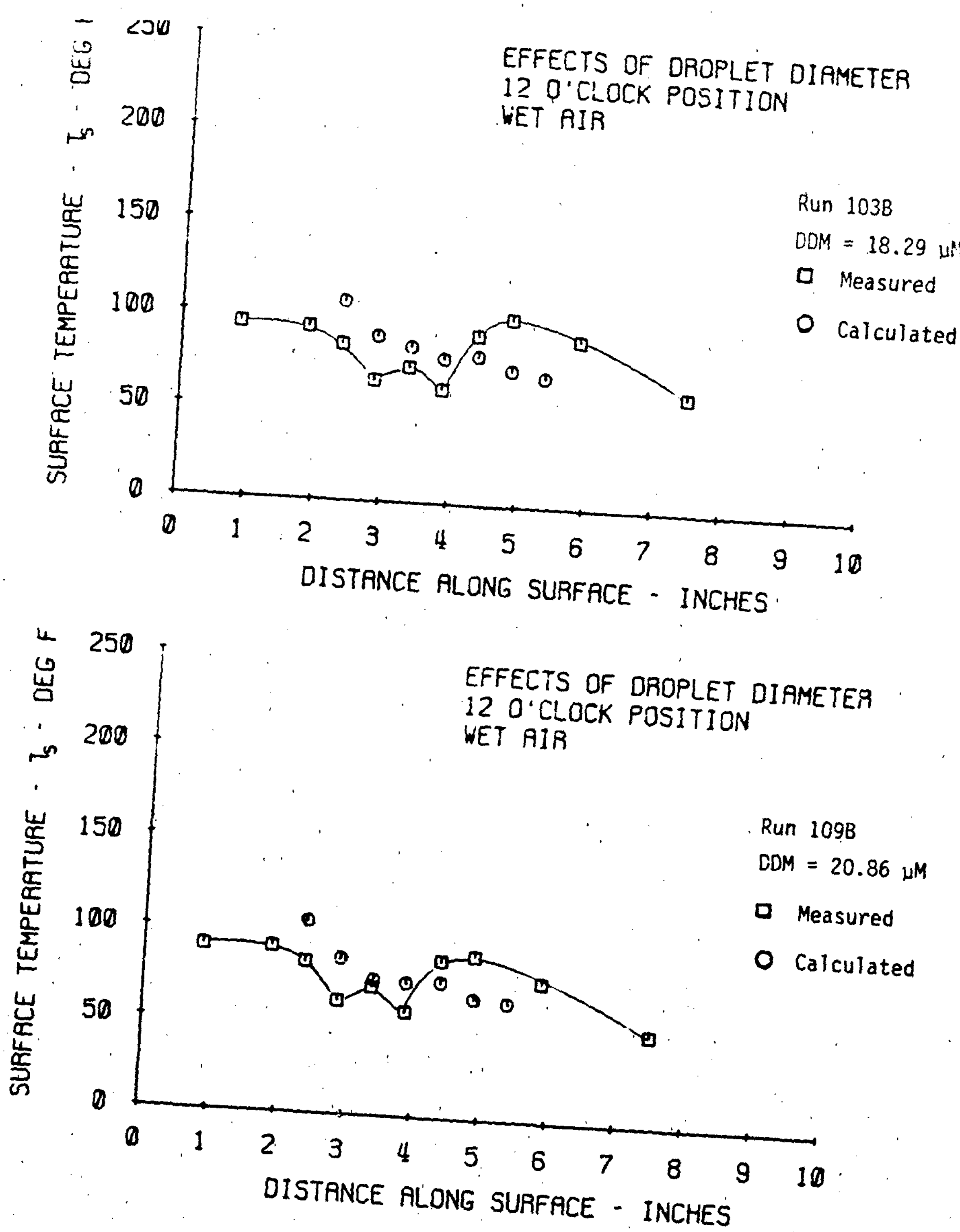

Figure 4-19 - (Cont.) - Double Skin

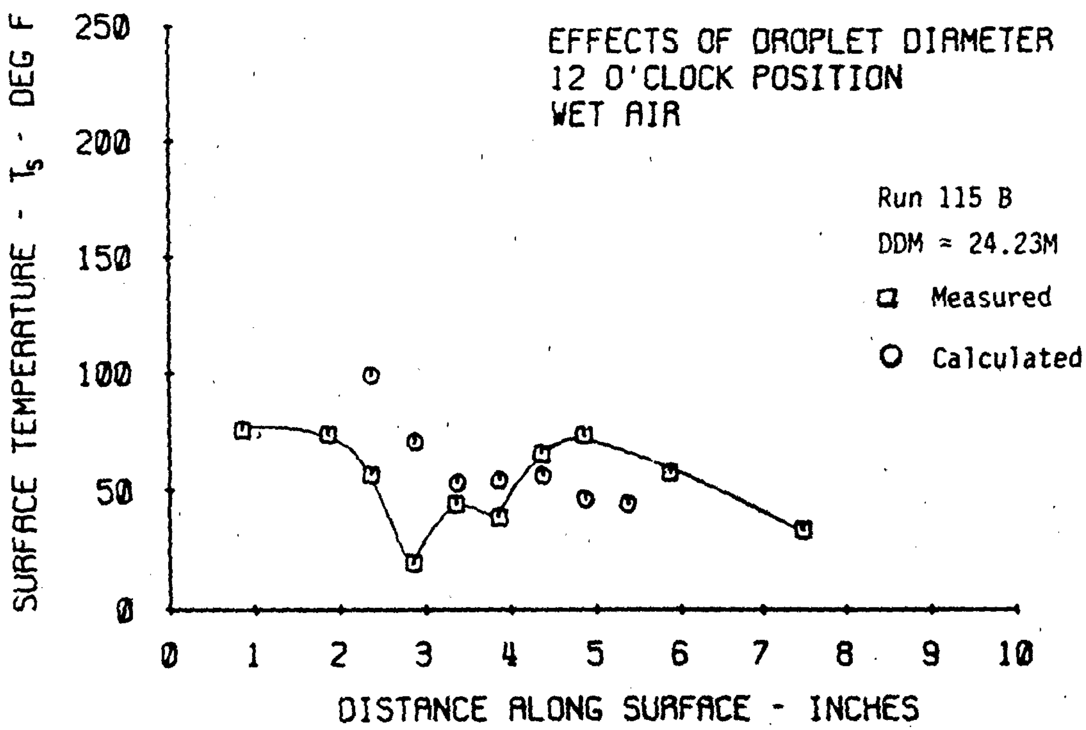

Figure 4-19 - (Cont.) - Double Skin

5.0 APPLICATION OF THE PROCEDURES

The analysis method consists of two separate programs written in Fortran IV. As presently programmed, these can be run on PDP 11/70, IBM 370 or other compatible equipment.

The first program, CHANEFF, is used to determine the heat transfer efficiency of the inlet lip hot air distribution system. The intent is to determine the efficiency for the particular configuration to be employed in the nacelle design by running dry air tests in a wind tunnel. The test model can be two-dimensional with a configuration representing a partial section of the nacelle inlet design. Data to be collected during dry air tests and geometrical information that is required for running program Ch. ..FF are:

Nacelle Geometry

- Leadi edge radius
- Streamwise surface length of the heated surface
- High-light diameter

Flight Condition Data

- Flight/tunnel pressure altitude
- Ambient temperature
- Flight velocity/airspeed
- Bleed air mass flow rate
- Bleed air temperature

Inlet Lip Data

- Surface skin temperature profile streamwise around inlet lip
- Surface static pressure profile streamwise around inlet lip

Surface static pressures will be used to calculate the pressure coefficient characteristics of the inlet lip. With the above listed data the channel efficiency can be calculated for incremental intervals streamwise around the inlet lip. For the same nacelle geometry and engine flow characteristics, the pressure-coefficient profile will remain the same so long as the nacelle angle-of-attack is held constant.

The second program, ICEOFF, can be employed to evaluate the anti-icing performance of the nacelle inlet. This program can be used in any one or all of the following ways:

a. As a tool during the design phase to determine the bleed air requirements for anti-icing.
b. With incorporation of an engine performance routine into the present program this can be used to size the heating system.
c. As a means to demonstrate engine/nacelle anti-icing capability as part of the FAR anti-icing performance.

The data required for running program ICEOFF are:

<u>Nacelle and Aircraft Geometry</u>

Nacelle chord length
Nacelle thickness-to-chord ratio
Nacelle inlet leading edge radius
Nacelle inlet high-light diameter
Extent of inlet lip heated surface
Wing area.

<u>Flight Conditions</u>

Flight/tunnel pressure altitude
Aircraft gross weight
Flight velocity
Constants of the airplane drag polar

<u>Inlet Lip Data</u>

Surface pressure coefficient profile streamwise around the inlet lip
Channel efficiency profile streamwise around the inlet lip (From Program CHANEFF)

<u>Icing Conditions</u>

Ambient temperature
Droplet median diameter
Liquid water content
Cloud horizontal extent

Program ICEOFF is written to operate in two different modes as follows:

Mode I - This mode uses icing tunnel data and predicts evaporation and runback. In order to check run-data as it proceeds, this mode of operation prints out intermediate calculation of the point-by-point analysis.

Mode II - This mode is used for icing prediction under given flight and icing conditions.

Detailed instructions for use of these programs along with sample inputs and outputs are provided in Appendices A and B.

6.0 CONCLUSIONS

Two computer programs, based on a simplified heat transfer theory, have been developed. The channel efficiency program, CHANEFF, provides a means for evaluating the external and internal heat transfer characteristics of an engine inlet anti-icing system. The anti-icing program, ICEOFF, provides a means of evaluating the icing performance characteristics of an engine inlet anti-icing system. Both programs are developed for a continuous flow hot gas anti-icing system.

The program ICEOFF calculates the inlet lip skin temperature profile for dry air with very good agreement. The calculations for icing conditions, though useful, are not so good. The mean deviation of the calculated temperature is 6°F for dry air and 19°F for wet.

It is concluded that, although better accuracy could be desirable for wet air calculations, the method is simple to use and gives rapid and useable predictions for the surface temperature distribution on an engine nacelle inlet lip that is anti-iced with hot bleed air flow. The method is applicable to a wide range of independent variables in the problem and treats double skin distribution systems equally as well as single skin piccolo tube systems.

7.0 RECOMMENDATIONS

The underlying basis of the present approach is the characterization of the internal heat transfer that is used in the analysis published by the Federal Aviation Administration[1], by a single parameter, referred to as Channel Efficiency. This parameter is used in lieu of a more definite determination of an internal convective heat transfer coefficient. Channel Efficiency equates to the ratio of external heat transfer divided by internal heat transfer. Any errors caused by improper determination of the internal or external heat transfer will then appear in the value of Channel Efficiency when using the program for evaluating experimental data.

Based on the analysis of dry air data using program ICEOFF, it is concluded that the assumptions made in formulating the internal and external flow and heat transfer model are very reasonable. This is supported by the 6°F mean temperature deviation which is probably well within the data accuracy. This is considered excellant agreement and no change to this portion of the program is recommended.

The correlation accuracy for wet air (19°F mean deviation) is not as good as for dry air. It appears that there is possibility for improvement here. Brief analyses of the cause of major temperature differences between calculated and measured near the stagnation point indicated that the rate of heat transfer in this region is consistantly over predicted resulting in higher than measured temperature. On the other hand, near the aft limit of the heated region, the calculated temperatures tend to be lower than measured. A more in-depth investigation of these two regions would probably result in improved calculation procedures and better accuracy on temperature correlation. Potential candidates for improvement would be the modeling for evaporation and heat transfer.

---

1. op. cit.

The method presented does give accurate trends for a variety of external ambient conditions (i.e. droplet diameter, liquid water content, etc.) and no further improvements are recommended in this area.

APPENDIX A - Channel Efficiency Program

A.1 Flow Chart

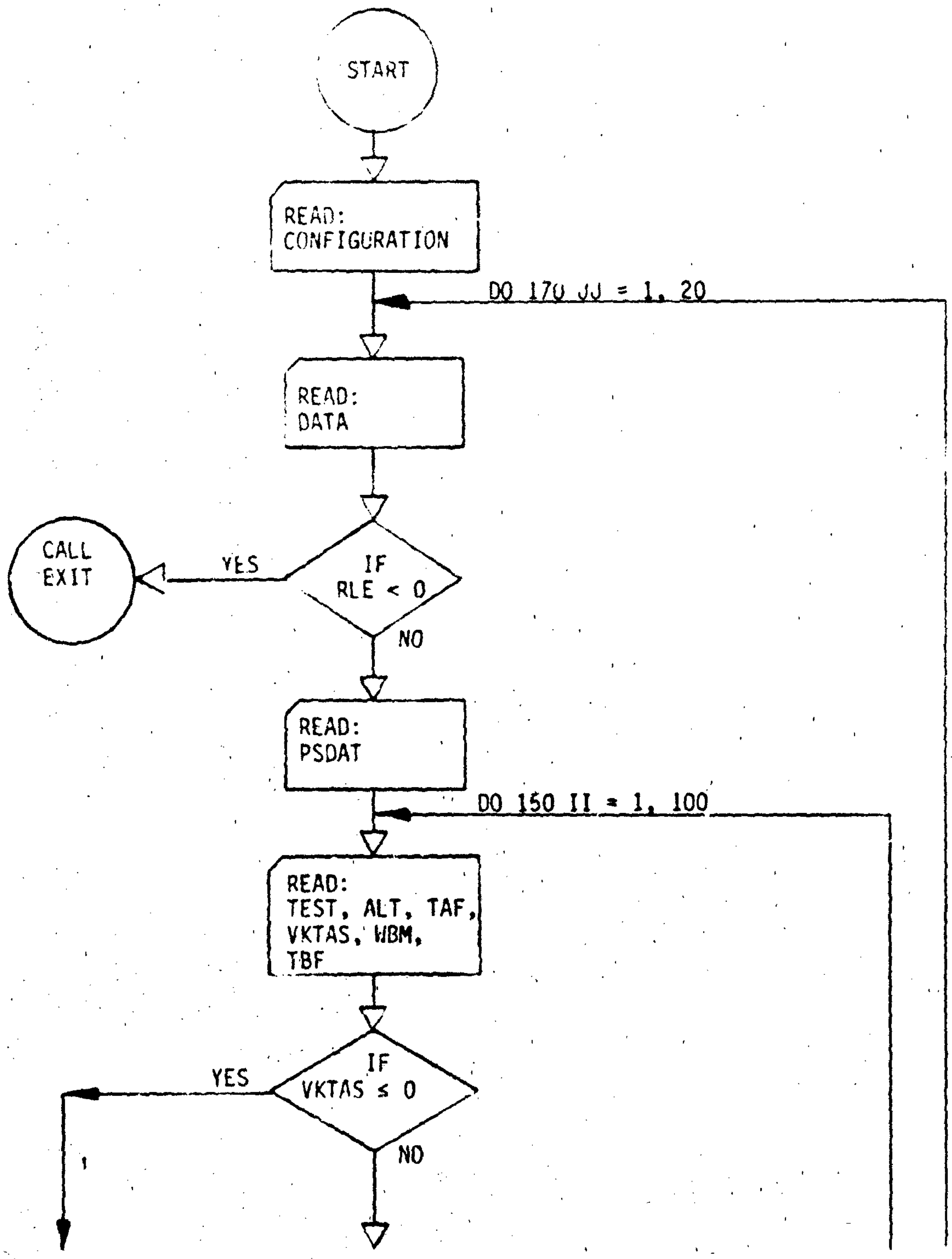

A.1 *Flow Chart (Cont.)*

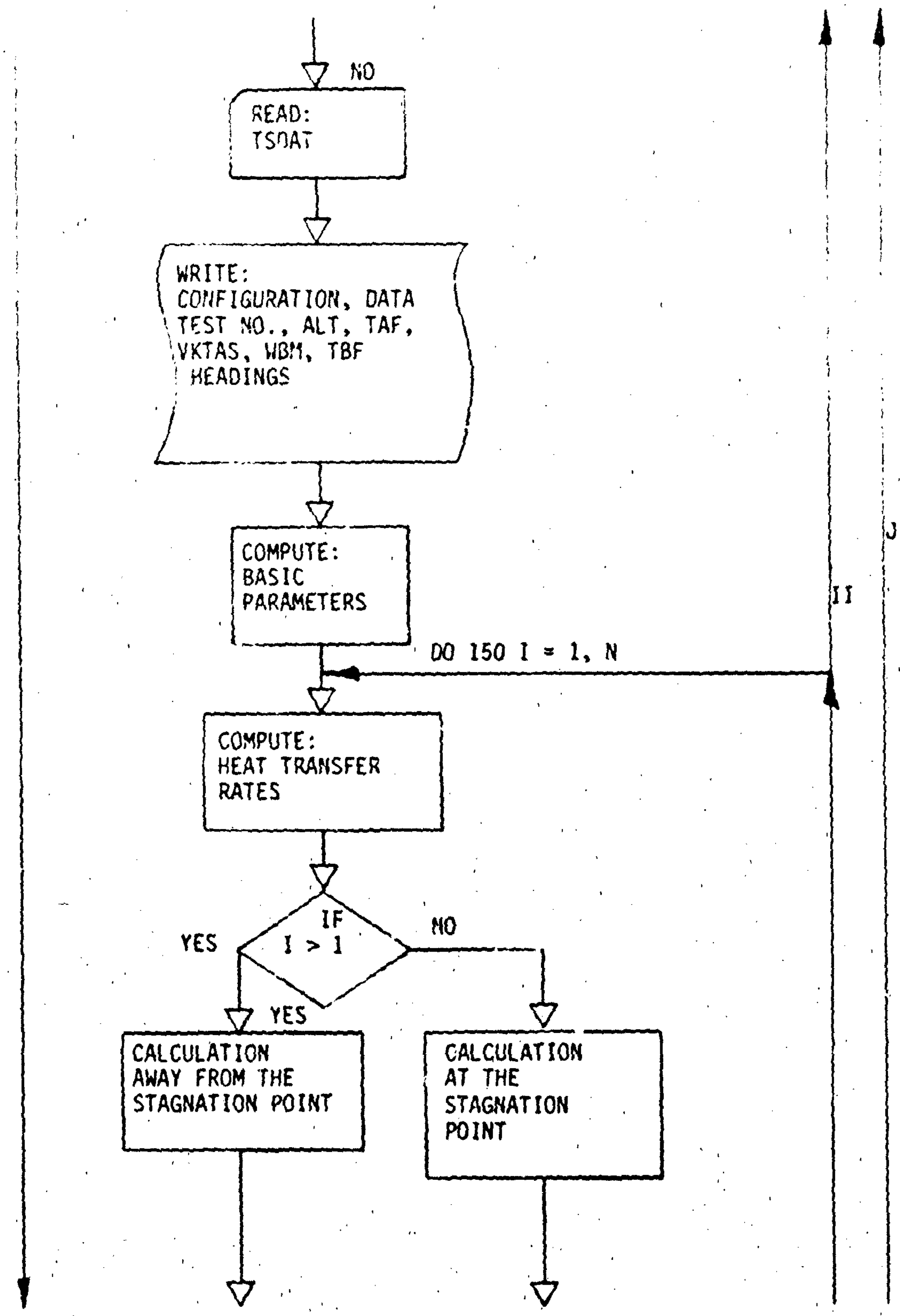

A.1 Flow Chart (Cont.)

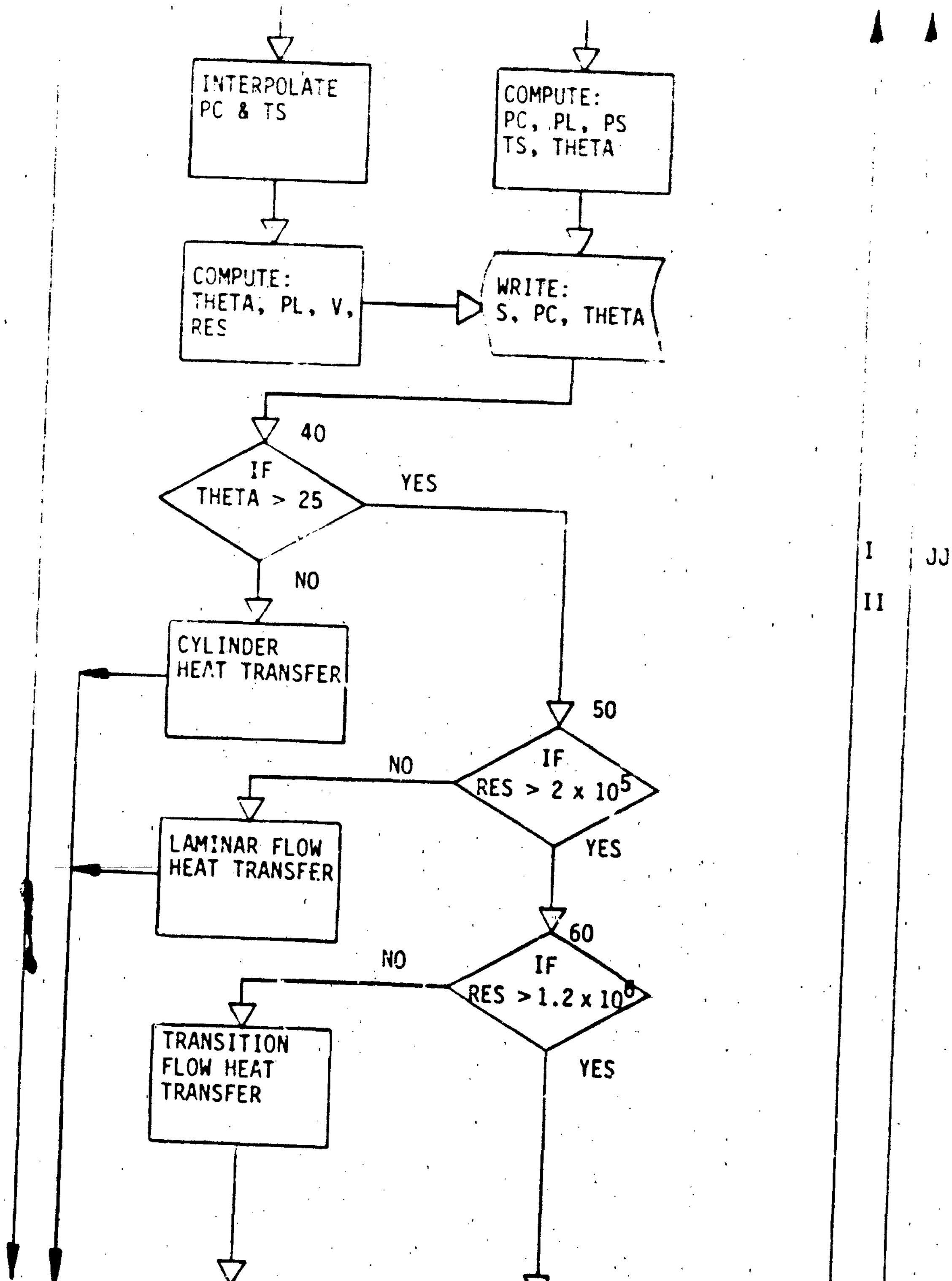

A.1 Flow Chart (Cont.)

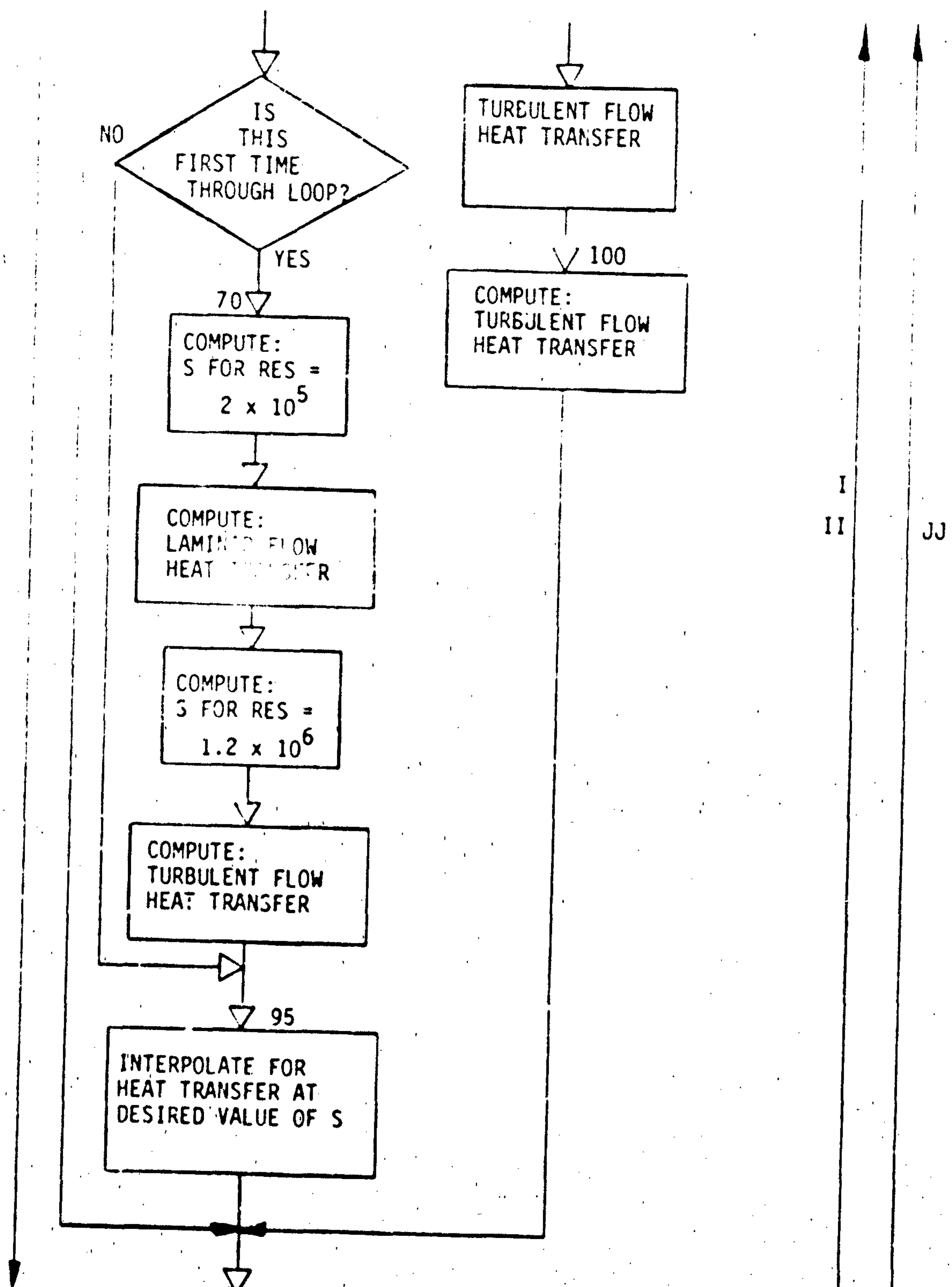

A.1 Flow Chart (Cont.)

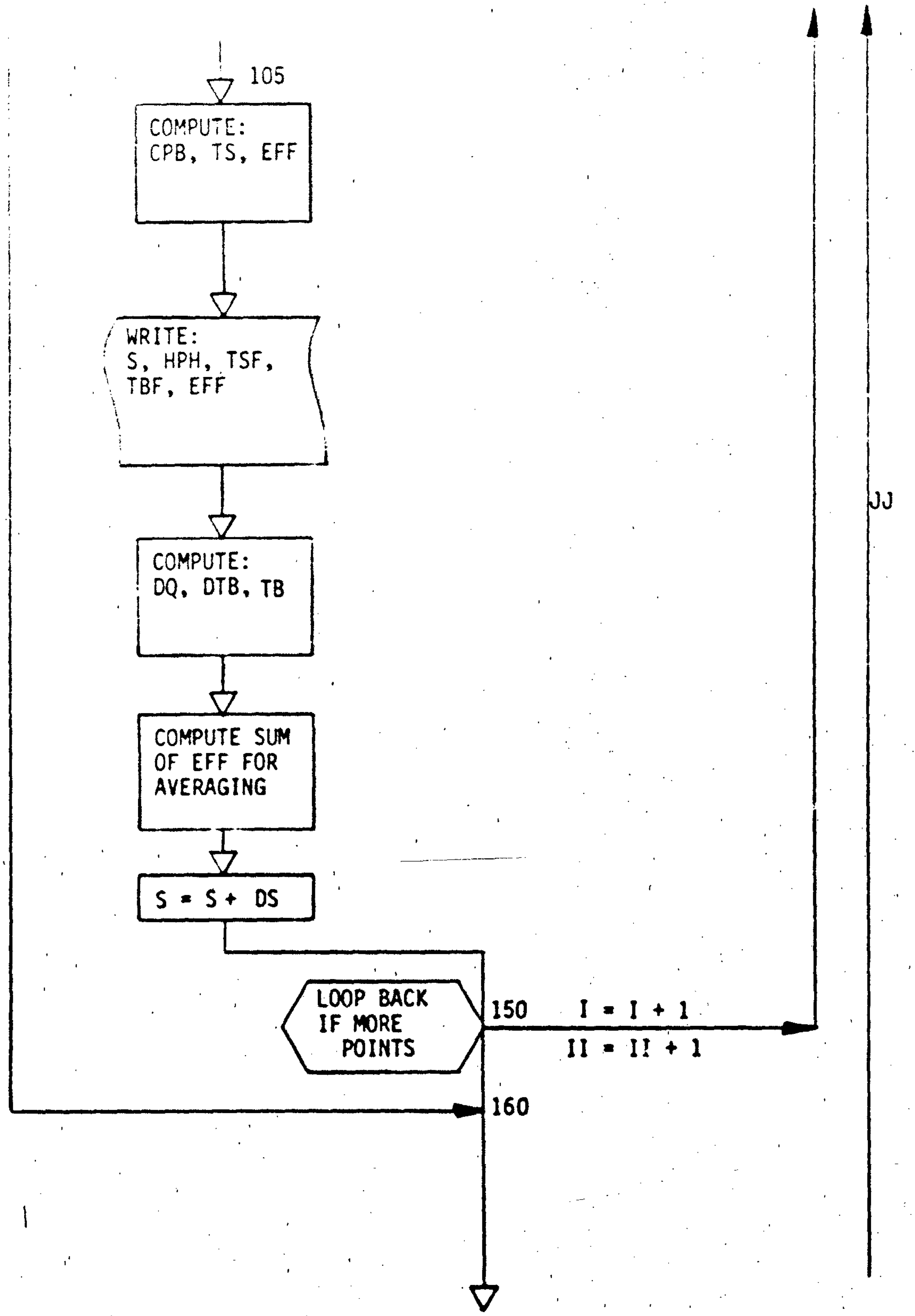

A.1 Flow Chart (Cont.)

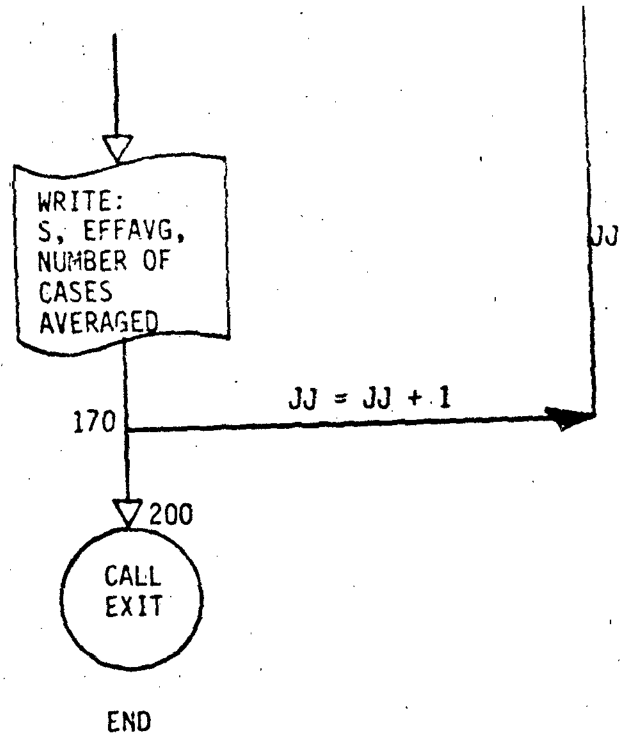

A.2 Input and Operation

This program uses experimental data for flight and bleed air conditions to compute a channel heat transfer efficiency on a point by point analysis.

INPUT PREPARATION

CARD 1 (40A2)	Title This card can contain up to 80 columns of alphanumeric information. It will be used as the heading for the output data sheet.
CARD 2 (4F8)	Nacelle Geometry This card has 4 fields of 8 columns each to contain the variables RLE, SH, DIA and DS (F8.2 format).
Column 1 RLE -	Radius of curvature for the leading edge of the nacelle inlet lip in feet.
Column 9 SH -	Streamwise length of the heated surface in feet. (Heated area per foot circumference).
Column 17 DIA -	Nacelle inlet highlight diameter in feet.
Column 25 DS -	Length of increment used between points of analysis in feet.
CARD 3 (16F5)	Pressure Coefficient Table. This card has 16 fields of 5 columns each to contain streamwise distance measurements, from the stagnation point to the point under analysis, in inches. The values should begin at zero (stagnation point) and increase at any desired interval until the aftmost heated region is reached (F5.2 format).

A.2 Input and Operation (Cont.)

CARD 4 (16F5)	Pressure Coefficient Table. This card has 16 fields of 5 columns each to contain pressure coefficient values for the corresponding points on Card 3 (F5.2 format).
CARD 5 (40A2)	Flight Title. Test or flight number and any pertinent information up to 80 columns (40A2 format).
CARD 6 (5F8)	Flight Parameters. This card has 5 fields of 8 columns each to contain the variables ALT, TAF, VKTAS, WBM and TBF (F8.2 format).
Column 1 ALT -	Altitude (MSL) of aircraft in feet.
Column 9 VKTAS -	True airspeed of the aircraft in knots.
Column 17 TAF -	Ambient temperature in °F.
Column 25 WBM -	Bleed air mass flow per engine in lb/min.
Column 33 TBF -	Bleed air temperature in °F.
CARD 7 (16F5)	Surface Temperature Table. This card has 16 fields of 5 columns each to contain streamwise distance measurements, from the stagnation point to the point under analysis, in inches. The values should begin at zero (stagnation point) and increase at any desired interval until the aftmost heated region is reached (F5.2 format).
CARD 8 (16F5)	Surface Temperature Table. This card has 16 fields of 5 columns each to contain surface temperature values corresponding to the points on Card 7 (F5.1 format).

Up to 100 cases of cards 5, 6, 7 and 8 can be handled at one submission. Card 8 followed by a blank card will cause the routine to calculate point-by-point average efficiencies and then loop back to read new nacelle geometry and pressure distribution data (cards 2, 3 and 4). As many as 20 such configurations can be handled at one submission. Card 8 followed by 2 blank cards will terminate the program.

A.3 Program Listing

```
C.................PROGRAM CHANEFF......6/22/79.........................
C.................ENGINE INLET LIP ANTI-ICE ANALYSIS......................
C.................DETERMINATION OF BLEED AIR CHANNEL EFFICIENCY.........
C
      REAL J,K1,MU
      DIMENSION TITLE(40),FLT(40)
      DIMENSION PSDAT(16,2)
      DIMENSION TSDAT(16,2)
      DIMENSION EFFIC(16)
      DIMENSION SINCH(16)
      OPEN(UNIT=2,NAME='CHANEFF.DAT',TYPE='OLD')
      OPEN(UNIT=3,NAME='CHANEFF.OUT',DISP='PRINT')
C
C-------------------CONSTANTS
C
      IR=2
      IW=3
      NPS=16
      NTS=16
      G=32.174
      J=778.
      PI=3.1416
      R=53.35
C
C-------------------INPUTS
C
      READ(IR,400) TITLE
      DO 170 JJ=1,20
      XM=0.0
      DO 5 L=1,7
      EFFIC(L)=0.0
    5 CONTINUE
      READ(IR,300) RLE,SH,DIA,DS
      IF(RLE .LE. 0.0) CALL EXIT
      SL=SH/2.
      N=SL/DS+1
      READ(IR,1400) PSDAT
      DO 150 II=1,100
      READ(IR,400) FLT
      READ(IR,300) ALT,TAF,VKTAS,WBM,TBF
      IF(VKTAS .LE. 0.0) GO TO 160
      IF(VKTAS .GE. 1.0) GO TO 20
      XM=VKTAS
   20 CONTINUE
      NCASE=II
      READ(IR,1400) TSDAT
      DO 25 L=1, 16
      TSDAT(L,2)=TSDAT(L,2)+459.688
   25 CONTINUE
      TA=TAF+459.688
      TB=TBF+459.688
      WB=WBM/(60.*PI*DIA)
      WRITE(IW,410) TITLE
      WRITE(IW,600) RLE,SH,DIA
      WRITE(IW,400) FLT
      WRITE(IW,700) ALT,TAF,VKTAS,WBM,TBF
      WRITE(IW,800)
C
C-------------------CALCULATION OF BASIC PARAMETERS
C
      A=SQRT(1.4*G*R*TA)
      IF(XM .LE. 0.0) GO TO 30
      VKTAS=XM*A
   30 VO=VKTAS*1.6878
      CP=.2365+7.6*TA/10.**6
      MU=7.475*TA**1.5/(TA+216.)/10.**7
      K1=(4.722+.06944*TA)/10.**7
      PR=CP*MU/K1
      PA=2116.21/EXP(ALT/(27710.-.098774*ALT))
      RHO=PA/TA/R
      REFTO=RHO*VO/MU
      RELE=REFTO*2.*RLE
```

A.3 Program Listing (Cont.)

```
      DP=RHO/2.*VO*VO/G
      T2=VO*VO*PR**.5/(2.*CP*G*J)
C
C-------------------POINT-BY-POINT ANALYSIS OF HEAT TRANSFER
C                   RELATIONSHIPS, STARTING AT STAGNATION
C                   POINT AND ENDING A AFTMOST POINT OF
C                   HEATED REGION
C                   AT AFTMOST POINT OF HEATED REGION
C
C
C-------------------INITIALISE CONDITIONS AND START
C
      S=PSDAT(1,1)/12
      NN=1
      DO 150 I=1,N
      IF (I .GT. 1)  GO TO 35
C
C-------------------STAGNATION POINT CALCULATIONS
C
      PC=PSDAT(I,2)
      TS=TSDAT(I,2)
      THETA=S/RLE*57.30
      WRITE(IW,900)S,PC,THETA
      PL=PA+DP
      GO TO 40
   35 CONTINUE
C
C-------------------CALCULATIONS AWAY FROM THE STAGNATION POINT
C
      PC=TRP(S,PSDAT,NPS)
      TS=TRP(S,TSDAT,NTS)
      THETA=S/RLE*57.30
      WRITE(IW,900)S,PC,THETA
      V=VO*SQRT(1.-PC)
      PL=PA+PC*DP
      RES=REFTO*S*V/VO
   40 CONTINUE
      IF (THETA .GT. 25.0) GO TO 50
C
C-------------------CYLINDER REGION
C
      H=.57*K1*PR**.4*RELE**.5/RLE*(1.-(THETA/90.)**3)
      WRITE(IW,420)
      GO TO 105
   50 CONTINUE
      IF(RES .GT. 2.0E5)  GO TO 60
C
C-------------------LAMINAR FLOW REGION
C
      H=.332*K1*PR**(1./3.)*RES**.5/S
      WRITE(IW,430)
      GO TO 105
   60 CONTINUE
      IF(RES .GT. 1.2E6)  GO TO 100
C
C-------------------TRANSITION FLOW REGION
C
      S11=S
      REST11=RES
      S1=S11-DS
      GO TO (70,95), NN
   70 CONTINUE
C
C-------------------CALCULATION OF PC, V AND H AT THE BEGINNING OF
C                   THE TRANSITION REGION
C
      PC=TRP(S1,PSDAT,NPS)
      V=VO*SQRT(1.-PC)
      REST1=REFTO*S1*V/VO
      IF(ABS(REST1-2.0E5) .LE. 100.) GO TO 75
      S1I=S11+(S1-S11)/(REST1-REST11)*(2.0E5-REST11)
      S11=S1
      REST11=REST1
```

A.3 Program Listing (Cont.)

```
      S1=S11
      GO TO 70
   75 CONTINUE
      HLAM=.332*K1*PR**(1./3.)*REST1**.5/S1
C
C--------------------CALCULATION OF PC, V AND H AT THE END OF THE
C                    TRANSITION REGION
C
      S21=4.*S
      PC=TRP(S21,PSDAT,NPS)
      V=VO*SQRT(1.-PC)
      REST21=REFTO*S21*V/VO
      S2=S21+2.*DS
   80 CONTINUE
      PC=TRP(S2,PSDAT,NPS)
      V=VO*SQRT(1.-PC)
      REST2=REFTO*S2*V/VO
      IF(ABS(REST2-1.2E6) .LE. 100.) GO TO 90
      S2I=S21+(S2-S21)/(REST2-REST21)*(1.2E6-REST21)
      S21=S2
      REST21=REST2
      S2=S2I
      GO TO 80
   90 CONTINUE
      HTURB=0.0296*K1*PR**(1./3.)*REST2**.8/S2
      NU=2
   95 CONTINUE
C
C--------------------INTERPOLATION FOR H BETWEEN THE VALUES AT THE
C                    BEGINNING OF THE TRANSITION REGION AND AT THE
C                    END OF THE TRANSITION REGION
C
      H=HLAM+(HTURB-HLAM)/1.E6*(RES-2.E5)
      WRITE(IW,440)
      GO TO 105
  100 CONTINUE
C
C--------------------TURBULENT FLOW REGION
C
      H=.0296*K1*PR**(1./3.)*RES**.8/S
      WRITE(IW,450)
  105 CONTINUE
C
C--------------------CALCULATE LOCAL CONDITIONS
C
      T5=R*TA*(1.-PR**.5)*(1.-PL/PA)/CP/J
      CPB=.2365+7.6*TB/10.**6
      EFF=H*(TS-TA-T2+T5)*SH/(WB*CPB*(TB-TS))
C
C--------------------OUTPUT
C
      SIN=S*12.
      HPH=H*3600.
      TSF=TS-459.688
      TBF=TB-459.688
      WRITE(IW,500) SIN,HPH,TSF,TBF,EFF
      DQ=H*DS*(TS-TA-T2+T5)
      DTB=DQ/(WB*CPB)
      TB=TB-DTB
      EFFIC(I)=EFF+EFFIC(I)
      SINCH(I)=SIN
      S=S+DS
  150 CONTINUE
  160 CONTINUE
      WRITE(IW,1300)
      DO 165 I=1,N
      EFFAVG=EFFIC(I)/NCASE
      WRITE(IW,1100) SINCH(I), EFFAVG
  165 CONTINUE
      WRITE(IW,1200) NCASE
  170 CONTINUE
  200 CONTINUE
```

A.3 Program Listing (Cont.)

```
  300 FORMAT(10F8.2)
  400 FORMAT(40A2)
  410 FORMAT(1H1,40A2)
  420 FORMAT(5X,'** CYLINDER **')
  430 FORMAT(5X,'** LAMINAR **')
  440 FORMAT(5X,'** TRANSITION **')
  450 FORMAT(5X,'** TURBULENT **')
  500 FORMAT(4F15.2,F15.3//)
  600 FORMAT(//22X,'LEADING EDGE RADIUS',8X,F5.3,' FT'/
     122X,'HEATED AREA PER FOOT SPAN',F7.3,' SQFT'/
     222X'LIP HIGHLIGHT DIAMETER',4X,F6.3,' FT'//)
  700 FORMAT(/22X,'ALTITUDE',15X,F7.1,' FT'/22X,'AMB TEMP',17X,F5.1,' F'
     1/22X,'AIRSPEED',17X,F5.1,' KTAS'/22X,'BLEED FLOW PER ENGINE',5X,
     2F4.1,' LB/MIN'/22X,'BLEED TEMP',15X,F5.1,' F'/)
  800 FORMAT(///10X,'S(IN)',7X,'(F PER HR)',3X,'(SKIN TEMP,F)',2X,'(DIFF
     1D TEMP,F)',7X,'EFF'/)
  900 FORMAT(1H ,'S=', E15.8,5X,'PC=',E15.8,5X,'THETA = ',F6.2)
 1100 FORMAT(F15.2,F15.3)
 1200 FORMAT(1H0,10X,'NUMBER OF CASES AVERAGED = ',I3)
 1300 FORMAT(1H1,10X,'S(IN)',8X,'EFF(AVG)'//)
 1400 FORMAT(16F5.2)
      CALL EXIT
      END
```

A.4 Function TRF Listing

```
      FUNCTION TRF(S,PSDAT,IMAX)
      DIMENSION PSDAT(16,2)
      DO 140 K=1, IMAX, 2
      IF(S*12.-PSDAT(K+2,1))150, 130, 130
130   CONTINUE
      IF(PSDAT(K+2,1)-PSDAT(K+3,1)) 140, 140, 150
140   CONTINUE
150   CONTINUE
      PC=PSDAT(K,2)+(S*12.-PSDAT(K,1))*((PSDAT(K+1,2)-PSDAT(K,2))/
     1(PSDAT(K+1,1)-PSDAT(K,1))+(S*12.-PSDAT(K+1,1))/(PSDAT(K+2,1)-
     2PSDAT(K,1))*((PSDAT(K+2,2)-PSDAT(K+1,2))/(PSDAT(K+2,1)-
     3PSDAT(K+1,1))-(PSDAT(K+1,2)-PSDAT(K,2))/(PSDAT(K+1,1)-PSDAT(K,1)))
     4)
      TRF = PC
      RETURN
      END
```

A.5 Sample Input Data

```
                    MODEL 35 ENGINE INLET LIP BLEED AIR CHANNEL EFFICIENCY
.125     .558     7.237     .041667
0.0  0.5  1.0  1.5  2.0  2.5  3.0  3.5  4.0  4.5  5.0
1.    .97  .13-1.47-1.30 -.94 -.81 -.77 -.81 -.92-1.09
                    CONFIGURATION 10A UPPER LIP                TAF CORRECTED
3154.   1.33        224.4        14.95     407.4
0.0  0.5  1.0  1.5  2.0  2.5  3.0  3.5  4.5
184. 192. 204. 223. 160. 100.  94.  94.  94.
                    CONFIGURATION 11A UPPER LIP                TAF CORRECTED
3193.   1.9         226.1        12.07     451.1
0.0  0.5  1.0  1.5  2.0  2.5  3.0  3.5  4.5
196. 199. 212. 237. 168. 103.  95.  95.  95.
                    CONFIGURATION 12A UPPER LIP                TAF CORRECTED
3187.   3.2         226.0        14.97     453.2
0.0  0.5  1.0  1.5  2.0  2.5  3.0  3.5  4.5
208. 218. 232. 258. 184. 114. 108. 108. 108.
                    CONFIGURATION 13A UPPER LIP                TAF CORRECTED
1756.  -6.95        142.6        11.94     351.0
0.0  0.5  1.0  1.5  2.0  2.5  3.0  3.5  4.5
155. 162. 175. 185. 145.  86.  74.  74.  74.
                    CONFIGURATION 14A UPPER LIP                TAF CORRECTED
1740.  -7.3         142.1        14.94     349.6
0.0  0.5  1.0  1.5  2.0  2.5  3.0  3.5  4.5
172. 180. 193. 200. 166.  96.  88.  88.  88.
                    CONFIGURATION 15A UPPER LIP                TAF CORRECTED
1748.  -6.6         142.7        12.09     402.0
0.0  0.5  1.0  1.5  2.0  2.5  3.0  3.5  4.5
182. 190. 203. 218. 171. 102.  92.  92.  92.
                    CONFIGURATION 16A UPPER LIP                TAF CORRECTED
1738.  -6.9         142.2        15.46     399.7
0.0  0.5  1.0  1.5  2.0  2.5  3.0  3.5  4.5
199. 208. 224. 237. 166. 113. 105. 105. 105.
                    CONFIGURATION 17A UPPER LIP                TAF CORRECTED
1740.  -7.          142.7        12.01     450.6
0.0  0.5  1.0  1.5  2.0  2.5  3.0  3.5  4.5
205. 214. 230. 250. 192. 116. 106. 106. 106.
                    CONFIGURATION 18A UPPER LIP                TAF CORRECTED
1740.  -7.2         142.4        15.04     457.6
0.0  0.5  1.0  1.5  2.0  2.5  3.0  3.5  4.5
225. 234. 252. 274. 210. 128. 121. 121. 121.
                    CONFIGURATION 19A UPPER LIP                TAF CORRECTED
2794.  -22.6        196.2        12.09     350.8
0.0  0.5  1.0  1.5  2.0  2.5  3.0  3.5  4.5
136. 139. 156. 165. 116.  62.  56.  56.  56.
                    CONFIGURATION 20A UPPER LIP                TAF CORRECTED
2816.  -20.9        197.6        15.2      350.2
0.0  0.5  1.0  1.5  2.0  2.5  3.0  3.5  4.5
152. 156. 174. 182. 130.  72.  68.  68.  68.
                    CONFIGURATION 21A UPPER LIP                TAF CORRECTED
2794.  -20.5        196.3        12.09     401.1
0.0  0.5  1.0  1.5  2.0  2.5  3.0  3.5  4.5
158. 161. 182. 196. 136.  75.  69.  69.  69.
                    CONFIGURATION 22A UPPER LIP                TAF CORRECTED
2786.  -20.8        196.         14.89     401.3
0.0  0.5  1.0  1.5  2.0  2.5  3.0  3.5  4.5
176. 180. 202. 216. 153.  85.  82.  82.  82.
                    CONFIGURATION 23A UPPER LIP                TAF CORRECTED
2775.  -20.7        196.1        12.03     451.1
0.0  0.5  1.0  1.5  2.0  2.5  3.0  3.5  4.5
180. 185. 208. 226. 158.  87.  81.  81.  81.
                    CONFIGURATION 24A UPPER LIP                TAF CORRECTED
2741.  -20.5        194.1        14.76     451.7
0.0  0.5  1.0  1.5  2.0  2.5  3.0  3.5  4.5
200. 205. 230. 248. 176. 100.  96.  96.  96.
```

A.6 Sample Output Data

```
            MODEL 35 ENGINE INLET LIP BLEED AIR CHANNEL EFFICIENCY

                    LEADING EDGE RADIUS            0.125 FT
                    HEATED AREA PER FOOT SPAN      0.558 SQFT
                    LIP HIGHLIGHT DIAMETER         2.237 FT

        CONFIGURATION 10A UPPER LIP       TAF CORRECTED

                    ALTITUDE                    3154.0 FT
                    AMB TEMP                       1.3 F
                    AIRSPEED                     224.8 KTAS
                    BLEED FLOW PER ENGINE         14.9 LB/MIN
                    BLEED TEMP                   402.4 F

         S(IN)          (H PER HR)   (SKIN TEMP,F)  (BLEED TEMP,F)        EFF

S= 0.00000000E+00     PC= 0.10000000E+01      THETA =   0.00
   ** CYLINDER **
         0.00             43.00          184.00          402.40           0.601

S= 0.41666999E-01     PC= 0.96999657E+00      THETA =  19.10
   ** CYLINDER **
         0.50             42.59          192.00          392.54           0.683

S= 0.83333999E-01     PC= 0.12996030E+00      THETA =  38.20
   ** TRANSITION **
         1.00             21.74          204.00          382.32           0.422

S= 0.12500100E+00     PC=-0.14700172E+01      THETA =  57.30
   ** TRANSITION **
         1.50             39.10          223.00          376.70           0.941

S= 0.16666800E+00     PC=-0.12999848E+01      THETA =  76.40
   ** TRANSITION **
         2.00             47.34          160.00          365.44           0.626

S= 0.20833500E+00     PC=-0.93999022E+00      THETA =  95.50
   ** TRANSITION **
         2.50             52.81          100.00          355.83           0.336

S= 0.25000200E+00     PC=-0.80999613E+00      THETA = 114.60
   ** TRANSITION **
         3.00             59.56           94.00          349.41           0.353
```

A.6 Sample Output Data (Cont.)

S(IN)	EFF(AVG)
0.00	0.627
0.50	0.598
1.00	0.445
1.50	0.397
2.00	0.379
2.50	0.317
3.00	0.328

NUMBER OF CASES AVERAGED = 15

APPENDIX B - ICING ANALYSIS PROGRAM

B.1 Flow Chart

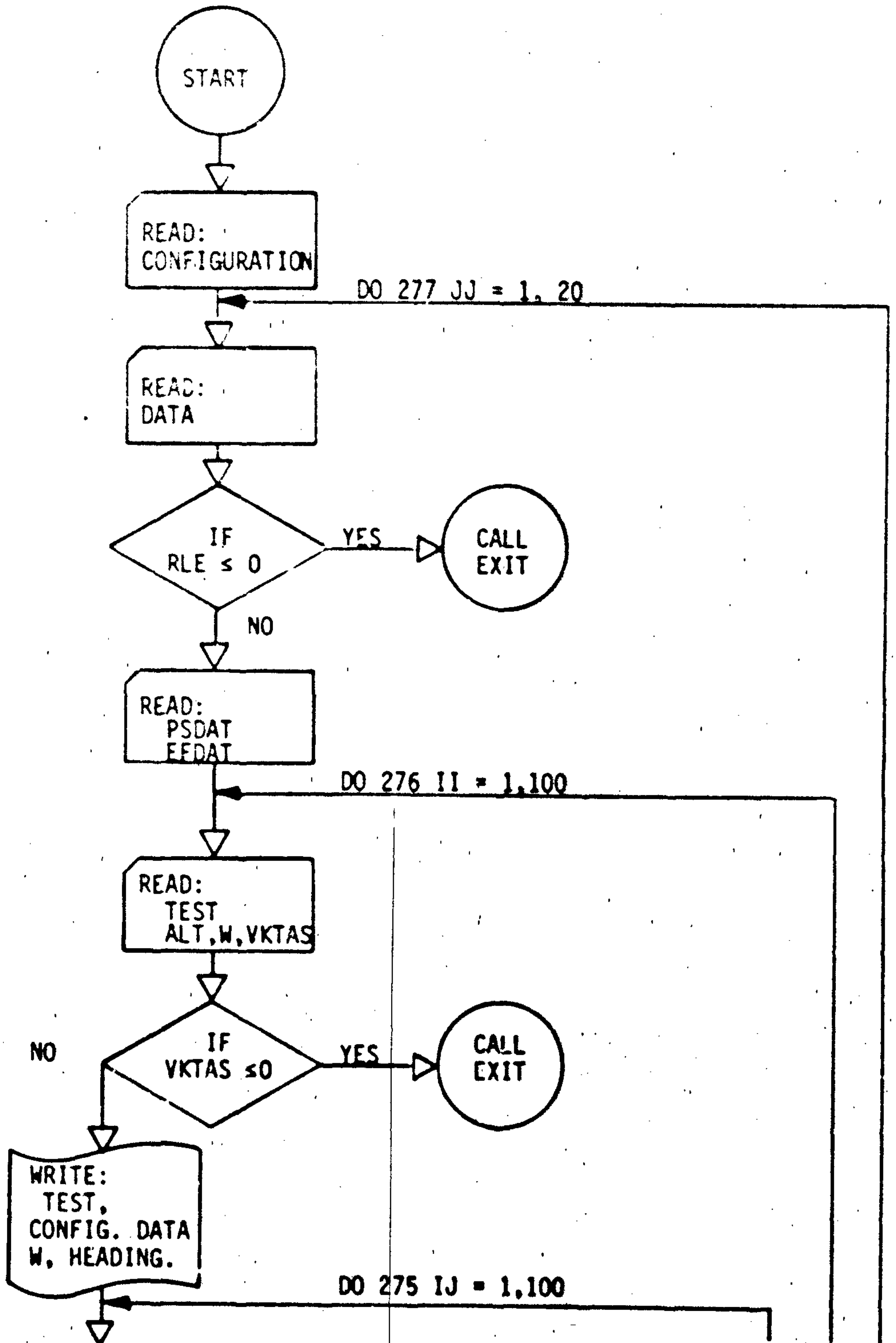

B.1 Flow Chart (Cont.)

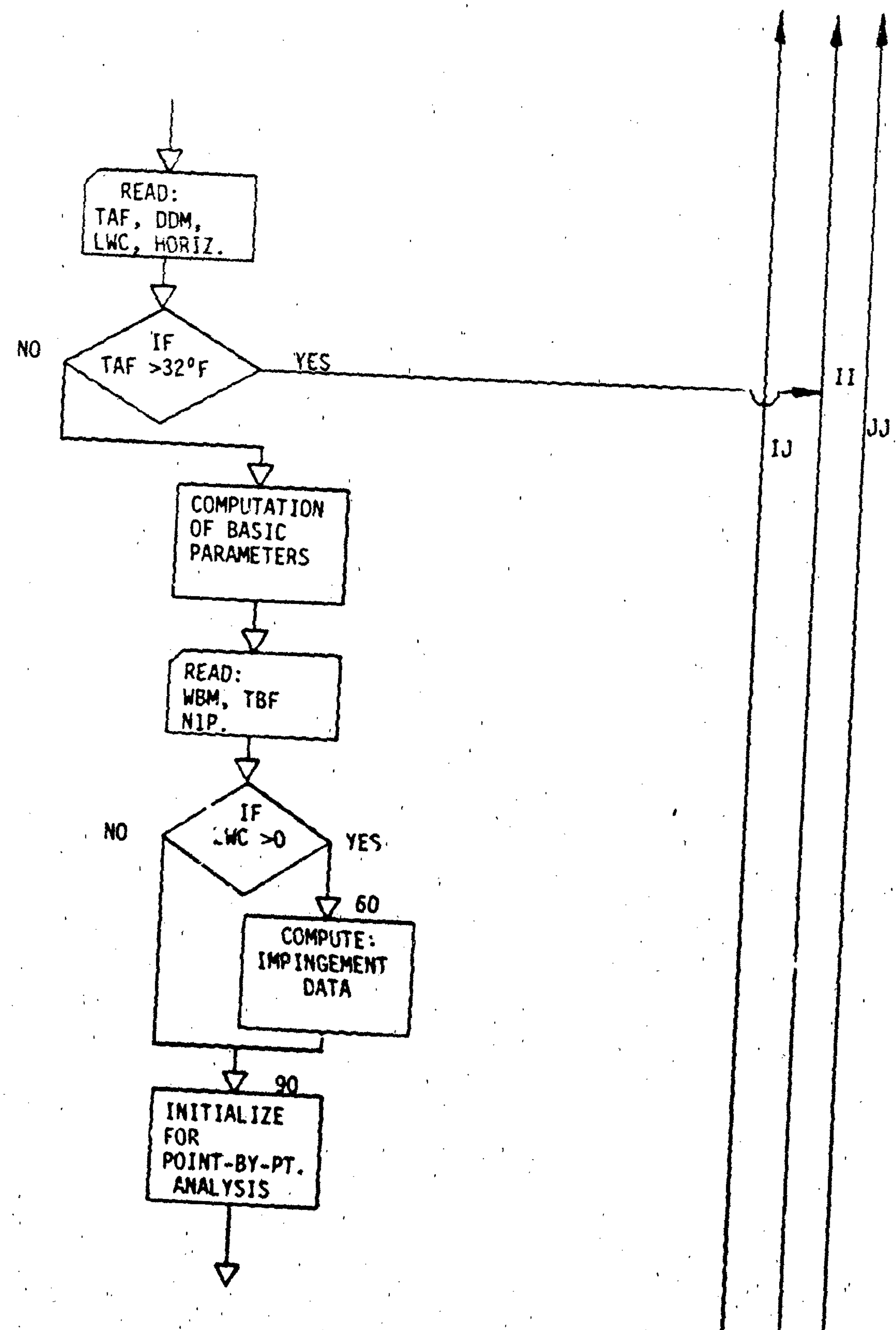

B.1 Flow Chart(Cont.)

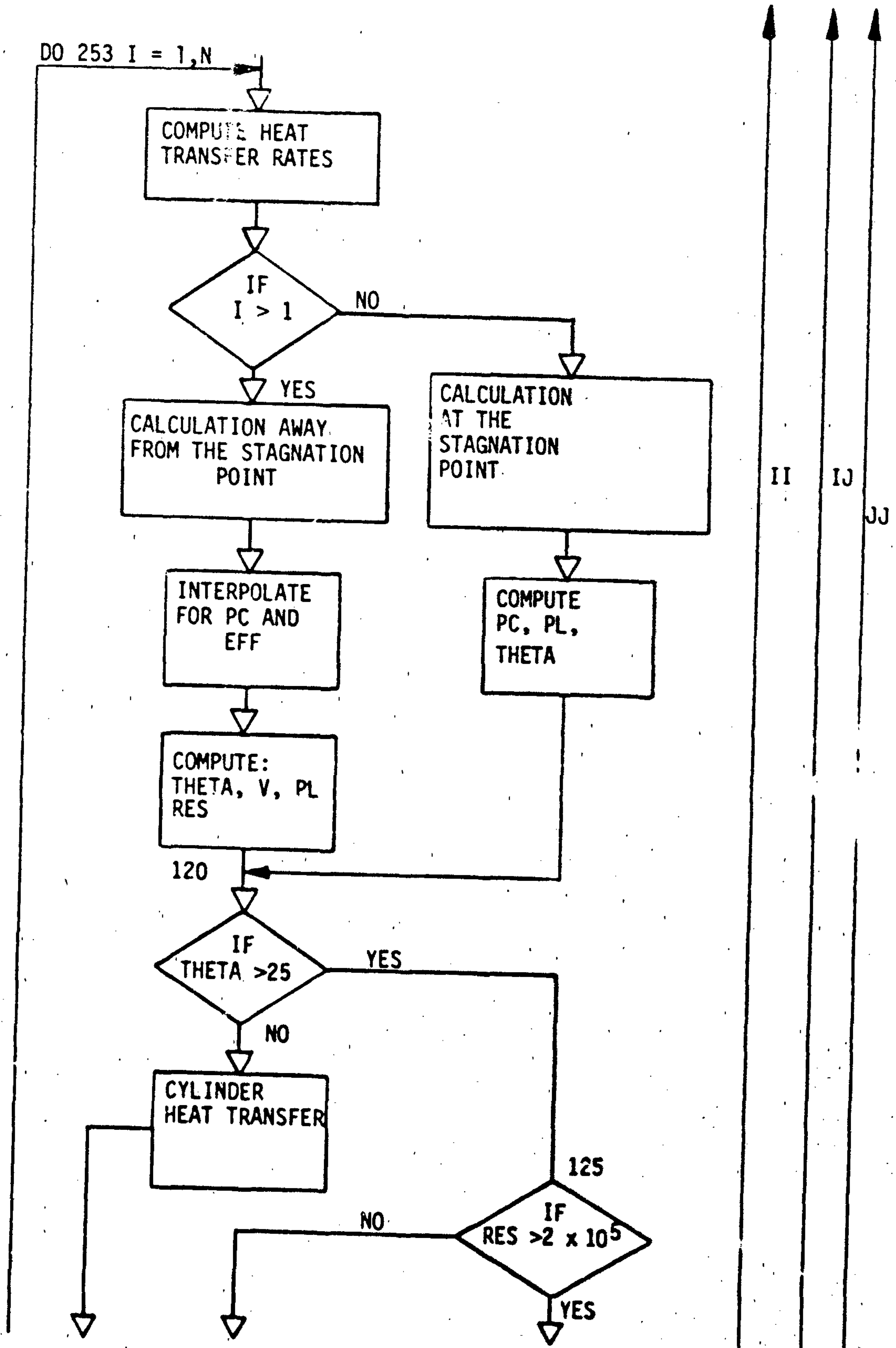

B.1 Flow Chart(Cont.)

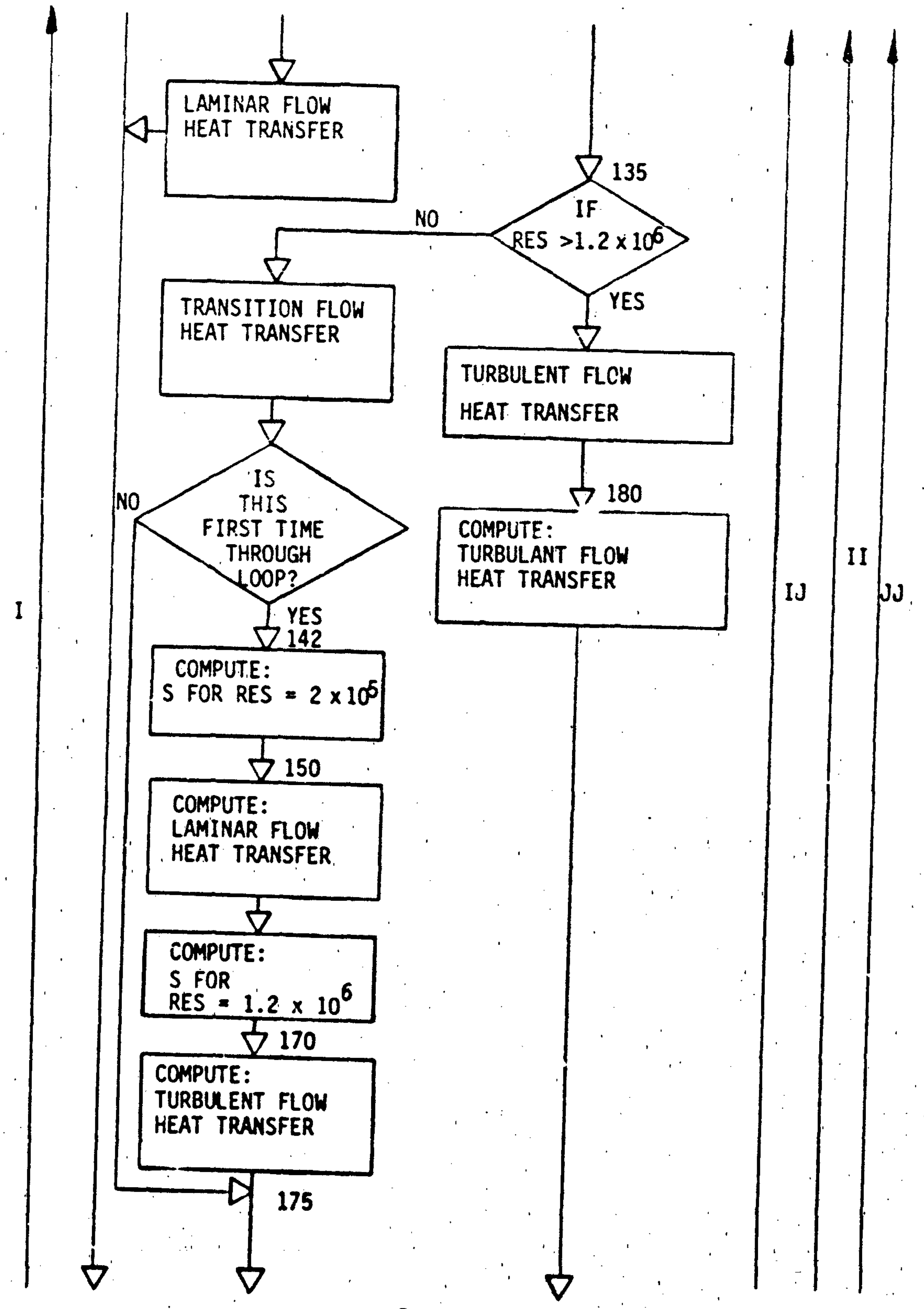

B.1 Flow Chart(Cont.)

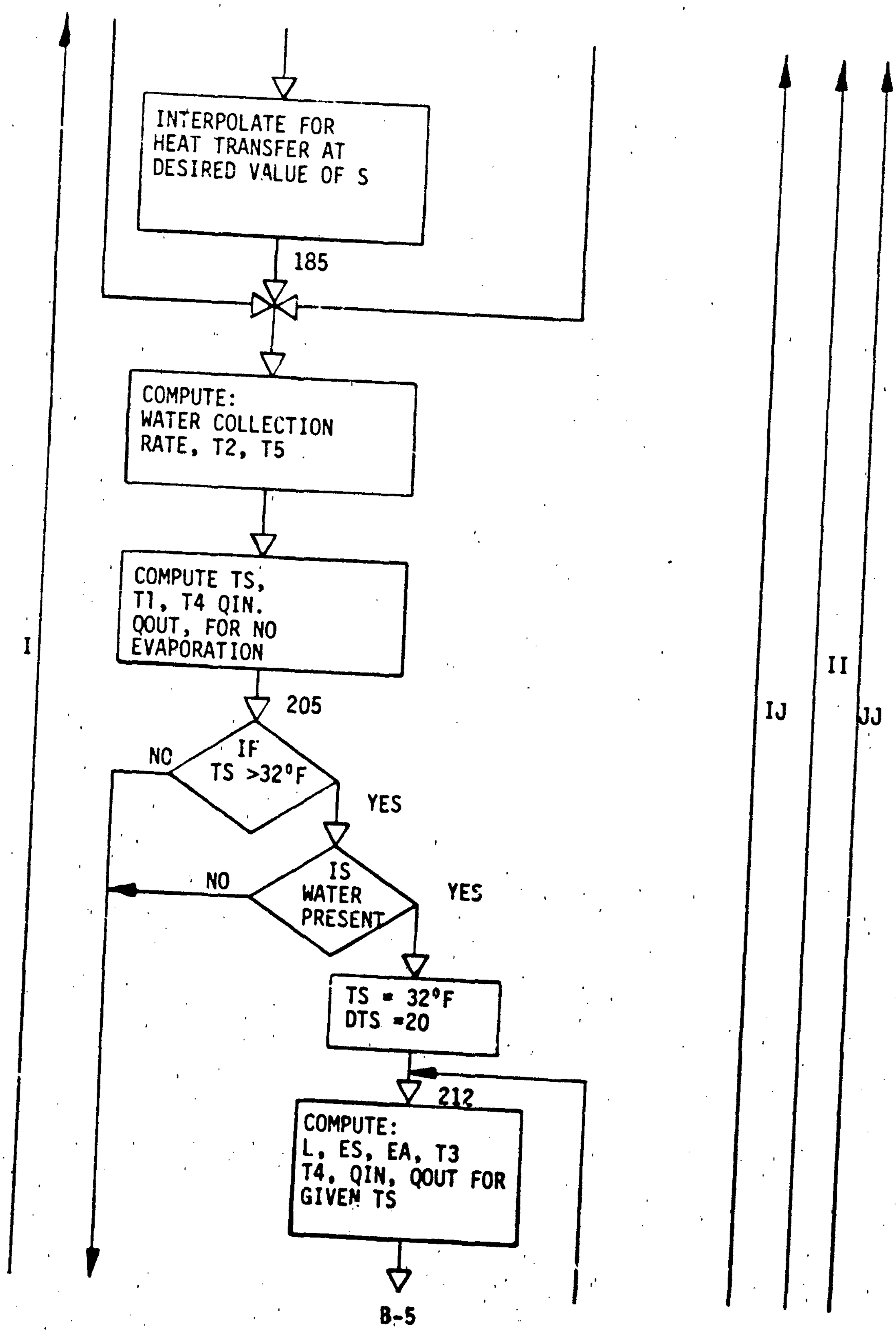

B.1 Flow Chart (Cont.)

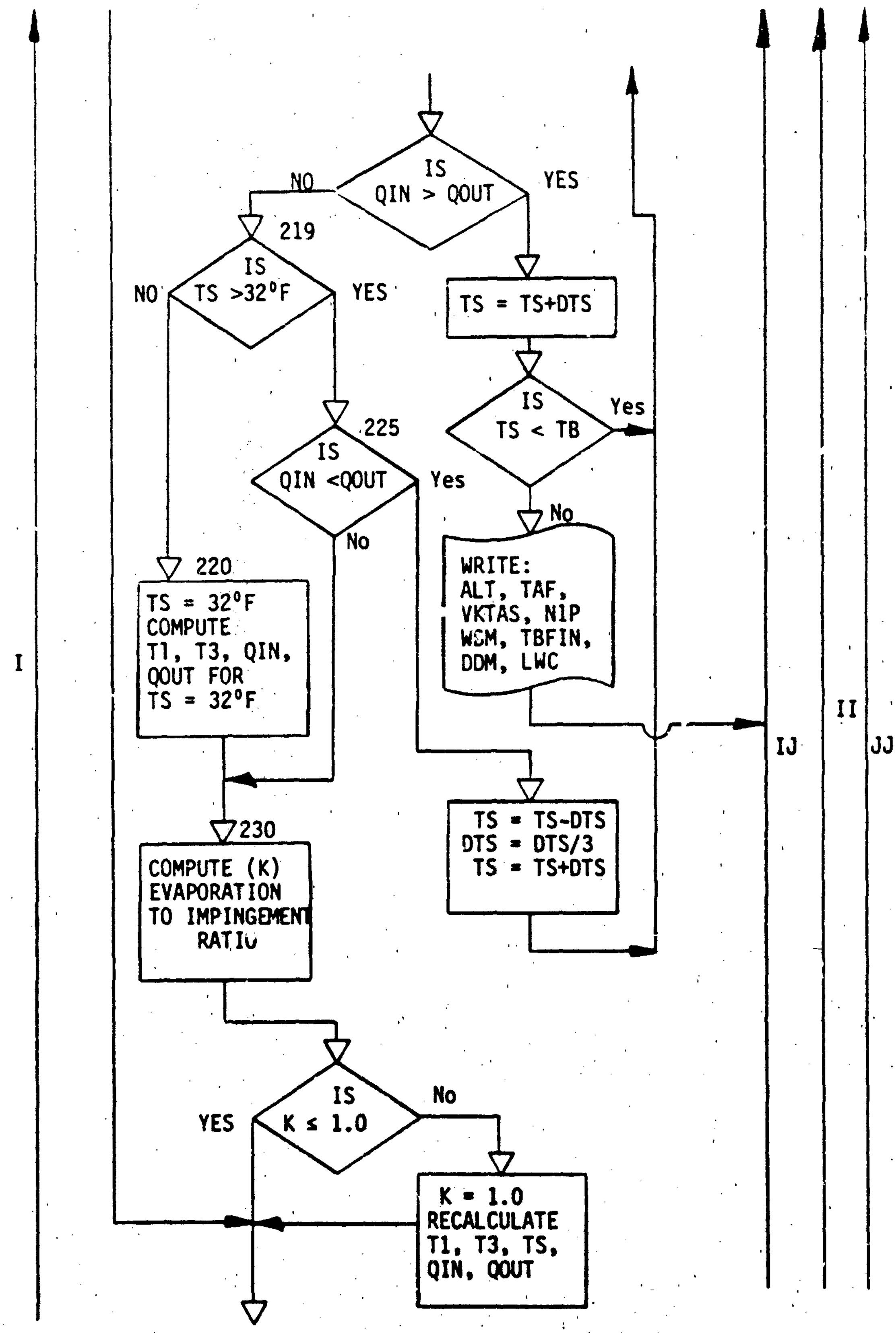

B.1 Flow Chart (Cont.)

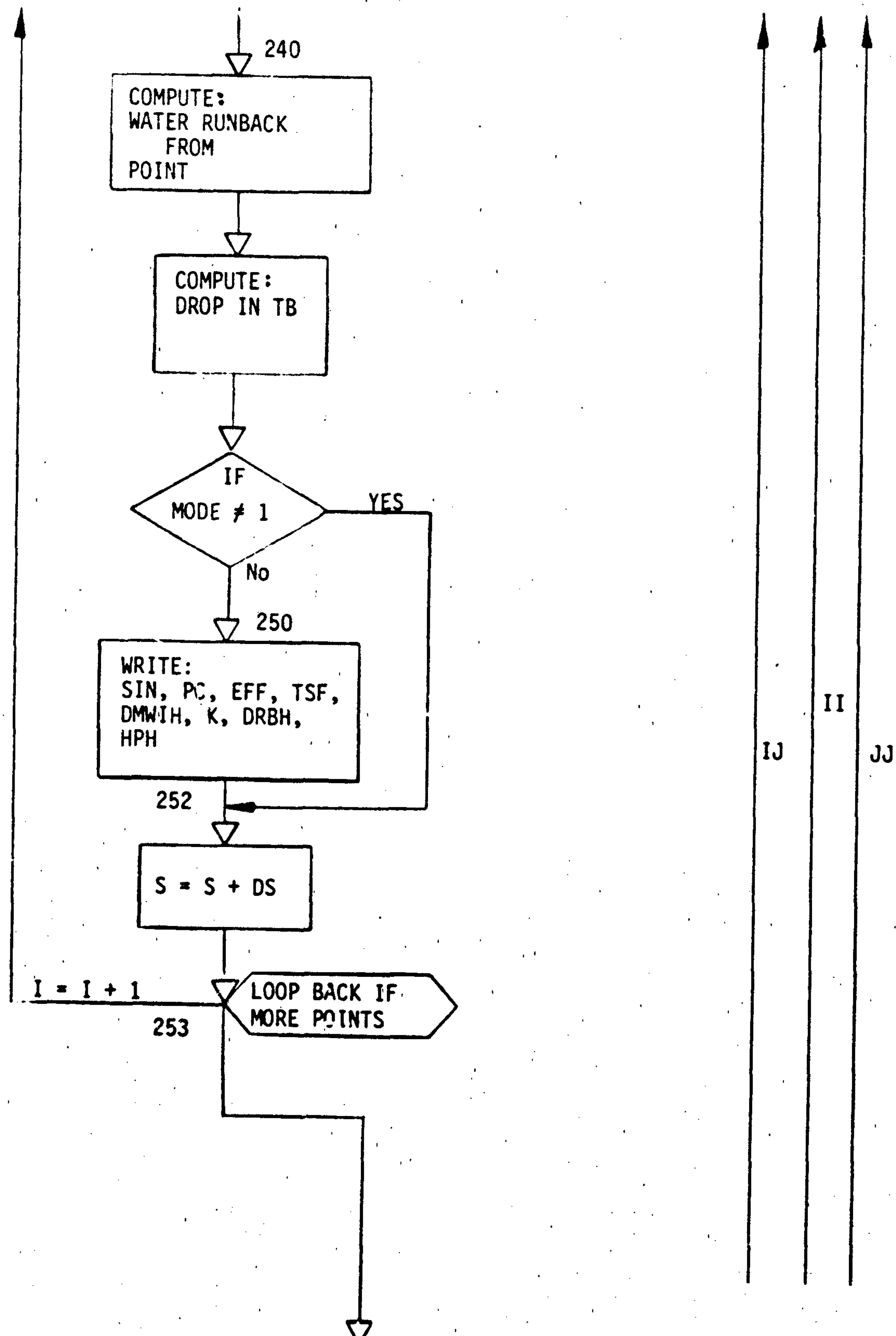

B.1 Flow Chart(Cont.)

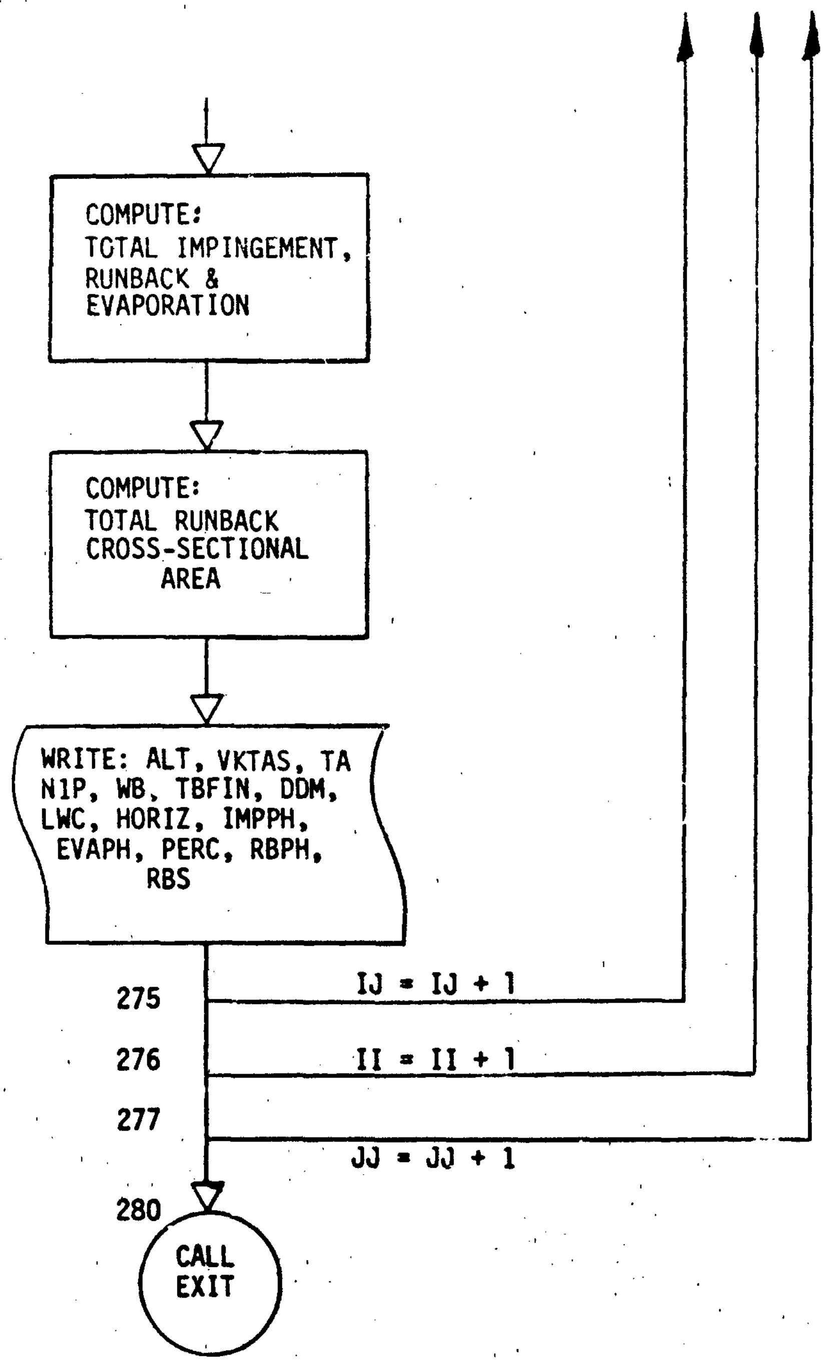

END

B.2 Input and Operation

MODE - 1

This mode of operation reduces experimental data to check for accuracy. An expanded output shows results of intermediate calculations in the point-by-point analysis.

INPUT PREPARATION FOR MODE - I

CARD 1 (20A4)	Title This card can contain up to 80 columns of alphanumeric information. It will be used as the heading on the putput data sheet (20A4 format).
CARD 2 (1F10)	Mode Enter a "1." in column 1 for Mode I operation (F10.3 format).
CARD 3 (8F10)	Nacelle Geometry. This card has 8 fields of 10 columns each to contain the variables C, TOC, RLE, DIA, SH, SW, CDO. (F10.3 format).

Column 1	C	-	Chordwise length of nacelle in feet.
Column 11	TOC	-	Thickness ratio (maximum nacelle thickness/chordwise length) non-dimensional.
Column 21	RLE	-	Radius of curvature for the leading edge of nacelle inlet lip in feet.
Column 31	DIA	-	Nacelle inlet highlight diameter in feet.
Column 41	SH	-	Streamwise length of the heated surface in feet. (Heated area per foot circumference).
Column 51	SW	-	Aircraft wing area in square feet.
Column 61	CDO	-	Drag polar term (C_{Do} or $C_{Dintercept}$).
Column 71	DCD	-	Drag polar term (k or $C_{D_{slope}}$) (C_D = CDO + (DCD)C_L^2 Drag polar).

B.2 Input and Operation (Cont.)

CARD 4	(15F5)	Pressure Coefficient Table. This card has 15 fields of 5 columns each to contain streamwise distance measurements, from stagnation point to point under analysis, in inches. The values shall begin at zero (stagnation point) and increase at any desired interval until the aftmost heated region is reached (F5.0 format).
CARD 5	(15F5)	Pressure Coefficient Table. This card has 15 fields of 5 columns each to contain pressure coefficient values for the corresponding points on card 4 (F5.0 format).
CARD 6	(10F7)	Efficiency Profile Table. This card has 10 fields of 7 columns each containing the streamwise distance measurements from the stagnation point to the point under analysis, in inches. The values increase at any desired interval until the aftmost heated region is reached (F7.3 format).
CARD 7	(10F7)	Efficiency Profile Table. This card has 10 fields of 7 columns each containing the channel efficiency values for the corresponding points on Card 6. (F7.3 format).
CARD 8	(20A4)	Test Title. Test number and any pertinent information up to 80 columns (20A4 format).

B.2 Input and Operation (Cont.)

CARD 9 (3F10)		Flight Parameters. This card has 3 fields of 10 columns each to contain the variables ALT, W, VKTAS (F10.3 format).
Column 1 ALT	-	Altitude (MSL) of aircraft in feet.
Column 11 W	-	Weight of aircraft in pounds.
Column 21 VKTAS	-	True airspeed of aircraft in knots.
CARD 10 (4F10)		Icing Conditions. This card has 4 fields of 10 columns each to contain the variables TA, DDM, LWC, & HORIZ (F10.3 format).
Column 1 TA	-	Ambient Temperature (in°F).
Column 11 DDM	-	Water droplet median diameter in microns.
Column 21 LWC	-	Liquid water content of surrounding air in grams/cubic meter.
Column 31 HORIZ	-	Horizontal cloud extent in statute miles.
CARD 11 (3F10)		Bleed Air Data. This card has 3 fields of 10 columns each to contain the variables WBM, TBIN, N1P (F10.3) format).
Column 1 WBM	-	Bleed air mass flow rate per engine in lb/min.
Column 11 TBIN	-	Bleed air temperature in °F.
Column 21 N1P	-	Percent engine RPM.

In this mode a dummy card with "33." punched starting in column 1 should follow card 11. This will loop the routine back to read in a new set of test data. Cards 8, 9, 10 and 11 followed by a "33." card should be repeated for as many test cases desired up to 100 tests.

One blank card following a dummy "33." card will allow the input of new mode, nacelle geometry and pressure and efficiency data cards. Two blank cards following a dummy "33." card will terminate the program.

B.2 Input and Operation (Cont.)

Mode II

This mode of operation is for icing prediction under given flight and icing conditions. Intermediate information or calculations are not shown.

INPUT PREPARATION FOR MODE II

CARD 1 (20A4)	Title. Prepared same as for Mode I operation.
CARD 2 (1F10)	Mode. Enter a 2. in column 1 for Mode II operation (F10.3 format).
CARDS 3-7	Same input as described under Mode I operation.
CARD 8	Flight Parameters. This card has 3 fields of 10 columns each to contain the variables ALT, W, VKTAS, (F10.3 format). These variables are input the same as for Card 9 under Mode I operation.
CARD 9 (4F10)	Icing Conditions. This card has 4 fields of 10 columns each to contain the variables TA, DDM, LWC, & HORIZ (F10.3 format). This data is input the same as for Card 10 under Mode I operation.
CARD 10 (3F10)	Bleed Air Data. This card has 3 fields of 10 columns each to contain the variables WBM, TBIN and N1P (F10.3 format). This data is input the same as for Card 11 under Mode I operation.

In this mode up to 100 sets of cards 9 and 10 may follow a Flight Parameter card. A dummy "33." card following a card 9 and 10 set will allow input of a new Flight Parameter Card 8. One or two blank cards following a dummy "33." card has the same effect on the program as during Mode I operation.

B.3 Program Listing

```
C.................. PROGRAM ICEOFF ..........6/22/79.....................
C.................. ENGINE INLET LIP ANTI-ICE ANALYSIS .....................
C.................. DETERMINATION OF ANTI-ICING PERFORMANCE ..................
C
      REAL J,K,K0,K1,K2,L,LOLS,LWC,MU,MW,MWAV,MWIMP,MWLE,N1P,IMPPH
      REAL MODE
      DIMENSION PSDAT(16,2)
      DIMENSION EFDAT(16,2)
      DIMENSION TITLE(20)
      DIMENSION TEST(20)
      OPEN(UNIT=2,NAME='ICFOFF.DAT',TYPE='OLD')
      OPEN(UNIT=3,NAME='ICFOFF.OUT',DISP='PRINT')
C
C-------------------CONSTANTS
C
      IR=2
      IW=3
      NPS=16
      NES=10
      G=32.174
      PI=3.1416
      J=778.
      R=53.35
      DS=.0416667
      DTSIN=20.
C
C-------------------INPUTS
C
      READ(IR,300) TITLE
      DO 277 JJ=1,20
      READ(IR,310) MODE
      READ(IR,310) C,TOC,RLE,DIA,SH,SW,CDO,DCD
      IF(RLE .LE. 0.0) GO TO 280
      READ(IR,1100) ((PSDAT(I,N), I=1,NPS), N=1,2)
      READ(IR,1200) ((EFDAT(I,N), I=1,NES), N=1,2)
      DO 276 II=1,100
      XM=0.0
      IF(MODE .NE. 1.0) GO TO 15
      READ(IR,300) TEST
   15 CONTINUE
      READ(IR,310) ALT,W,VKTAS
      IF(VKTAS .LE. 0.0) CALL EXIT
      IF(VKTAS .GE. 1.)  GO TO 20
      XM=VKTAS
   20 CONTINUE
      WRITE(IW,330) TITLE
      IF(MODE .NE. 1.0) GO TO 25
      WRITE(IW,320) TEST
   25 CONTINUE
C
C-------------------CONVERSION OF INPUT DATA TO INCHES
C
      CIN=12.*C
      RLEIN=12.*RLE
      DIAIN=12.*DIA
      SHIN=12.*SH
      WRITE(IW,400) CIN,TOC,RLEIN,DIAIN,SHIN,SW,CDO,DCD
      WRITE(IW,500) W
      WRITE(IW,600)
      DO 275 IJ=1,100
      READ(IR,310) TAF,DDM,LWC,HORIZ
      IF(TAF .GT. 32.) GO TO 276
C
C-------------------CONVERSION OF UNITS
C
      SL=SH/2.
      N=SL/DS+1
      TA=TAF+459.688
      DD=DDM*3.281/10.**6
C
C-------------------CALCULATION OF BASIC PARAMETERS
C
```

B.3 Program Listing (Cont.)

```
      A=SQRT(1.4*G*R*TA)
      IF(XM .LE. 0.0) GO TO 40
      VKTAS=XM*A/1.6878
   40 VO=VKTAS*1.6878
      CP=.2365+7.6*TA/10.**6
      MU=7.475*TA**1.5/(TA+216.)/10.**7
      K1=(4.722+.0694*TA)/10.**7
      PR=CP*MU/K1
      PA=2116.21/EXP(ALT/(27710.-.098774*ALT))
      RHO=PA/TA/R
      REFTO=RHO*VO/MU
      RELE=REFTO*2.*RLE
      XM=VO/A
C
C--------------------CALCULATION OF BLEED-AIR DATA
C
      DP=RHO/2.*VO*VO/G
      CL=W/DP/SW
      FN=(CDO+DCD*CL*CL)*DP*SW/2.
C
C--------------------INSERT CALL FOR ENGINE PERFORMANCE
C                    PROGRAM TO OBTAIN BLEED AIR FLOW
C                    RATE AND TEMPERATURE OR READ THIS
C                    DATA FROM INPUT
C
      READ(IR,310) WBM,TBF,N1P
      TBIN=TBF+459.688
      WB=WBM/60./PI/DIA
C
C--------------------CALCULATION OF IMPINGEMENT DATA
C
      IF(LWC .GT. 0.0) GO TO 60
      MWLE=0.
      GO TO 90
   60 CONTINUE
      RED=REFTO*DD
      IF(RED .GT. 200.) GO TO 70
   68 LOLS=.98-.134*ALOG(RED)
      GO TO 71
   70 LOLS=.74-.0887*ALOG(RED)
   71 K2=.108*VO/MU/C*DD*DD*G
      KO=K2*LOLS
      IF(KO .GT. .01) GO TO 80
      IF(KO .LT. .004)  GO TO 77
   75 EM=.0873*(ALOG(KO)+5.522)
      GO TO 85
   77 EM=0.
      GO TO 85
   80 IF(KO .GT. .4)  GO TO 83
      EM=.08+.31*(2.+.4342*ALOG(KO))**1.55
      GO TO 85
   83 WRITE(IW,900)  KO
      GO TO 275
   85 WM=VO*LWC*TOC*C*EM*.623/10.**4
      MWAV=WM/SH
      MWLE=2.*MWAV
   90 CONTINUE
C
C--------------------POINT-BY-POINT ANALYSIS OF HEAT/MASS
C                    TRANSFER RELATIONSHIPS STARTING AT STAGNATION
C                    POINT AND ENDING AT AFTMOST POINT OF HEATED
C                    REGION
C                    HEATED REGION
C
C
C--------------------INITIALISE CONDITIONS AND START
C
      S=PSDAT(1,1)/12.
      NN=1
      TB=TBIN
      TBFIN=TBIN-459.688
      DRB=0.0
```

B.3 Program Listing (Cont.)

```
      TOTIM=0.0
      DO 253 I=1,N
      IF(S .LE. SL)  GO TO 100
      S=SL
  100 SP=S/SL
C
C--------------------CALCULATION OF LOCAL HEAT TRANSFER COEFFICIENT
C
      IF(I .GT. 1) GO TO 115
C
C--------------------CALCULATION AT THE STAGNATION POINT
C
      PC=PSDAT(I,2)
      PL=PA+DP
      THETA=S/RLE*57.30
      RES=0.0
      GO TO 120
  115 CONTINUE
C
C--------------------CALULATION AWAY FROM THE STAGNATION POINT
C
      PC=TRP(S,PSDAT,NPS,IW)
      THETA=S/RLE*57.30
      V=VO*SQRT(1.-PC)
      PL=PA+PC*DP
      RES=REFTO*S*V/VO
  120 CONTINUE
      IF (THETA .GT. 25.) GO TO 125
C
C--------------------CYLINDER REGION
C
      H=.57*K1*PR**.4*RELE**.5/RLE*(1.-(THETA/90.)**3)
      GO TO 185
  125 CONTINUE
      IF(RES .GT. 2.E5) GO TO 135
C
C--------------------LAMINAR FLOW REGION
C
      H=.332*K1*PR**(1./3.)*RES**.5/S
      GO TO 185
  135 CONTINUE
      IF(RES .GT. 1.2E6) GO TO 180
C
C--------------------TRANSITION FLOW REGION
C
      S11=S
      REST11=RES
      S1=S11-DS
      GO TO (142,175), NN
  142 CONTINUE
C
C--------------------CALCULATION OF PC, V AND H AT THE BEGINNING OF
C                    THE TRANSITION REGION
C
      PC=TRP(S1,PSDAT,NPS)
      V=VO*SQRT(1.-PC)
      REST1=REFTO*S1*V/VO
      IF(ABS(REST1-2.0E5) .LE. 100.) GO TO 150
      S1I=S11+(S1-S11)/(REST1-REST11)*(2.0E5-REST11)
      S11=S1
      REST11=REST1
      S1=S1I
      GO TO 142
  150 CONTINUE
      HLAM=.332*K1*PR**(1./3.)*REST1**.5/S1
C
C------------------CALCULATION OF PC, V AND H AT THE END OF THE
C                  TRANSITION REGION
C
      S21=4.*S
      PC=TRP(S21,PSDAT,NPS)
      V=VO*SQRT(1.-PC)
```

B.3 Program Listing (Cont.)

```
      REST21=REFTO*S21*V/VO
      S2=S21+2.*DS
  160 CONTINUE
      PC=TRP(S2,PSDAT,NPS)
      V=VO*SQRT(1.-PC)
      REST2=REFTO*S2*V/VO
      IF(ABS(REST2-1.2E6) .LE. 100.) GO TO 170
      S2I=S21+(S2-S21)/(REST2-REST21)*(1.2E6-REST21)
      S21=S2
      REST21=REST2
      S2=S2I
      GO TO 160
  170 CONTINUE
      HTURB=0.0296*K1*PR**(1./3.)*REST2**.8/S2
      NN=2
  175 CONTINUE
C
C-------------------INTERPOLATION FOR H BETWEEN THE VALUES AT THE
C                   BEGINNING OF THE TRANSITION REGION AND AT THE
C                   END OF THE TRANSITION REGION
C
      H=HLAM+(HTURB-HLAM)/1.E6*(RES-2.E5)
      GO TO 185
  180 CONTINUE
C
C-------------------TURBULENT FLOW REGION
C
      H=.0296*K1*PR**(1./3.)*RES**.8/S
C
C------------------ CALCULATE LOCAL IMPINGEMENT(+RUNBACK) RATE
C
  185 IF(SP .GT. .3333) GO TO 188
      MWIMP=MWLE*(1.-.385*(3.*SP)**1.75)
      GO TO 189
  188 MWIMP=MWLE*1.177*(1.-SP)**1.6
  189 MW=MWIMP+DRB
      TOTIM=TOTIM+MWIMP
C
C------------------ CALCULATE T2,T5
C
      PL=PA+PC*DP
      T2=VO*VO/(2.*CP*G*J)*(PR**.5+CP*MW/H)
      T5=(1.-PR**.5)*R*TA/CP/J*(1.-PL/PA)
C
C-------------------CALCULATE TS,T1,T3,T4
C
C                   CASE 1. NO EVAPORATION
C
      K=0.
      CPB=.2365+7.6*TB/10.**6
      EFF=TRP(S,EFDAT,NES)
  200 TS=(WB*CPB*EFF*TB+H*SH*(TA*(1.+MW/H)+T2-T5))/(WB*CPB*EFF+H*SH*(1.+
     1MW/H))
      T1=(TS-TA)*(1.+MW/H)
      QIN =WB*CPB*EFF*(TB-TS)
      QOUT=H*SH*(T1-T2+T5)
  205 IF(TS .LE. 491.688) GO TO 240
      IF(MW .LE. 0.) GO TO 240
C
C-------------------CASE 2. WITH EVAPORATION
C                                      FIND EQUILIBRIUM VALUE OF TS
C                                      SUCH THAT QIN=QOUT
C                                      BY ITERATING BETWEEN 492 AND TB
C
  210 TS=491.688
      DTS=DTSIN
  212 T1=(TS-TA)*(1.+MW/H)
      L=1348.21-.562*TS
      ES=PP(TS)
      T3=0.622*L*ES/CP/PL*144.
      EA=PP(TA)
      T4=0.622*L*EA/CP/PA*144.
      QIN=WB*CPB*EFF*(TB-TS)
```

```
      QOUT=H*SH*(T1-T2+T3-T4+T5)
      IF(QIN .LE. QOUT) GO TO 219
C                                          IF QIN.GT.QOUT, INCREMENT TS BY DTS
      TS=TS+DTS
      IF(TS .LT. TB) GO TO 212
      WRITE(IW,700) ALT,VKTAS,TAF,N1P,WBM,TBFIN,CDM,LWC
      GO TO 275
  219 IF(TS .GT. 491.688) GO TO 225
C                                          IF QIN.LT.QOUT BUT TS.LT.491.688,
C                                          EQUILIBRIUM TS = 491.688
C                                          FIND EVAPORATION RATE FOR TS = 491.688
  220 TS=491.688
      QIN=WB*CPB*EFF*(TB-TS)
      QOUT=QIN
      T1=(TS-TA)*(1.+MW/H)
      T3=QOUT/(H*SH)-(T1-T2-T4+T5)
      GO TO 230
  225 IF(QOUT/QIN .LE. 1.001) GO TO 230
C                                          IF QIN.LT.QOUT BUT TS.GT.492,
C                                          DECREMENT TS BY SMALLER AND SMALLER
C                                          AMOUNTS TO OBTAIN CONVERGENCE
      TS=TS-DTS
      DTS=DTS/3.
      TS=TS+DTS
      GO TO 212
C                                          IF QIN = QOUT, CONFIRM THAT EVAPORATION
C                                          RATE DOES NOT EXCEED IMPINGEMENT RATE
  230 K=(T3-T4)*H/(L*MW)
      IF(K .LE. 1.)  GO TO 240
C                                          IF EVAPORATION RATE EXCEEDS IMPINGEMENT
C                                          RATE, FIND NEW TS FOR FULL EVAPORATION
      K=1.
      T3=T4+L*MW/H
      TS=(WB*CPB*EFF*TB+H*SH*(TA*(1.+MW/H)+T2-L*MW/H-T5))/(WB*CPB*EFF+H*
     1SH*(1.+MW/H))
      QIN=WB*CPB*EFF*(TB-TS)
      T1=(TS-TA)*(1.+MW/H)
      QOUT=H*SH*(T1-T2+T3-T4+T5)
C
C----------------- CALCULATE ELEMENTAL RUNBACK RATE
C
  240 DRB=(1.-K)*MW
C
C------------------ CALCULATE DROP IN TB AND GO TO NEXT POINT(SEGMENT)
C
      DQ=QOUT*DS
      DTB=DQ/(WB*CPB)
      TB=TB-DTB
      SIN=S*12.
      TSF=TS-459.688
      HPH=H*3600.
      DRBH=DRB*3600.*DS
      DMWIH=MWIMP*3600.*DS
      IF(MODE .NE. 1.0) GO TO 252
  250 CONTINUE
      WRITE(IW,1000) SIN,PC,EFF,TSF,DMWIH,K,DRBH,HPH
  252 CONTINUE
      S=S+DS
  253 CONTINUE
C
C------------------ CALCULATE TOTAL IMPINGEMENT, EVAPORATION
C                   AND RUNBACK RATES
C
      RBPH=DRB*3600.*DS
      IMPPH=TOTIM*3600.*DS
      EVAPH=IMPPH-RBPH
      IF(IMPPH .GT. 0.0) GO TO 262
  260 PERC=0.
      GO TO 265
  262 PERC=EVAPH/IMPPH*100.
C
C------------------ CALCULATE RUNBACK CROSS-SECTIONAL AREA
C
```

B.3 Program Listing (Cont.)

```
  265 TIME=HORIZ/VKTAS/1.151
      RBS=DRB*3600.*DS*TIME/62.4*144.
C
C------------------ OUTPUT
C
      WRITE(IW,800)  ALT,VKTAS,TAF,R1P,WRM,TBFIN,DDM,LWC,HORIZ,IMPPH,
     1    EVAPH,PERC,RBPH,RBS
  275 CONTINUE
  276 CONTINUE
  277 CONTINUE
  280 CONTINUE
  300 FORMAT(20A4)
  310 FORMAT(8F10.3)
  320 FORMAT(1H0,5X,20A4//)
  330 FORMAT(1H1,19X,20A4//)
  400 FORMAT(23X,'NACELLE LENGTH',F18.2,'  IN'/23X,'THICKNESS-TO-LENGTH
     1RATIO',F8.3/23X,'LEADING-EDGE RADIUS',F13.2,'  IN'/23X,
     2'LIP DIAMETER',F20.2,'  IN'/23X,'STREAMWISE SURFACE'/23X,'LENGTH
     3OF HEATED AREA',F11.2,'  IN'/23X,'WING AREA',F23.2,'  SQ FT'//
     423X,'DRAG POLAR....CD=',F6.4,'+',F6.4,'*CL*CL'/)
  500 FORMAT(23X,'WEIGHT',F26.2,'  LB'///)
  600 FORMAT(3X,'ALT   VEL    AMB PERC BLEED BLEED DROP LWC   HOR   IMPING
     1 EVAP   PERC RUNBK RUNBK'/13X,'TEMP   HI    FLOW TEMP   DIA   (GM/ EXT
     2    RATE   RATE  EVAP RATE   SEC1'/'   (FT) (KTAS) (F)',6X,'(PPM)   (F)
     3  (MIC) CM) (M)     (PPH) (PPH)',6X,'(PPH) (SQIN)')
  700 FORMAT(F8.0,2F5.0,F6.0,F7.2,F6.0,F5.0,F8.3,5X,'NO CONVERGENCE ON
     1TS')
  800 FORMAT(1H0,F7.0,3F5.0,F6.2,2F5.0,F6.3,3F6.2,F5.0,F6.2,F6.3)
  900 FORMAT(11X,'KO=',E10.3,10X,'OUTSIDE ASSUMED RANGE'/)
 1000 FORMAT(/5X,'SIN=',F6.3,3X,'PC=',F5.2,3X,'EFF=',F5.3,3X,'TSF=',F6.1
     1/10X,'DMWIH=',F5.1,3X,'K=',F5.3,3X,'DRBH=',F5.1,3X,'HPH=',F5.1)
 1100 FORMAT(16F5.2)
 1200 FORMAT(10F7.3)
      CALL EXIT
      END
```

B.4 Function PP Listing

```
      FUNCTION PP(T)
C
C--------------FUNCTION PP CALCULATES THE PARTIAL PRESSURE
C              OF SATURATED AIR IN POUNDS PER SQUARE INCH.
C
      ZT=1000.0/T
      IF(T .GT. 491.688) GO TO 100
      A=19.598997
      B=-10.4310[illegible]5
      C=-0.27550[illegible]73
      D=0.039404[illegible]93
      E=0.0
      GO TO 300
  100 CONTINUE
      IF(T .GT. 671.688) GO TO 200
      A=13.435296
      B=-5.0988424
      C=-1.6896174
      D=0.17829154
      F=0.0
      GO TO 300
  200 CONTINUE
      A=16.625544
      B=-14.213106
      C=7.5567694
      D=-4.0151569
      F=0.71697364
  300 CONTINUE
      XP=A+B*ZT+C*ZT**2+D*ZT**3+F*ZT**4
      PP=EXP(XP)
      RETURN
      END
```

B.5 Sample Input Data

```
MODEL 35 ENGINE INLET LIP ANTI-ICE ANALYSIS - 12 O'CLOCK POSITION
1.
  7.814    .058        0.125     2.237        0.558      253.       .0225        .050
 0.0   0.5  1.0  1.5  2.0  2.5  3.0  3.5  4.0  4.5  5.0
 1.    .97  .13-1.47-1.30 -.94 -.81 -.77 -.81 -.92-1.09
   .0       .5      1.0     1.5     2.0     2.5     3.0     3.5     4.5
  0.627  0.698  0.445  0.897  0.609  0.317  0.328  0.350  0.350
TEST RUN   1A - DRY   CORRECTED
3195.      13000.     235.8
16.33       0.        0.          0.
11.98      348.9
33.
TEST RUN   2A - DRY   CORRECTED
3181.      13000.     235.9
15.86       0.        0.          0.
14.94      350.6
33.
TEST RUN   3A - DRY   CORRECTED
3189.      13000.     236.8
16.08       0.        0.          0.
12.14      400.9
33.
TEST RUN   4A - DRY   CORRECTED
3179.      13000.     236.4
15.37       0.        0.          0.
15.0       399.3
33.
TEST RUN   5A - DRY   CORRECTED
3123.      13000.     235.4
15.80       0.        0.          0.
12.12      449.1
33.
TEST RUN   6A - DRY   CORRECTED
3150.      13000.     234.2
16.44       0.        0.          0.
15.05      451.3
33.
TEST RUN   7A - DRY   CORRECTED
3135.      13000.     231.7
1.48        0.        0.          0.
12.14      352.2
33.
TEST RUN   8A - DRY   CORRECTED
3160.      13000.     232.5
0.71        0.        0.          0.
15.06      352.2
33.
TEST RUN   9A - DRY   CORRECTED
3160.      13000.     232.7
0.50        0.        0.          0.
12.19      399.3
33.
TEST RUN  10A - DRY   CORRECTED
3154.      13000.     224.8
1.33        0.        0.          0.
14.95      402.4
33.
    TEST RUN  11A - DRY CORRECTED
3193.      13000.     226.1
1.91       0.         0.          0.
12.07      451.1
33.
    TEST RUN  12A - DRY CORRECTED
3187.      13000.       226.0
3.23       0.
14.97      453.2
33.
    TEST RUN  13A - DRY CURRECTED
1756.      13000.     142.6
-8.95      0.
11.94      351.
33.
```

B.5 Sample Input Data (Cont.)

```
 TEST RUN  14A - DRY CORRECTED
1740.     13000.     142.1
-7.34     0.
14.94     349.0
33.
 TEST RUN  15A - DRY CORRECTED
1748.     13000.     142.7
-6.58     0.
12.09     402.
33.
 TEST RUN  16A - DRY CORRECTED
1738.     13000.     142.2
-6.87     0.
15.46     399.7
33.
 TEST RUN  17A - DRY CORRECTED
1740.     13000.     142.7
-6.98     0.
12.01     450.
33.
 TEST RUN  18A - DRY CORRECTED
1740.     13000.     142.4
-7.22     0.
15.04     452.6
33.
 TEST RUN  19A - DRY CORRECTED
2794.     13000.     196.2
-22.63    0.
12.09     350.8
33.
 TEST RUN  20A - DRY CORRECTED
2816.     13000.     197.6
-20.88    0.
15.19     350.2
33.
 TEST RUN  21A - DRY CORRECTED
2794.     13000.     196.3
-20.54    0.
12.09     401.1
33.
 TEST RUN  22A - DRY CORRECTED
2786.     13000.     196.0
-20.76    0.
14.89     401.3
33.
 TEST RUN  23A - DRY CORRECTED
2775.     13000.     196.1
-20.66    0.
12.03     451.1
33.
 TEST RUN  24A - DRY CORRECTED
2741.     13000.     194.1
-20.51    0.
14.76     451.7
33.
```

B.5 Sample Input Data (Cont.)

```
MODEL 35 ENGINE INLET LIP ANTI-ICE ANALYSIS - 12 O'CLOCK POSITION
1.
  7.814    .058        0.125     2.237      0.558      253.      .0225      .050
 0.0  0.5  1.0  1.5  2.0  2.5  3.0  3.5  4.0  4.5  5.0
 1.    .97  .13-1.47-1.30 -.94 -.81 -.77 -.81 -.92-1.09
   .0      .5     1.0     1.5     2.0     2.5     3.0     3.5     4.5
  0.627  0.698  0.445  0.897  0.609  0.317  0.328  0.350  0.350
TEST RUN 60A - WET   CORRECTED
3208.       13000.     231.0
18.05       18.45      .901        20.5
12.09       351.6
33.
TEST RUN 61A - WET   CORRECTED
3266.       13000.     234.1
17.45       18.29      .890        20.8
15.16       351.
33.
TEST RUN 62A - WET   CORRECTED
3295.       13000.     235.2
14.82       18.25      .887        20.9
12.11       400.2
33.
TEST RUN 63A - WET   CORRECTED
3259.       13000.     234.5
17.4        18.30      .890        20.6
15.30       398.9
33.
TEST RUN 64A - WET   CORRECTED
3222.       13000.     233.0
17.40       18.35      .894        20.7
12.10       452.1
33.
TEST RUN 65A - WET   CORRECTED
2831.       13000.     234.7
18.49       18.21      .888        20.8
11.35       452.1
33.
TEST RUN 66A - WET   CORRECTED
3253.       13000.     231.0
1.02        20.66      .762        20.5
12.02       35[illegible].4
33.
TEST RUN 67A - WET   CORRECTED
3262.       13000.     231.1
1.95        20.70      .763        20.5
15.17       351.5
33.
TEST RUN 68A - WET   CORRECTED
3297.       13000.     233.0
2.83        20.58      .757        20.7
12.03       399.5
33.
TEST RUN 69A - WET   CORRECTED
3280.       13000.     232.2
3.53        20.65      .760        20.6
15.16       401.3
33.
   TEST RUN  70A - WET CORRECTED
3266.       13000.     231.2
2.01        20.7       .763        20.5
12.10       451.1
33.
   TEST RUN 71A - WET CORRECTED
3291.       13000.      232.6
2.40        20.64      .760        20.7
14.93       452.4
33.
   TEST RUN 72A - WET CORRECTED
1637.       13000.      141.3
-2.97       23.76      1.944        5.4
12.06       350.6
33.
```

B.5 Sample Input Data (Cont.)

```
 TEST RUN 73A - WET CORRECTED
1661.        13000.      143.2
-4.13        23.61       1.917       5.5
15.17        352.5
33.
 TEST RUN 74A - WET CORRECTED
1645.        13000.      143.4
-3.64        23.61       1.917       5.5
11.90        401.3
33.
 TEST RUN 75A - WET CORRECTED
1667.        13000.      144.6
-4.66        23.54       1.904       5.5
15.37        399.3
33.
 TEST RUN 76A - WET CORRECTED
1602.        13000.      142.6
-2.81        23.67       1.930       5.5
11.91        452.1
33.
 TEST RUN 77A - WET CORRECTED
1552.        13000.      143.8
-4.53        23.62       1.917       5.5
15.40        452.8
33.
 TEST RUN 78A - WET CORRECTED
2389.        13000.      193.4
-18.17       24.21       1.442       7.4
12.14        348.8
33.
 TEST RUN 79A - WET CORRECTED
2385.        13000.      193.2
-18.22       24.21       1.441       7.4
12.02        351.7
33.
 TEST RUN 80A - WET CORRECTED
2413.        13000.      194.9
-19.63       24.14       1.434       6.5
12.04        399.9
33.
 TEST RUN 81A - WET CORRECTED
2541.        13000.      196.5
-20.07       24.00       1.420       7.5
15.35        397.4
33.
 TEST RUN 82A - WET CORRECTED
2488.        13000.      194.8
-17.6        24.14       1.434       7.5
12.24        451.7
33.
 TEST RUN 83A - WET CORRECTED
2492.        13000.      195.
-17.7        24.06       1.427       7.5
15.16        449.9
33.
```

B.6 Sample Output Data

```
MODEL 35 ENGINE INLET LIP ANTI-ICE ANALYSIS - 12 O'CLOCK POSITION

TEST RUN 10A - DRY   CORRECTED

               NACELLE LENGTH                   93.77  IN
               THICKNESS-TO-LENGTH RATIO         0.058
               LEADING-EDGE RADIUS               1.50  IN
               LIP DIAMETER                     26.84  IN
               STREAMWISE SURFACE
               LENGTH OF HEATED AREA             6.70  IN
               WING AREA                       253.00  SQ FT

               DRAG POLAR....CD=0.0225+0.0500*CL*CL

               WEIGHT                        13000.00  LB


 ALT   VEL    AMB PERC BLEED BLEED DROP LWC   HOR   IMPING EVAP  PERC RUNBK RUNBK
             TEMP  N1   FLOW  TEMP  DIA  (GM/ EXT    RATE  RATE  EVAP RATE  SECT
(FT) (KTAS) (F)       (PPH)   (F)  (MIC) CM)  (M)   (PPH) (PPH)       (PPH) (SQIN)

  SIN= 0.000    PC= 1.00   EFF=0.627    TSF= 187.5
       DMWIH=   0.0   K=0.000   DRBH=   0.0    HPH= 43.0

  SIN= 0.500    PC= 0.97   EFF=0.698    TSF= 196.1
       DMWIH=   0.0   K=0.000   DRBH=   0.0    HPH= 42.6

  SIN= 1.000    PC=-0.81   EFF=0.445    TSF= 212.7
       DMWIH=   0.0   K=0.000   DRBH=   0.0    HPH= 21.7

  SIN= 1.500    PC=-1.47   EFF=0.897    TSF= 221.1
       DMWIH=   0.0   K=0.000   DRBH=   0.0    HPH= 39.1

  SIN= 2.000    PC=-1.30   EFF=0.609    TSF= 164.3
       DMWIH=   0.0   K=0.000   DRBH=   0.0    HPH= 47.3

  SIN= 2.500    PC=-0.94   EFF=0.317    TSF= 101.3
       DMWIH=   0.0   K=0.000   DRBH=   0.0    HPH= 52.8

  SIN= 3.000    PC=-0.81   EFF=0.328    TSF=  94.8
       DMWIH=   0.0   K=0.000   DRBH=   0.0    HPH= 59.6

3154. 225.   1.   0. 14.95 402.   0. 0.000  0.00  0.00  0.00  0.  0.00 0.000
```

B.6 Sample Output Data (Cont.)

```
                MODEL 35 ENGINE INLET LIP ANTI-ICE ANALYSIS - 12 O'CLOCK POSITION

TEST RUN 69A - WET   CORRECTED

                   NACELLE LENGTH                        93.77  IN
                   THICKNESS-TO-LENGTH RATIO              0.058
                   LEADING-EDGE RADIUS                    1.50  IN
                   LIP DIAMETER                          26.84  IN
                   STREAMWISE SURFACE
                   LENGTH OF HEATED AREA                  6.70  IN
                   WING AREA                            253.00  SQ FT

                   DRAG POLAR....CD=0.0225+0.0500*CL*CL

                   WEIGHT                             13000.00  LB

 ALT   VEL    AMB PERC BLEED BLEED DROP LWC   HOR  IMPING EVAP  PERC RUNBK RUNBK
             TEMP  N1   FLOW TEMP  DIA  (GM/  EXT   RATE  RATE  EVAP RATE  SECT
(FT) (KTAS)  (F)        (PPH)  (F) (MTC) CM)  (M)  (PPH) (PPH)       (PPH) (SQIN)
   SIN= 0.000   PC= 1.00   EFF=0.627    TSF=  93.8
        DMWIH=  4.2   K=0.424   DRBH=   2.4   HPH= 43.6
   SIN= 0.500   PC= 0.97   EFF=0.698    TSF=  95.1
        DMWIH=  3.8   K=0.296   DRBH=   4.3   HPH= 43.2
   SIN= 1.000   PC=-0.80   EFF=0.445    TSF=  91.4
        DMWIH=  2.8   K=0.138   DRBH=   6.2   HPH= 22.2
   SIN= 1.500   PC=-1.47   EFF=0.897    TSF=  97.3
        DMWIH=  1.9   K=0.290   DRBH=   5.7   HPH= 40.3
   SIN= 2.000   PC=-1.30   EFF=0.609    TSF=  77.1
        DMWIH=  1.1   K=0.209   DRBH=   5.4   HPH= 48.9
   SIN= 2.500   PC=-0.94   EFF=0.317    TSF=  53.4
        DMWIH=  0.5   K=0.106   DRBH=   5.4   HPH= 54.7
   SIN= 3.000   PC=-0.81   EFF=0.326    TSF=  51.7
        DMWIH=  0.1   K=0.120   DRBH=   4.8   HPH= 61.7
3280. 232.   4.   0. 15.16 401.  21. 0.760 20.60 14.49  9.66  67.  4.83 0.122
```

APPENDIX C

C-1

Table C-1 Summary of Dry Run Skin Temperature Prediction - 6 o'clock Position

RUN NO.	ALTITUDE (FT)	VEL (KTAS)	BLEED RATE (LB/MIN)	BLEED TEMP (°F)	AMB TEMP (°F)	SKIN TEMPERATURE (°F) S = 0.0 PRED	S = 0.0 MEAS	S = 0.5 PRED	S = 0.5 MEAS	S = 1.0 PRED	S = 1.0 MEAS	S = 1.5 PRED	S = 1.5 MEAS	S = 2.0 PRED	S = 2.0 MEAS	S = 2.5 PRED	S = 2.5 MEAS	S = 3.0 PRED	S = 3.0 MEAS
1A	3195	236	12.0	349	16	165	166	198	196	230	227	199	200	167	173	143	151	124	131
2A	3181	236	14.9	351	16	183	181	216	215	246	242	217	213	185	188	160	165	141	145
3A	3189	231	12.1	401	16	188	191	226	228	263	260	227	230	190	197	162	172	141	150
4A	3171	236	15.0	399	15	207	205	244	245	280	273	245	243	208	212	180	185	157	161
5A	3123	235	12.1	449	16	209	212	252	258	294	289	253	258	211	224	180	195	155	170
6A	3150	234	15.1	451	16	233	232	276	272	316	307	278	274	236	241	204	211	178	186
7A	3135	232	12.1	352	1	159	159	194	195	228	223	192	197	158	167	132	141	113	120
8A	3160	233	15.1	352	1	177	176	211	213	243	235	210	207	175	179	149	154	128	133
9A	3160	233	12.2	399	1	179	180	219	217	257	249	217	219	177	187	148	159	126	136
10A	3154	225	15.0	402	1	202	200	242	239	278	267	242	236	204	201	174	171	150	147
11A	3193	226	12.1	451	2	203	203	248	248	291	283	248	250	204	214	171	183	146	157
12A	3187	226	15.0	453	3	227	224	271	265	312	301	272	267	229	230	196	198	169	173
13A	1756	143	11.9	351	-9	166	167	202	209	236	230	216	209	194	179	172	154	153	133
14A	1740	142	14.9	349	-7	185	189	220	222	251	247	233	224	214	195	193	170	174	149
15A	1748	143	12.1	402	-7	193	200	234	235	272	269	250	244	226	211	201	183	174	160
16A	1738	142	15.5	400	-7	216	217	256	255	291	285	271	258	249	227	225	199	203	176
17A	1740	143	12.0	450	-7	215	223	261	266	304	304	279	274	252	239	224	208	199	183
18A	1740	142	15.0	453	-7	242	245	287	285	327	322	304	291	278	257	251	227	227	202
19A	2794	196	12.1	351	-23	149	147	187	179	222	218	189	185	153	153	125	126	104	104
20A	2816	198	15.2	350	-21	170	163	207	199	240	230	209	200	174	168	147	141	124	119
21A	2794	196	12.1	401	-21	173	170	215	209	256	250	219	216	178	180	147	150	123	125
22A	2786	196	14.9	401	-21	194	191	236	231	275	269	240	233	200	196	168	166	143	140
23A	2775	196	12.0	451	-21	195	194	242	239	288	286	246	247	200	207	166	174	139	147
24A	2741	194	14.8	452	-21	219	217	266	257	309	306	271	265	226	225	191	192	163	165
29A	3270	232	11.8	402	-1	151	151	173	171	205	201	244	239	223	216	190	182	157	149
30A	3241	231	12.0	402	-1	140	140	150	149	168	165	193	190	236	230	226	218	180	172
31A	3322	235	11.9	352	-3	146	146	174	172	213	208	196	191	166	160	137	131	114	108
32A	3264	232	12.2	350	0	147	147	165	163	197	193	208	203	174	168	144	138	120	115
35B	3112	234	12.0	349	16	166	166	164	161	165	165	159	154	166	159	164	157	159	151
36B	3100	234	15.0	350	15	184	182	182	175	182	178	177	167	184	170	182	168	177	162
37B	3100	234	12.0	401	16	188	190	185	184	186	187	180	176	188	182	186	178	180	175
38B	3084	234	15.2	399	16	209	206	206	201	207	202	201	193	209	198	207	195	201	186
39B	3102	235	11.9	450	16	209	215	206	208	207	211	200	198	208	206	206	203	200	197
40B	3100	235	15.2	448	16	233	235	230	230	231	229	224	219	233	226	230	223	224	214
41B	3119	232	12.0	348	1	157	160	155	154	156	155	147	144	153	152	151	147	145	140
42B	3102	231	15.0	352	1	179	178	176	172	177	172	168	163	175	168	172	163	167	158
43B	3115	231	12.0	401	1	180	184	177	179	180	181	169	170	176	176	173	172	167	166
44B	3162	233	15.0	398	1	200	201	197	196	198	196	188	194	195	191	192	186	186	180
45B	3117	231	12.1	446	1	201	205	198	201	199	202	189	190	197	199	194	195	187	187
46B	3139	231	14.9	454	1	228	226	224	223	225	223	215	213	223	219	220	215	213	206
53B	2565	195	12.2	351	-23	150	152	148	148	149	148	143	141	151	146	149	143	144	135
54B	2547	195	14.9	349	-21	169	168	167	165	168	163	163	157	171	162	169	158	164	151
55B	2555	195	12.2	400	-22	173	174	170	171	171	170	166	163	174	170	172	167	166	159
56B	2545	194	14.8	399	-22	193	191	190	189	191	188	186	179	195	186	192	181	186	178
57B	2571	196	12.0	450	-23	194	199	191	194	192	196	185	186	195	196	192	193	186	184
58B	2576	196	15.0	450	-23	221	221	217	217	219	218	212	207	222	217	219	215	212	205

Table C-2 Summary of Dry Run Skin Temperature Prediction - 9 o'clock Position

RUN NO.	ALTITUDE (FT)	VEL (KTAS)	BLEED RATE (LB/MIN)	BLEED TEMP (°F)	AMB TEMP (°F)	SKIN TEMPERATURE (°F) S = 0.0 PRED	S = 0.0 MEAS	S = 0.5 PRED	S = 0.5 MEAS	S = 1.0 PRED	S = 1.0 MEAS	S = 1.5 PRED	S = 1.5 MEAS	S = 2.0 PRED	S = 2.0 MEAS	S = 2.5 PRED	S = 2.5 MEAS	S = 3.0 PRED	S = 3.0 MEAS
1A	3195	236	12.0	349	16	140	147	150	163	163	171	181	194	151	164	87	97	72	80
2A	3181	236	14.9	351	16	157	161	167	170	181	185	199	210	169	177	99	105	81	89
3A	3189	237	12.1	401	16	159	167	171	177	185	196	206	224	172	188	97	103	79	90
4A	3179	236	15.0	399	15	176	182	189	195	204	210	225	240	190	200	110	118	89	99
5A	3123	235	12.1	449	16	176	187	189	196	206	213	230	253	192	208	106	126	86	100
6A	3150	234	15.1	451	16	199	204	212	214	231	230	255	269	215	225	124	130	100	106
7A	3135	232	12.1	352	1	133	135	143	144	155	155	173	176	142	147	74	81	58	66
8A	3160	233	15.1	352	1	149	160	260	157	173	168	190	187	158	158	85	94	67	74
9A	3160	233	12.2	399	1	149	151	161	161	175	173	194	195	159	166	82	102	64	72
10A	3154	225	15.0	402	1	170	164	183	168	199	184	221	223	185	180	100	102	78	80
11A	3193	226	12.1	451	2	168	170	182	180	200	198	224	238	184	192	95	94	74	78
12A	3187	226	15.0	453	3	191	189	206	201	224	220	249	258	208	210	113	114	89	92
13A	1756	143	11.9	351	-9	137	140	149	149	166	160	205	184	176	166	95	76	74	61
14A	1740	142	14.9	349	-7	156	157	168	166	185	178	223	200	196	182	114	99	90	73
15A	1748	143	12.1	402	-7	160	164	173	175	193	192	238	218	205	156	113	87	88	75
16A	1738	142	15.5	400	-7	183	182	197	193	216	208	260	237	229	212	134	113	107	86
17A	1740	143	12.0	450	-7	178	186	193	198	215	217	266	251	229	223	126	118	98	86
18A	1740	142	15.0	453	-7	204	207	220	219	242	237	291	274	256	240	149	127	118	99
19A	2794	196	12.1	351	-23	120	120	132	132	148	146	169	165	136	135	60	56	41	40
20A	2816	198	15.2	350	-21	141	136	153	147	169	162	190	182	157	150	76	76	55	51
21A	2794	196	12.1	401	-21	140	140	153	153	172	170	197	195	158	158	72	75	51	50
22A	2786	196	14.9	401	-21	160	159	174	172	193	190	218	216	180	175	88	92	54	62
23A	2775	196	12.0	451	-21	156	161	173	174	194	195	222	226	179	182	82	91	59	61
24A	2741	194	14.8	452	-21	181	176	197	198	219	220	247	256	205	199	101	100	74	74
29A	3270	232	11.8	402	-1	135	135	145	143	154	151	163	162	179	174	205	195	124	114
30A	3241	231	12.0	402	-1	92	92	114	113	124	123	132	130	140	138	147	147	163	159
31A	3322	235	11.9	352	-3	132	132	148	146	170	166	167	161	96	91	58	55	51	48
32A	3264	232	12.2	350	0	138	138	149	147	159	155	161	156	139	132	70	66	49	46
35B	3112	234	12.0	349	16	157	155	154	150	147	146	146	142	144	138	134	128	114	106
36B	3100	234	15.0	350	15	174	169	171	164	165	163	164	158	162	156	150	143	129	119
37B	3100	234	12.0	401	16	177	176	174	171	167	167	165	163	164	160	151	146	128	121
38B	3084	234	15.2	399	16	198	194	194	190	187	185	186	181	184	178	171	161	146	136
39B	3102	235	11.9	450	16	196	198	193	193	185	188	183	184	181	180	167	163	141	136
40B	3100	235	15.2	448	16	220	220	216	216	209	212	207	210	205	206	190	189	162	156
41B	3119	232	12.0	348	1	147	146	144	141	136	137	133	134	131	130	120	116	99	97
42B	3102	231	15.0	352	1	168	166	165	161	157	157	154	154	152	150	140	137	117	113
43B	3115	231	12.0	401	1	169	170	165	165	156	160	153	156	151	153	138	137	114	114
44B	[illegible]	233	15.0	398	1	189	189	185	184	176	179	172	176	169	172	155	155	133	129
45B	3117	231	12.1	446	1	188	193	184	188	174	182	172	178	169	174	154	156	123	129
46B	3139	231	14.9	454	1	214	216	210	208	200	199	197	191	194	182	178	167	149	148
53B	2565	195	12.2	351	-23	134	157	136	147	130	140	129	134	127	129	115	125	91	120
54B	2547	195	14.9	349	-21	158	158	155	152	149	147	149	144	147	140	134	124	110	98
55B	2555	195	12.2	400	-22	161	162	157	156	150	152	150	147	148	143	133	125	107	96
56B	2545	194	14.8	399	-22	181	181	177	176	170	171	170	168	168	163	153	145	125	114
57B	2571	196	12.0	450	-23	180	184	175	177	169	172	168	167	165	163	149	146	120	112
58B	2576	196	15.0	450	-23	206	208	202	203	195	198	194	193	191	189	175	170	143	134

C-2

APPENDIX C

Table C-3 Summary of Dry Run Skin Temperature Prediction - 12 o'clock Position

RUN NO.	ALTITUDE (FT)	VEL (KTAS)	BLEED RATE (LB/MIN)	BLEED TEMP (°F)	AMB TEMP (°F)	SKIN TEMPERATURE (°F) S = 0.0 PRED	S = 0.0 MEAS	S = 0.5 PRED	S = 0.5 MEAS	S = 1.0 PRED	S = 1.0 MEAS	S = 1.5 PRED	S = 1.5 MEAS	S = 2.0 PRED	S = 2.0 MEAS	S = 2.5 PRED	S = 2.5 MEAS	S = 3.0 PRED	S = 3.0 MEAS
1A	3195	236	12.0	349	16	154	159	160	163	174	174	181	194	135	142	88	98	84	96
2A	3181	236	14.9	351	16	171	174	178	178	192	190	199	210	152	154	109	106	95	105
3A	3169	231	12.1	401	16	175	181	183	186	198	200	206	224	153	164	98	108	93	107
4A	3179	236	15.0	399	15	193	197	201	202	217	217	225	240	171	176	111	116	105	117
5A	3123	235	12.1	449	16	194	203	203	210	220	226	230	253	170	183	103	120	107	119
6A	3150	234	15.1	451	16	217	222	227	228	245	244	255	269	194	199	125	130	118	131
7A	3135	232	12.1	352	1	147	154	154	158	167	169	173	176	124	135	75	86	70	81
8A	3160	233	15.1	352	1	164	168	172	172	185	185	190	187	141	146	87	92	81	90
9A	3160	233	12.2	399	1	165	172	174	177	188	190	194	195	139	150	93	94	78	90
10A	3154	225	15.0	402	1	183	194	196	192	213	204	221	223	164	160	101	100	95	94
11A	3193	226	12.1	451	2	187	190	196	199	215	212	224	237	161	168	97	103	90	95
12A	3187	226	15.0	453	3	211	208	220	218	239	232	249	25P	185	184	115	114	107	108
13A	1756	143	11.9	351	-9	153	155	160	162	178	175	205	185	157	145	97	86	92	74
14A	1740	142	14.9	349	-7	172	172	180	180	197	193	223	200	178	160	115	98	110	88
15A	1748	143	12.1	402	-7	178	182	187	190	207	203	238	218	184	171	115	102	109	92
16A	1738	142	15.5	400	-7	201	199	210	208	230	224	260	237	208	186	136	113	129	105
17A	1740	143	12.0	450	-7	198	205	208	214	231	230	266	250	205	192	178	116	121	106
18A	1740	142	15.0	453	-7	225	225	235	234	257	252	291	274	232	210	151	128	144	121
19A	2794	196	12.1	351	-23	136	136	144	139	160	156	169	165	117	116	61	62	55	56
20A	2816	198	15.2	350	-21	157	152	165	156	181	174	190	182	138	130	77	72	71	68
21A	2794	196	12.1	401	-21	158	158	167	161	186	182	197	196	137	136	74	75	68	69
22A	2786	196	14.9	401	-21	179	176	188	180	208	202	218	216	158	153	90	85	82	82
23A	2775	196	12.0	451	-21	178	180	188	185	210	208	222	226	155	158	84	87	77	81
24A	2741	194	14.8	45[illegible]	-21	202	200	212	205	235	230	247	248	180	176	103	100	95	96
29A	3270	232	11.8	402	-1	135	135	145	143	154	151	163	162	179	174	205	195	124	114
30A	3241	231	12.0	402	-1	92	92	114	113	124	123	132	130	140	138	147	147	163	159
31A	3322	235	11.9	352	-3	149	149	163	161	174	169	169	163	100	95	80	75	76	71
32A	3264	232	12.2	350	0	157	157	170	168	181	176	156	150	106	101	87	82	83	78
35B	3112	[illegible]	12.0	349	16	179	176	142	138	152	144	135	126	135	130	117	107	110	102
36B	3100	234	15.0	350	15	197	192	159	152	170	160	152	140	152	142	133	118	124	112
37B	3100	234	12.0	401	16	203	202	160	158	172	168	153	146	153	148	132	123	123	117
38B	3084	234	15.2	399	16	224	220	180	174	193	168	173	163	173	163	150	147	141	128
39B	3102	235	11.9	450	16	225	230	177	178	191	192	169	167	169	166	145	141	135	131
40B	3100	235	15.2	448	16	250	252	200	198	215	213	192	188	192	186	167	156	155	146
41B	3119	232	12.0	348	1	170	171	132	130	141	141	122	121	121	120	103	99	95	92
42B	3102	231	15.0	352	1	192	192	152	147	162	160	142	138	141	136	121	114	112	106
43B	3115	231	12.0	401	1	195	200	151	152	162	164	140	142	139	140	118	117	109	108
44B	3162	233	15.0	398	1	215	218	170	168	181	182	158	158	158	155	135	131	124	121
45B	3117	231	12.1	446	1	218	225	168	172	181	187	157	162	156	159	132	133	122	113
46B	3139	231	14.9	454	1	245	250	193	194	207	210	181	183	180	180	154	152	142	140
53B	2565	195	12.2	351	-23	165	164	122	122	135	134	116	110	116	106	95	89	86	79
54B	2547	195	14.9	349	-21	184	181	141	138	155	150	136	127	136	122	114	104	104	93
55B	2555	195	12.2	400	-22	189	189	141	143	157	156	135	130	135	126	111	106	101	97
56B	2545	194	14.8	399	-22	209	208	160	160	177	174	155	148	155	142	130	122	119	109
57B	2571	196	12.0	450	-23	212	216	158	164	175	177	152	150	15[illegible]	146	125	124	113	110
58B	2576	196	15.0	450	-23	239	240	184	186	202	200	177	172	177	167	149	142	136	128

C-3

APPENDIX C

Table C-4 Summary of Wet Run Skin Temperature Prediction - 6 O'clock Position

RUN NO.	ALTITUDE (FT)	VEL KTAS	BLEED RATE (LB/MIN)	BLEED TEMP (°F)	AMB TEMP (°F)	DROP DIA (MIC)	LWC (G/m³)	SPRAY TIME (MIN)	IMP RATE (LB/HR)	EVAP RATE (LB/HR)	PER CENT EVAP	RUNBACK (IN²/FT) PRED	RUNBACK (IN²/FT) MEAS	S = 0.0 PRED	S = 0.0 MEAS	S = 0.5 PRED	S = 0.5 MEAS	S = 1.0 PRED	S = 1.0 MEAS	S = 1.5 PRED	S = 1.5 MEAS	S = 2.0 PRED	S = 2.0 MEAS	S = 2.5 PRED	S = 2.5 MEAS	S = 3.0 PRED	S = 3.0 MEAS
60A	3208	231	12.09	352	18	18	.901	4.63	29.23	6.04	21	.59	-	86	71	96	87	95	100	76	98	65	77	59	65	54	59
61A	3266	234	15.16	351	17	18	.890	4.63	29.14	8.16	28	.53	-	94	79	105	95	105	107	85	103	73	87	66	74	61	67
62A	3295	235	12.11	400	15	18	.887	4.63	29.17	7.39	25	.55	-	91	78	102	93	102	112	81	104	69	92	61	60	56	71
63A	3259	235	15.30	399	17	18	.890	4.63	29.23	10.45	36	.48	-	100	83	112	97	115	126	94	121	81	97	73	85	67	90
64A	3222	233	12.10	452	17	18	.894	4.63	29.18	9.42	32	.50	-	98	84	110	101	112	141	90	138	78	110	69	94	63	86
65A	2831	235	11.35	452	18	18	.888	4.63	28.85	8.75	30	.5[illegible]	-	96	88	108	112	109	151	88	146	75	116	67	101	67	94
66A	3253	231	12.02	352	1	21	.762	4.63	28.63	4.91	17	.60	-	81	68	91	83	87	102	65	93	53	76	46	66	41	57
67A	3262	231	15.17	352	2	21	.763	4.63	28.76	6.93	24	.55	-	90	74	101	93	100	106	77	100	64	82	55	69	50	61
68A	3297	233	12.03	400	3	21	.757	4.63	28.67	6.38	22	.57	-	87	73	99	93	97	110	74	103	61	84	53	71	42	63
69A	3280	232	15.16	401	4	21	.760	4.63	28.77	9.16	32	.50	-	97	80	109	103	111	127	87	115	73	91	64	79	57	69
70A	3266	231	12.10	451	2	21	.763	4.63	28.78	8.00	28	.53	-	93	79	106	103	106	128	82	114	68	94	59	83	52	72
71A	3291	233	14.93	452	2	21	.760	4.63	28.82	11.25	39	.45	-	102	85	116	109	119	141	95	127	80	101	70	89	63	79
72A	1637	141	12.06	351	-3	24	1.944	2.0	41.74	2.64	6	.43	-	80	62	88	84	71	106	50	101	40	84	35	70	32	61
73A	1661	143	15.17	353	-4	24	1.917	2.0	41.65	4.08	10	.41	-	89	69	99	92	85	112	61	107	49	91	43	78	39	68
74A	1645	143	11.90	401	-4	24	1.917	2.0	41.73	3.58	9	.42	-	86	67	95	88	80	114	57	109	45	91	39	79	35	68
75A	1667	145	15.37	399	-5	24	1.904	2.0	41.81	5.38	13	.40	-	97	75	107	98	96	121	70	116	57	96	50	85	44	75
76A	1602	143	11.91	452	-3	24	1.930	2.0	41.78	4.69	11	.41	-	94	74	104	96	90	123	65	120	53	93	46	87	41	76
77A	1552	144	15.40	453	-5	24	1.917	2.0	41.88	7.06	17	.38	-	105	75	116	112	107	152	81	152	66	119	58	107	52	98
78A	2389	193	12.14	349	-18	24	1.442	2.0	50.65	1.72	3	.53	-	68	37	74	67	52	87	31	81	21	63	16	52	13	42
79A	2385	193	12.02	352	-18	24	1.441	2.0	50.53	1.72	3	.53	-	67	35	74	56	52	90	31	82	21	66	16	55	13	45
80A	2413	195	12.04	400	-20	24	1.434	2.0	50.82	2.31	5	.46	-	75	39	82	73	59	101	34	93	25	73	19	61	15	53
81A	2541	197	15.35	397	-20	24	1.420	2.0	50.63	3.60	7	.51	-	86	52	94	73	74	104	47	95	33	79	28	69	24	59
82A	2488	195	12.24	452	-18	24	1.434	2.0	50.77	3.27	6	.52	-	83	38	92	62	71	101	44	91	32	77	27	63	22	53
83A	2492	195	15.16	450	-18	24	1.427	2.0	50.38	4.92	10	.50	-	94	53	104	83	86	112	57	97	42	83	34	73	32	64
95A	3199	230	12.1	404	1	21	.767	4.63	28.82	7.43	26	.54	-	77	70	80	74	70	82	90	130	86	138	74	110	63	86
96A	3108	225	12.1	403	3	21	.783	4.63	28.98	7.63	26	.27	-	72	61	70	65	50	71	62	80	91	128	92	133	74	106
97A, 98A	This data not available.																										
100B	3040	232	12.0	350	16	19	.902	4.63	29.45	5.54	19	.61	-	85	76	80	72	60	73	55	73	62	72	64	77	66	79
101B	3040	233	15.0	350	15	18	.895	4.63	29.24	7.45	25	.55	-	93	81	87	78	67	78	62	72	69	82	72	87	73	88
102B	3051	232	12.1	399	14	18	.899	4.63	29.18	6.97	24	.56	-	92	82	86	77	65	78	60	74	67	82	70	88	71	90
103B	3117	235	15.0	400	13	18	.888	4.63	29.18	9.44	32	.50	-	99	86	94	82	74	81	68	78	75	84	78	90	79	94
104B	3069	233	12.1	451	14	18	.895	4.63	29.20	8.55	29	.52	-	97	86	91	83	71	82	65	78	73	88	76	96	77	99
105B	3141	236	15.0	451	14	18	.884	4.63	29.17	11.93	41	.44	-	105	91	100	89	82	90	75	84	83	97	86	108	87	112
106B	3152	231	12.1	352	1	21	.764	4.63	28.82	4.67	16	.61	0	82	73	74	67	50	67	45	57	52	47	55	58	57	64
107B	3137	230	15.1	351	1	21	.767	4.63	28.85	6.36	22	.57	0	90	80	83	72	59	73	53	68	61	72	64	74	65	73
108B	3137	231	12.0	401	2	21	.763	4.63	28.69	5.91	21	.58	0	88	79	81	72	57	72	51	66	59	71	62	73	63	73
109B	3055	229	15.0	401	-1	21	.770	4.63	28.76	7.94	28	.53	0	96	86	89	80	65	79	58	79	67	95	70	102	72	103
110B	3092	231	12.0	450	0	21	.763	4.83	28.68	7.18	25	.55	0	93	83	87	78	62	77	55	74	63	84	67	91	68	93
111B	3038	228	15.2	451	-0	21	.773	4.63	28.88	10.37	36	.47	0	103	90	97	86	74	84	67	80	76	86	74	91	80	95
112B	2547	196	12.1	351	-20	24	1.420	2.0	50.56	1.10	2	.54	0	68	37	52	31	16	46	12	47	19	53	24	53	27	57
113B	2539	195	15.1	350	-21	24	1.427	2.0	50.30	2.25	4	.53	.04	78	49	63	50	24	54	19	54	27	59	32	59	34	57
114B	2563	195	11.9	400	-21	24	1.427	2.0	50.53	1.51	3	.54	0	75	43	59	42	20	51	15	52	23	56	29	57	32	56
115B	2643	193	15.0	400	-21	24	1.442	2.0	50.90	3.06	6	.52	.04	85	54	70	52	29	61	23	60	32	64	36	66	40	64
116B	2563	195	12.0	450	-18	24	1.427	2.0	50.44	2.79	6	.52	0	83	53	68	49	28	60	23	62	32	64	35	65	38	65
117B	2622	197	15.0	449	-20	24	1.413	2.0	50.59	4.21	8	.51	0	93	61	79	59	34	68	30	66	38	74	44	76	47	74

C-4

Table C-5 Summary of Wet Run Skin Temperature Prediction - 9 O'clock Position

RUN NO.	ALTITUDE (FT)	VEL KTAS	BLEED RATE (LB/MIN)	BLEED TEMP (°F)	AMB TEMP (°F)	DROP DIA (MIC)	LWC (G/m³)	SPRAY TIME (MIN)	IMP RATE (LB/HR)	EVAP RATE (LB/HR)	PER CENT EVAP	RUNBACK (IN²/FT) PRED	RUNBACK (IN²/FT) MEAS	SKIN TEMPERATURE, °F S = 0.0 PRED	S = 0.0 MEAS	S = 0.5 PRED	S = 0.5 MEAS	S = 1.0 PRED	S = 1.0 MEAS	S = 1.5 PRED	S = 1.5 MEAS	S = 2.0 PRED	S = 2.0 MEAS	S = 2.5 PRED	S = 2.5 MEAS	S = 3.0 PRED	S = 3.0 MEAS
60A	3208	231	12.09	352	18	18	.901	4.63	14.73	6.02	41	.22	-	78	58	80	65	77	72	88	79	76	84	50	71	44	45
61A	3266	234	15.16	351	17	18	.890	4.63	14.68	8.01	55	.17	-	85	57	87	65	83	77	94	92	83	92	56	65	49	57
62A	3295	235	12.11	400	15	18	.887	4.63	14.69	7.31	50	.19	-	82	57	84	63	79	75	91	91	80	94	52	69	45	54
63A	3259	235	15.30	399	17	18	.890	4.63	14.72	10.01	68	.12	-	91	63	94	70	93	80	101	104	89	104	61	79	53	62
64A	3222	233	12.10	452	17	18	.894	4.63	14.70	9.08	62	.14	-	88	66	91	71	97	82	99	110	87	111	58	80	51	66
65A	2831	235	11.35	452	18	18	.888	4.63	14.53	8.44	58	.15	-	87	70	89	77	95	87	96	121	85	139	56	87	49	76
66A	3253	231	12.02	352	1	21	.762	4.63	14.42	5.03	35	.24	-	71	51	73	53	66	66	79	74	67	74	38	52	32	36
67A	3262	231	15.17	352	2	21	.763	4.63	14.49	6.99	48	.19	-	80	56	82	59	77	72	89	88	77	78	46	52	38	36
68A	3297	233	12.03	400	3	21	.757	4.63	14.44	6.44	45	.20	-	78	57	80	62	74	73	86	83	74	80	43	55	36	40
69A	3280	232	15.16	401	4	21	.760	4.63	14.49	8.98	62	.14	-	87	64	90	70	87	80	97	93	85	92	52	61	44	45
70A	3266	231	12.10	451	2	21	.763	4.63	14.50	7.92	55	.17	-	84	66	86	69	81	81	93	94	81	100	48	71	40	48
71A	3291	233	14.93	452	2	21	.760	2.0	14.52	10.78	74	.10	-	92	70	95	75	91	86	102	117	90	114	57	74	48	54
72A	1637	141	12.06	351	-3	24	1.944	2.0	21.03	3.13	15	.20	-	72	45	71	54	59	67	85	83	71	87	35	64	32	34
73A	1661	143	15.17	353	-4	24	1.917	2.0	20.98	4.67	22	.18	-	81	52	81	56	70	74	96	85	82	91	43	77	34	42
74A	1645	143	11.90	401	-4	24	1.917	2.0	21.02	4.13	20	.19	-	79	50	77	59	66	73	92	90	79	91	40	66	32	43
75A	1667	145	15.37	399	-5	24	1.904	2.0	21.06	6.15	29	.16	-	89	57	88	58	79	80	105	102	91	100	59	64	40	51
76A	1602	143	11.91	452	-3	24	1.930	2.0	21.04	5.34	25	.17	-	85	56	84	57	74	80	101	102	87	100	46	72	37	52
77A	1552	144	15.40	453	-5	24	1.917	2.0	21.10	8.03	38	.14	-	95	58	96	56	88	86	115	128	101	116	58	82	47	60
78A	2389	193	12.14	349	-18	24	1.442	2.0	25.25	2.23	9	.25	-	61	24	58	29	42	45	64	64	49	51	18	28	11	17
79A	2385	193	12.02	352	-18	24	1.441	2.0	25.46	2.23	9	.25	-	61	25	58	32	42	46	64	70	49	64	18	41	11	23
80A	2413	195	12.04	400	-20	24	1.434	2.0	25.60	2.89	11	.22	-	67	32	64	36	47	59	71	80	56	73	21	42	13	30
81A	2541	197	15.35	397	-20	24	1.420	2.0	25.51	4.39	17	.23	-	78	36	76	36	59	59	83	82	68	79	32	47	21	36
82A	2488	195	12.24	452	-18	24	1.434	2.0	25.58	3.95	15	.24	-	75	34	73	32	58	61	82	82	65	77	30	43	20	36
83A	2492	195	15.16	450	-18	24	1.427	2.0	25.38	6.00	24	.21	-	85	43	84	42	70	69	93	93	77	89	34	56	30	47
95A	3199	230	12.1	404	1	21	.767	4.63	14.52	11.53	79	.08	-	74	64	74	61	56	58	63	59	83	71	93	105	66	80
96A	3108	225	12.1	403	3	21	.783	4.63	14.60	2.85	20	.15	-	55	80	60	75	36	71	35	66	36	62	55	61	78	64
97A, 98A	This data not available.																										
100B	3040	232	12.0	350	16	19	.902	4.63	14.84	6.40	43	.21	-	84	70	80	64	67	61	70	62	71	68	68	72	61	68
101B	3040	233	15.0	350	15	18	.895	4.63	14.73	8.46	57	.16	-	91	76	88	70	75	67	77	67	78	80	75	83	68	77
102B	3051	232	12.1	399	14	18	.899	4.63	14.70	7.97	54	.17	-	90	74	86	69	73	67	76	73	77	77	74	77	66	73
103B	3117	235	15.0	400	13	18	.888	4.63	14.70	10.55	72	.11	-	97	81	94	75	81	73	83	76	84	90	81	90	73	83
104B	3069	233	12.1	451	14	18	.895	4.63	14.71	9.66	66	.13	-	95	79	92	74	79	71	81	77	87	85	79	84	71	80
105B	3141	236	15.0	451	14	18	.884	4.63	14.69	13.03	89	.04	-	103	86	100	81	88	79	89	89	90	103	87	102	79	99
106B	3152	231	12.1	352	1	21	.764	4.63	14.52	5.62	39	.23	0	80	64	76	58	60	56	63	56	64	58	61	58	53	57
107B	3137	230	15.1	351	1	21	.767	4.63	14.53	7.53	52	.18	0	88	72	84	65	69	63	72	65	73	68	69	68	61	68
108B	3137	231	12.0	401	2	21	.763	4.63	14.45	7.02	49	.19	0	86	72	82	65	67	61	70	62	71	65	67	66	59	65
109B	3055	229	15.0	401	-1	21	.770	4.63	14.49	9.32	64	.13	0	94	76	90	70	75	68	78	75	79	84	75	85	66	82
110B	3092	231	12.0	450	0	21	.763	4.63	14.45	8.46	59	.15	0	92	72	88	77	72	63	75	64	75	73	72	74	63	74
111B	3038	228	15.2	451	-0	21	.773	4.63	14.55	11.90	82	.07	0	101	82	98	78	84	72	85	74	87	82	83	84	74	84
112B	2547	196	12.1	351	-20	24	1.420	2.0	25.47	2.57	10	.25	0	70	42	59	31	32	24	42	26	44	39	40	44	32	47
113B	2539	195	15.1	350	-21	24	1.427	2.0	25.34	3.81	15	.24	.04	80	52	70	45	42	39	53	46	54	53	50	54	40	55
114B	2563	195	11.9	400	-21	24	1.427	2.0	25.48	3.35	13	.24	0	77	48	66	43	38	34	49	39	50	47	46	48	36	48
115B	2643	193	15.0	400	-21	24	1.442	2.0	25.64	4.93	19	.23	.04	87	58	77	50	50	45	61	49	62	57	57	61	47	63
116B	2563	195	12.0	450	-18	24	1.427	2.0	25.41	4.52	18	.23	0	84	56	75	53	47	45	58	50	60	59	55	60	45	61
117B	2622	197	15.0	449	-20	24	1.413	2.0	25.48	6.53	26	.21	0	94	64	85	58	57	52	68	60	70	68	65	72	54	72

C-5

APPENDIX C

Table C-6 Summary of Wet Run Skin Temperature Prediction - 12 O'clock Position

RUN NO.	ALTITUDE (FT)	VEL KTAS	BLEED RATE (LB/MIN)	BLEED TEMP (°F)	AMB TEMP (°F)	DROP DIA (MIC)	LWC (G/m³)	SPRAY TIME (MIN)	IMP RATE (LB/HR)	EVAP RATE (LB/HR)	PER CENT EVAP	RUNBACK (IN²/FT) PRED	RUNBACK (IN²/FT) MEAS	SKIN TEMPERATURE, °F S = 0.0 PRED	S = 0.0 MEAS	S = 0.5 PRED	S = 0.5 MEAS	S = 1.0 PRED	S = 1.0 MEAS	S = 1.5 PRED	S = 1.5 MEAS	S = 2.0 PRED	S = 2.0 MEAS	S = 2.5 PRED	S = 2.5 MEAS	S = 3.0 PRES	S = 3.0 MEAS
60A	3208	231	12.09	352	18	18	.901	4.63	14.73	6.42	44	.21	.00	84	54	84	55	82	70	88	85	69	82	51	60	50	57
61A	3266	234	15.16	351	17	18	.890	4.63	14.68	8.56	58	.16	.00	91	59	92	62	89	77	95	92	76	92	56	65	55	58
62A	3295	235	12.11	400	15	18	.887	4.63	14.69	7.82	53	.17	.00	89	61	89	62	85	75	91	91	73	96	52	68	51	57
63A	3259	235	15.30	399	17	18	.890	4.63	14.72	10.72	73	.10	.00	87	70	99	69	96	80	102	104	83	109	62	76	60	66
64A	3222	233	12.10	452	17	18	.894	4.63	14.70	9.72	66	.13	.00	95	73	96	74	93	82	99	110	80	113	59	79	57	69
65A	2831	235	11.35	452	18	18	.988	4.63	14.53	9.03	62	.14	.00	93	77	94	78	91	85	96	120	76	128	57	87	56	81
66A	3253	231	12.02	352	1	21	.762	4.63	14.42	5.43	38	.23	.00	78	57	79	59	72	66	79	76	60	74	38	48	37	40
67A	3262	231	15.17	352	2	21	.763	4.63	14.49	7.51	52	.18	.00	87	59	88	61	83	72	89	88	69	78	47	52	45	46
68A	3297	233	12.03	400	3	21	.757	4.63	14.44	6.92	48	.19	.00	85	60	85	62	80	72	87	83	67	79	44	54	43	47
69A	3280	232	15.16	401	4	21	.760	4.63	14.49	9.66	67	.12	.00	94	68	95	68	91	80	97	93	77	94	53	61	52	54
70A	3266	231	12.10	451	2	21	.763	4.63	14.50	8.54	59	.15	.00	91	70	92	68	87	79	94	94	73	96	49	64	47	29
71A	3291	233	14.93	452	2	21	.760	4.63	14.52	11.64	80	.07	.00	99	77	101	72	98	86	103	117	83	113	58	74	56	70
72A	1637	141	12.06	351	-3	24	1.944	2.0	21.03	3.56	17	.19	.00	80	40	77	36	66	58	85	83	62	83	36	59	35	51
73A	1661	143	15.17	353	-4	24	1.917	2.0	20.98	5.11	24	.17	.022	89	48	87	44	77	66	97	91	73	91	44	64	44	60
74A	1645	143	11.90	401	-4	24	1.917	2.0	21.02	4.55	22	.18	.043	86	45	83	42	73	63	93	90	69	90	41	64	40	57
75A	1667	145	15.37	399	-5	24	1.904	2.C	21.06	6.74	32	.16	.054	96	54	95	50	87	73	106	102	81	100	51	68	50	63
76A	1602	143	11.91	452	-3	24	1.930	2.0	21.04	5.86	28	.17	.043	93	53	91	50	82	72	102	107	78	102	48	72	47	64
77A	1552	144	15.40	453	-5	24	1.917	2.0	21.10	8.82	42	.13	.048	103	49	103	45	96	79	116	128	92	118	60	81	59	76
78A	2389	193	12.14	349	-18	24	1.442	2.0	25.52	2.45	10	.25	.06	69	32	64	24	48	37	64	59	40	62	19	40	18	32
79A	2385	193	12.02	352	-18	24	1.441	2.0	25.46	2.45	10	.25	.027	69	66	64	27	48	22	65	64	40	62	19	39	18	23
80A	2413	195	12.04	400	-20	24	1.434	2.0	25.60	3.18	12	.21	.027	75	21	71	29	54	38	71	78	46	74	22	42	21	38
81A	2541	197	15.35	397	-20	24	1.420	2.0	25.51	4.83	19	.23	.011	86	31	82	16	68	47	84	79	58	75	32	41	32	38
82A	2488	195	12.24	452	-18	24	1.434	2.0	25.58	4.33	17	.23	.00	84	26	80	13	66	44	82	79	55	72	31	37	30	35
83A	2492	195	15.16	450	-18	24	1.427	2.0	25.38	6.82	27	.20	.00	93	35	91	25	79	57	94	92	67	87	36	48	34	46
95A	3199	230	12.1	404	1	21	.767	4.63	14.52	11.53	79	.08	-	74	50	74	53	56	53	63	54	83	71	93	106	66	57
96A	3108	225	12.1	403	3	21	.783	4.63	14.60	2.85	20	.15	-	55	46	60	49	36	52	35	54	36	54	55	55	78	57
97A, 98A	This data not available.																										
100B	3040	232	12.0	350	16	19	.902	4.63	14.84	6.14	41	.22	-	93	70	75	52	69	60	66	48	67	69	61	77	59	74
101B	3040	233	15.0	350	15	18	.895	4.63	14.73	8.08	55	.17	-	101	78	83	59	77	67	73	56	74	81	68	88	65	75
102B	3051	232	12.1	399	14	18	.899	4.63	14.62	7.64	52	.18	-	100	78	81	58	76	67	71	53	73	77	66	84	64	82
103B	3117	235	15.0	400	13	18	.888	4.63	14.70	10.07	68	.12	-	107	84	89	64	84	72	78	61	80	91	73	100	70	96
104B	3069	233	12.1	451	14	18	.895	4.63	14.71	9.23	63	.14	-	105	82	86	63	81	71	76	58	78	85	71	96	68	94
105B	3141	236	15.0	451	14	18	.884	4.63	14.69	12.43	85	.06	-	114	91	95	70	91	77	84	68	86	99	79	116	77	106
106B	3152	231	12.1	352	1	21	.764	4.63	14.52	5.39	37	.23	.10	91	70	70	50	63	58	58	44	60	58	53	68	51	64
107B	3137	230	15.1	351	1	21	.767	4.63	14.53	7.20	50	.19	.10	98	76	78	57	72	63	67	50	68	70	61	80	58	75
108B	3137	231	12.0	401	2	21	.763	4.63	14.45	6.72	46	.20	.10	97	74	77	55	69	63	65	48	66	68	59	78	56	74
109B	3055	229	15.0	401	-1	21	.770	4.63	14.49	8.89	61	.14	.03	105	82	85	62	79	70	73	57	74	85	66	89	64	84
110B	3092	231	12.0	450	0	21	.763	4.63	14.45	8.09	56	.16	.10	103	79	82	57	75	66	69	50	71	78	63	82	60	77
111B	3038	228	15.2	451	-0	21	.773	4.63	14.55	11.34	78	.08	0	112	88	92	64	87	74	80	57	82	88	74	94	71	90
112B	2547	196	12.1	351	-20	24	1.420	2.0	25.47	2.41	9	.25	.09	82	36	52	30	35	30	36	20	39	50	32	46	32	36
113B	2539	195	15.1	350	-21	24	1.427	2.0	25.34	3.78	15	.24	.08	92	47	63	27	45	37	46	22	49	39	40	43	37	38
114B	2563	195	11.9	400	-21	24	1.427	2.0	25.48	3.36	13	.24	.09	89	45	59	15	41	36	42	28	45	52	36	60	33	56
115B	2643	193	15.0	400	-21	24	1.442	2.0	25.64	4.86	19	.23	.08	99	56	70	18	53	43	54	38	56	64	46	72	44	65
16B	2563	195	12.0	450	-18	24	1.427	2.0	25.41	4.47	18	.23	.06	97	54	68	18	51	34	52	34	54	62	44	67	42	61
7B	2622	197	15.0	449	-20	24	1.413	2.0	25.48	6.38	25	.21	.04	106	64	78	23	61	54	61	46	64	79	54	82	51	74

C-6

REFERENCES

1. Bowden, D.T., et. al.: "Engineering Summary of Airframe Icing Technical Data". Technical Report ADS-4, Federal Aviation Administration, March 1964.

2. Eshbach, O.W. and Souders, M.: "Handbook of Engineering Fundamentals". Third Edition, Wiley and Sons, New York, 1974.

3. Baumeister, T.: "Standard Handbook for Mechanical Engineers". 7th Edition, McGraw-Hill, New York, 1966.

4. Langmuir, I. and Blodgett, K.: "A Mathematical Investigation of Water Droplet Trajectories". AAFTR 5418, Feb. 19, 1946.

5. Neel, C.G.: "A Procedure for the Design of Air-Heated Ice Prevention". NACA TN 3130, 1954.

6. Gray. V.H.: "Simple Graphical Solution on Heat-Transfer and Evaporation from Surface Heated to Prevent Icing". NACA TN 2799, 1952.

7. Gelder, F.P., et. al.: "Icing Protection for a Turbojet Transport Airplane: Heating Requirements, Methods of Protection, and Performance Penalties". NACA TN 2866, 1953.

8. "SAE Aerospace Applied Thermodynamics Manual". Second Edition, Society of Automotive Engineers, Inc., New York, Oct. 1969.

BIBLIOGRAPHY

1. Kline, D.B.: "Investigation of Meteorological Conditions Associated with Aircraft Icing in Layer-Type Clouds for 1947-48 Winter". NACA TN 1793, 1949.

2. Jones, A.R. and Lewis, W.: "Recommended Values of Meteorological Factors to be Considered in the Design of Aircraft Ice Prevention Equipment". NACA TN 1855, 1949.

3. Kline, D.B. and Walker, J.A.: "Meteorological Analysis of Icing Conditions Encountered in Low-Altitude Stratiform Clouds". NACA TN 2306, 1951.

4. Hacker, P.T. and Dorsch, R.G.: "A Summary of Meteorological Conditions Associated with Aircraft Icing and a Proposed Method of Selecting Design Criteria for Ice Protection Equipment". NACA TN 2569, 1951.

5. Bergrun, N.R. and Lewis, W.: "A Probability Analysis of the Meteorological Factors Conducive to Aircraft Icing in the United States". NACA TN 2738, 1952.

6. Airworthiness Standards: "Transport Category Airplanes, Appendix C". Federal Aviation Regulations, Part 25, Federal Aviation Administration.

7. Sogin, H.H.: "A Design Manual for Thermal Anti-Icing". Wright Air Development Center, TR-54-313, 1954.

8. Kutty, T.M.: "A Comprehensive Approach to Icing Certification". SAE Paper No. 750507, Business Aircraft Meeting, April 1975.

9. Bergrun, N.R.: "A Method for Numerically Calculating the Area and Distribution of Water Impingement on the Leading Edge of an Airfoil in a Cloud". NACA TN 1397, 1947.

10. Dorsch, R.G. and Brun, R.J.: "A Method of Determining Cloud-Droplet Impingement on Swept Wings". NACA TN 2931, 1953.

11. Gelder, T.F.; Smyers, W.H. and Von Glahn, V.H.: "Experimental Droplet Impingement on Several Two-Dimensional Airfoils with Thickness Ratios of 6 to 16 Percent". NACA TN 3839, 1956.

12. Tribus, Myron: "Modern Icing Technology". Lecture Notes, Project M 992-E, Airesearch and Development Command, USAF Contract AF 18(600)-51, E.O. No. 462 Br-1, January, 1952.

13. Kutty, T.M.: "Gates Learjet Models 35/36 Engine Inlet Anti-Icing Analysis". Gates Learjet Corp. Report No. 26-PR-09, September, 1974.

BIBLIOGRAPHY (Cont.)

14. Anon: "Aircraft Ice Protection". Department of Transportation, FAA, Advisory Circular No. 20-73, April, 1971.

15. Neel, Carr B.: "The Design of Air-Heated Thermal Ice-Prevention Systems". NACA Lecture No. 7, Univ. Michigan. Airplane Icing Information Course. (Unpublished Report)